VOLUME LXIV NUMBER 5

THE ASTROPHYSICAL JOURNAL

AN INTERNATIONAL REVIEW OF SPECTROSCOPY AND ASTRONOMICAL PHYSICS

Edited by

GEORGE E. HALE
Mount Wilson Observatory of the Carnegie Institution of Washington

EDWIN B. FROST
Yerkes Observatory of the University of Chicago

HENRY G. GALE
Ryerson Physical Laboratory of the University of Chicago

DECEMBER 1926

THE UNIVERSITY OF CHICAGO PRESS
CHICAGO, ILLINOIS, U.S.A.

THE CAMBRIDGE UNIVERSITY PRESS, London
THE MARUZEN-KABUSHIKI-KAISHA, Tokyo, Osaka, Kyoto, Fukuoka, Sendai
THE COMMERCIAL PRESS, LIMITED, Shanghai

December 1926 Vol. LXIV, No. 5

THE ASTROPHYSICAL JOURNAL

AN INTERNATIONAL REVIEW OF SPECTROSCOPY AND ASTRONOMICAL PHYSICS

The Astrophysical Journal is published by the University of Chicago at the University of Chicago Press, 5750 Ellis Avenue, Chicago, Illinois, during each month except February and August. ¶ The subscription price is $6.00 a year; the price of single copies is 75 cents. Orders for service of less than a half-year will be charged at the single-copy rate. ¶ Postage is prepaid by the publishers on all orders from the United States, Mexico, Cuba, Porto Rico, Panama Canal Zone, Republic of Panama, Dominican Republic, Canary Islands, El Salvador, Argentina, Bolivia, Brazil, Colombia, Chile, Costa Rica, Ecuador, Guatemala, Honduras, Nicaragua, Peru, Hayti, Uruguay, Paraguay, Hawaiian Islands, Philippine Islands, Guam, Samoan Islands, Balearic Islands, and Spain. ¶ Postage is charged extra as follows: for Canada and Newfoundland, 30 cents on annual subscriptions (total $6.30); on single copies, 3 cents (total 78 cents); for all other countries in the Postal Union, 50 cents on annual subscriptions (total $6.50), on single copies 5 cents (total 80 cents). ¶ Patrons are requested to make all remittances payable to The University of Chicago Press in postal or express money orders or bank drafts.

The following are authorized to quote the prices indicated:

For the British Empire: The Cambridge University Press, Fetter Lane, London, E.C. 4. Yearly subscriptions, including postage, £1 12*s.* 6*d.* each; single copies, including postage, 4*s* each.

For China: The Commercial Press, Ltd., Paoshon Road, Shanghai. Yearly subscriptions, $6.00; single copies, 75 cents, or their equivalents in Chinese money. Postage extra, on yearly subscriptions 50 cents, on single copies 5 cents.

Claims for missing numbers should be made within the month following the regular month of publication. The publishers expect to supply missing numbers free only when losses have been sustained in transit, and when the reserve stock will permit.

Business Correspondence should be addressed to The University of Chicago Press, Chicago, Illinois.

Communications for the editors and manuscripts should be addressed to the Editors of THE ASTROPHYSICAL JOURNAL, Yerkes Observatory, Williams Bay, Wisconsin.

The cable address is "University, Chicago."

The articles in this Journal are indexed in the *International Index to Periodicals*, New York, N.Y.

Entered as second-class matter, January 17, 1895, at the Post-office at Chicago, Ill., under the Act of March 3, 1879.
Acceptance for mailing at special rate of postage provided for in Section 1103, Act of October, 3, 1917, authorized on July 15, 1918.

PRINTED IN THE U.S.A.

THE ASTROPHYSICAL JOURNAL

AN INTERNATIONAL REVIEW OF SPECTROSCOPY AND ASTRONOMICAL PHYSICS

VOLUME LXIV DECEMBER 1926 NUMBER 5

PHOTOMETRIC OBSERVATIONS OF THE SOLAR CORONA AT THE ECLIPSE OF JANUARY 24, 1925, BY THE LATE JOHN A. PARKHURST

By ALICE H. FARNSWORTH

ABSTRACT

Visual measures of the total light of the corona were made by matching the illumination produced in the field of the ocular of the Hartmann microphotometer with that from a glow-lamp of known candle-power. The light from the lamp passed through a blue filter and a photographic wedge, the match being produced by motion of the wedge. Settings made through blue, green, and no ocular filters were most satisfactory with the green filter. The effect of the sky-background was indicated by measures of the sky 8° east of the sun. *Comparison* with similar observations of the *moon* on six nights showed the *illumination produced by the corona* to be 0.27 that of the full moon. Selective transmission of the atmosphere is suggested by the different factors for the transmission of the lamp-filter necessary on different nights. The *candle-power* deduced for the corona is 0.04 meter-candles; for the full moon, 0.16 meter-candles.

INTRODUCTION

Visual measures of the total light of the corona were made on January 24, 1925, by Mr. Parkhurst, at Ithaca, New York. His instrument was located before an east window on the third floor of the physics building (Rockefeller Hall), Cornell University. Mrs. Parkhurst assisted by arranging the window shades, reading meters, and counting audibly the 104 seconds of totality. Weather conditions were good with the temperature at 0° F., thin clouds having disappeared from the region of the sun half an hour before totality at 9^h9^m E.S.T. Mr. Parkhurst was able to carry through his complete program. The reduction of his observations was in progress at

the time of his death. The completion of the work for publication was intrusted to the writer by Director Frost.

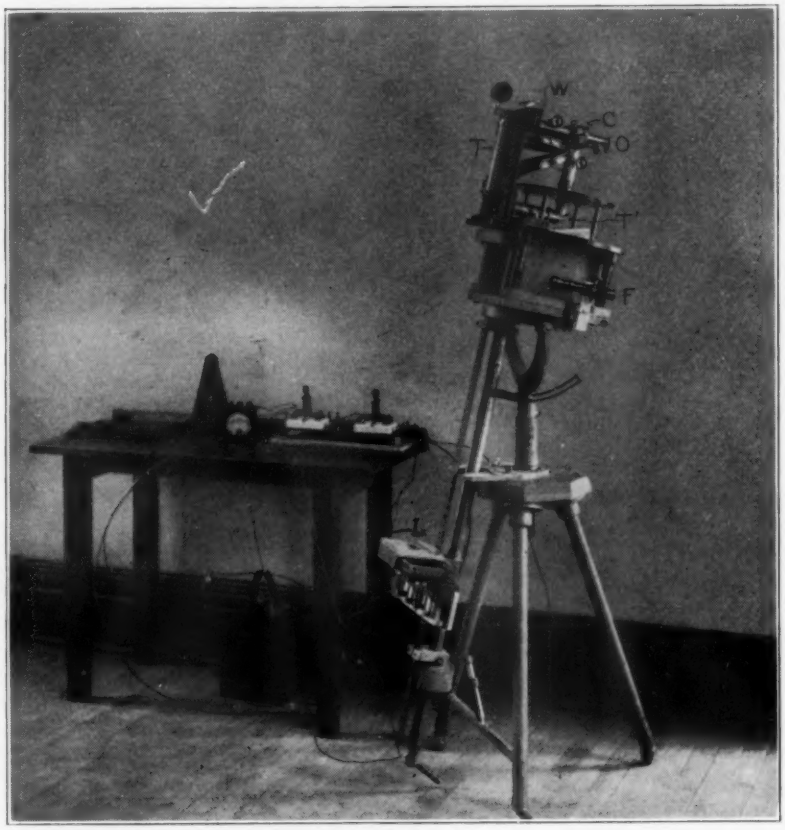

FIG. 1.—The Hartmann microphotometer mounted as an altazimuth for observation of the corona.

L, Lamp
T, Tube (vertical) for lamplight
W, Wedge
C, Cube
F, Finder
T', Tube (horizontal) for coronal light
O, Ocular

INSTRUMENT

The measures were made with a Hartmann microphotometer[1] on an altazimuth mounting shown in Figure 1. The lamp and ground-glass ordinarily used at the junction of the two tubes were

[1] *Astrophysical Journal*, **36**, 171, 1912.

removed. Light from a standard incandescent lamp (*L*), shining through a blue filter in order that it might approximate the color of the corona, passed by the tube (*T*) through a photographic wedge (*W*), then through the transparent portion of the Lummer-Brodhun cube (*C*) into the eyepiece. By means of a small finder (*F*), the other tube of the Hartmann (*T'*) was directed to the corona, the field included being 8°.3 in diameter. The coronal light reached the eyepiece after reflection from a silvered strip (5 mm wide) in the cube. The ocular (*O*) was provided with a rotating wheel carrying blue and green filters. An automatic device for recording the settings of the wedge precluded the necessity of taking time to read the wedge-scale.

OBSERVATION

The observation consisted in moving the wedge until it cut down the light from the combination of lamp and filter (appearing in the right and left segments of the field) sufficiently to bring it into equality with the coronal light (appearing as a vertical strip in the middle of the field). The microscopes in both tubes were thrown out of focus by the same amount. Three settings were made with the blue ocular filter, three with the green, and three with none. The photometer was then turned 8° in azimuth toward the east, and three settings on the sky were made with no ocular filter.

The color of the lamp shining through the blue filter (known as "8+11") proved to be a good match with the corona. The color-match was best, however, through the green ocular filter. This was noted at the time, and confirmed by the agreement among individual settings. The distance of the lamp from the photometer cube, determined from experiment on the full moon, proved right for the settings of the wedge both on corona *plus* sky and the sky alone.

DATA

It is evident that with the apparatus described the evaluation of the total light of the corona and a comparison of it with moonlight involves the following data which will be discussed in order.

1. *Candle-power of the naked lamp.*—According to tests made at the Eastman Research Laboratory, the lamp (No. 245) burning at a current of 1.15 amp. and color-temperature 2415° K. gave candle-

power 3.9 on January 2, and candle-power 4.4 when tested again on March 5. The candle-power used in the reductions is 4.0. The lamp was at a distance of 1.053 m from the microscope objective.

2. *Effect of blue lamp-filter.*—Mr. Parkhurst made several filters of varying density by soaking lantern-slide plates, which had been fixed and washed, in solutions of Eastman blue dye of varying concentrations. The filter finally adopted was a combination of two

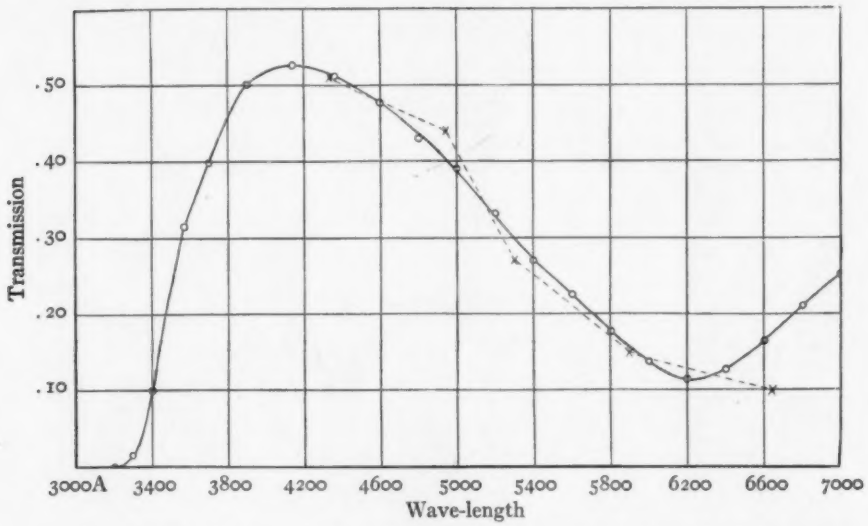

FIG. 2.—Spectral transmission of blue lamp-filter. The circles and full line show the transmission as derived from the Eastman curve of densities; the crosses were derived from measures made with the Hess-Ives tint photometer.

(Nos. 8 and 11) which were left in a solution of 1 dram of dye in 4 ounces of water for three and six minutes, respectively. Its maximum transmission is 52 per cent at λ 4150, as shown by Figure 2. This curve of transmission of the filter was deduced from its density-curve, as determined at the Eastman Research Laboratory and checked by Mr. Parkhurst's measures with the Hess-Ives tint photometer.

In order to determine the total transmission of the filter, integrated for all wave-lengths, it was necessary to plot the luminosity-curve of the naked lamp. For each wave-length the luminosity is proportional to the product of the ordinates of the curves of energy

and visibility (i.e., the relation between luminous sensation and radiant energy).[1] The energy-curve shown in Figure 3 was computed from the Wien-Paschen formula,[2]

$$E_\lambda = c_1 \lambda^{-5} e^{-\frac{c_2}{\lambda T}},$$

where $c_1 = 9226$ and $c_2 = 14{,}350$, for values of λ (expressed in microns) in the visible spectrum and $T = 2166°$ K. Color-temperature is de-

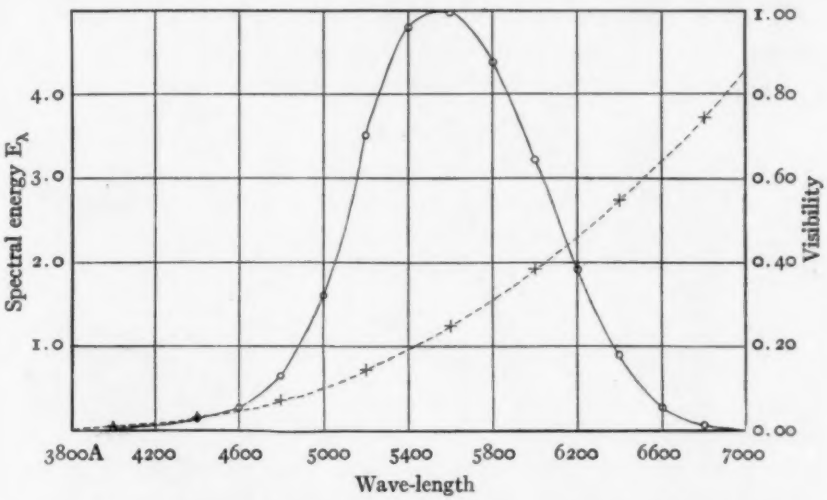

FIG. 3.—The dash-curve with crosses, co-ordinates at the left, gives the energy of a tungsten lamp calculated for $T = 2166°$. The full curve with circles, co-ordinates at the right, shows its visibility, or the ratio of luminous sensation to radiant energy.

fined as "the temperature of a black body which has the same integral color as the source studied."[3] The spectral emission of a tungsten lamp burning at a color-temperature of 2415° K. is equivalent to that of a black body at 2166° K.[4]

The data for the visibility-curve (also shown in Fig. 3) are mean values from Smithsonian Table 297,[5] and are practically the same as those recommended by the International Commission on Illumi-

[1] *Dictionary of Applied Physics*, **4**, 63.

[2] Nutting, *Outlines of Applied Optics*, p. 158.

[3] Forsythe and Worthing, *Astrophysical Journal*, **61**, 155, 1925.

[4] *Smithsonian Physical Tables* (7th ed.), 250, 1920. [5] *Ibid.*, p. 258.

nation.[1] The luminosity-curve of the naked lamp, obtained by multiplying the ordinates of the energy-curve by those of the visibility-curve, is shown in the dash-curve of Figure 4. The ordinates of this curve were then multiplied by the corresponding transmission of the lamp-filter to give the luminosity of lamp *plus* filter, as given by the

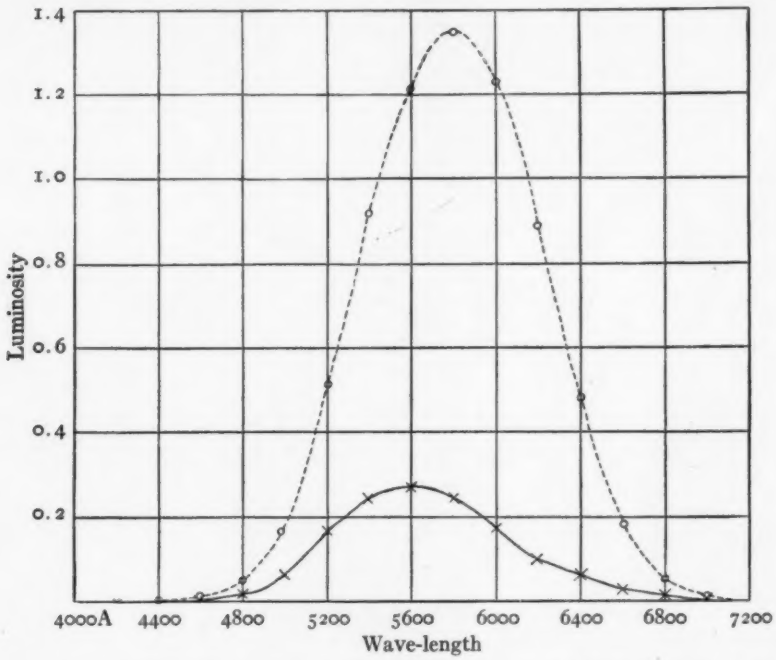

FIG. 4.—The luminosity of lamp 245 is shown by the dash-curve with circles; these ordinates were multiplied by the transmission of the lamp-filter to give the full curve with crosses, representing the luminosity of lamp *plus* filter.

full curve in Figure 4. The ratio of the areas of the two curves is 0.19, and represents the total transmission of the filter used with this lamp. The effect of the use of a further color-filter over the ocular upon this transmission of the lamp-filter is discussed below.

3. *Absorption of wedge.*—The transmission of the photographic wedge (*P*) at different scale-readings was determined by comparing it with various combinations of Eastman dye filters in two ways: First, as in ordinary measuring with a single source of light at the

[1] *Transactions of the Illuminating Engineering Society*, July, 1925.

junction of the two tubes of the Hartmann, the filters were laid on the plate-table, reducing by a known amount the light through one microscope, the wedge reducing the light through the other. Second, two lamps were pivoted in such a way that light from one passed through the wedge and from the other through the filters placed 60 mm outside the horizontal tube. The lamps were interchanged, and the means of the readings obtained adopted. It was further found that the wedge-scale read zero for equal lamps.

The wedge-settings made on the corona are shown in Table I, with the corresponding values of the transmission. Each setting given is the mean of three, the probable errors being indicated.

TABLE I

MEASURES OF LIGHT OF CORONA

Object	Ocular Filter	Wedge-Scale	Transmission of Wedge
Corona *plus* sky.....	Blue	29.0±0.6	0.058
Corona *plus* sky.....	Green	32.0± .0	.047
Corona *plus* sky.....	None	31.5± .3	.049
Sky only, 8° E.....	None	44.9±0.3	0.014

4. *Effect of ocular filters.*—The maximum transmission for the ocular filters as measured in the Hess-Ives tint photometer was 45 per cent at λ 4950 for the blue filter, and 46 per cent at λ 5300 for the green. From measures of the moon in October, 1925, it was found that this limiting of the spectrum reaching the eye had a very decided effect on the effective transmission of the lamp-filter, so that different transmission factors for the lamp-filter had to be used with the different ocular filters.

In order to check the values obtained from observation, to be described below, the total transmission ratios for each of the ocular filters used with naked lamp and with lamp *plus* lamp-filter were obtained as described earlier for the lamp-filter. That is to say, the ordinates of the luminosity-curve of the naked lamp were multiplied by the transmission ratios of each ocular filter and the ratio of the areas of the two curves determined. The same thing was then done with the luminosity-curve of lamp *plus* lamp-filter. Table III shows the computed values, in terms of the luminosity of lamp without

filter as unit, of the total transmission of the lamp *plus* lamp-filter, for each case. The last line of the table shows for each and for no ocular filter the wave-length of the maximum luminosity reaching the eye. It will be noted that the use of the ocular filter increases the effective transmission of the lamp-filter.

5. *Optical arrangements in photometer.*—The complicated optics of the situation is apparent when one considers that parallel rays such as came from the corona and lamp (which was far enough away to be considered a distant object) were brought by the microscopes to a focus so soon after passing through the objective that the rays from this focus were widely divergent and must have been largely lost in the tubes of the instrument. However, since the microscopes are identical, and acted in similar fashion on light from the lamp and from the corona, the consideration of relative brightness between image and object, absorption of light by optical parts, etc., drops out of the reduction.

6. *Effect of sky-background.*—The diameter of the field of the Hartmann is 8°.3; its area, 55.3 square degrees. The area of the full moon is 0.2 square degrees; that of the corona was estimated from photographs at 0.4 square degrees. Thus the corona occupied 1/138 of the field and the full moon 1/276. Since the settings on sky alone at the eclipse were made with no ocular filter, it is fair to compare with similar settings on corona *plus* sky. Reference to Table I shows that corona *plus* sky required for a match transmission of the wedge three and one-half times as great as sky only, 8° east. We have no means of estimating the relative brightness of the sky near and far from the corona. Stebbins[1] considers that there must be little difference. On this assumption the corona furnished 72 per cent of the total illumination.

7. *Atmospheric absorption.*—The question of the actual amount of atmospheric absorption on a given day is a difficult one, and makes uncertain comparisons of measures of the corona with measures of the moon on necessarily different dates. Observations of the corona were made at an altitude of $14\frac{1}{2}^\circ$; observations of the moon made at this altitude are given more weight in the comparisons than those made at a different altitude and reduced to it. No attempt has

[1] *Astrophysical Journal*, **49**, 144, 1919.

been made to reduce the final results to the zenith or outside the atmosphere.

8. *Change in brightness of moon with phase.*—The change of brightness of the moon with phase has been investigated by several observers. Russell's values as given in *Astrophysical Journal*, **43**, 114, 1916, were here used. The phases for the dates of observation of the moon were obtained with sufficient approximation by subtracting 180° from the difference between the longitudes of moon and sun for the date. The factor used to reduce the observed brightness to full moon is the reciprocal of the percentage given in Russell's Table III.

OBSERVATIONS OF THE MOON

Observations of the moon, for purposes of comparison, were made by Mr. Parkhurst in February after the eclipse, using the same apparatus as at the eclipse with the exception of the lamp (No. 245) which had been sent away to be retested. Lamp 241 showed candle-power 4.0 burning at 1.15 amp. in May, 1923, and is assumed in the reductions to be the equivalent of lamp 245. It was Mr. Parkhurst's intention to make measures with the eclipse lamp, and nearer to the time of full moon than February weather permitted.

In October, 1925, the apparatus was reassembled and measures on nights adjacent to full moon were made by the writer, using lamp 245. Table II gives the necessary data concerning the two series of observations of the moon. Uncertainty is introduced on February 5 and 6 because of the necessary reduction to altitude $14\frac{1}{2}°$, the observations having been made when the moon was higher. On the remaining dates, the settings given were made at altitude $14\frac{1}{2}°$. These facts as well as the recorded atmospheric conditions are taken into consideration in assigning weights for the different dates.

The relative transmissions indicated by the wedge-settings give a comparison between the light of the corona and that from the full moon. The elimination of the effect of the sky-background for the observations through the blue and green ocular filters is uncertain, because no measures were made of sky alone through these filters. However, the effect is assumed to be the same as in the case of no

ocular.filter, namely, that 72 per cent of the illumination from corona *plus* sky is due to corona. It may reasonably be asked what effect the sky-background for the moon produces. It was found in October that the light from the sky 8° from the moon was so faint that it was

TABLE II

OBSERVATIONS OF THE MOON

DATE	MEAN C.S.T.	RANGE IN ALTITUDE	PHASE-ANGLE	REDUCTION TO FULL	MEAN WEDGE-READING AT (OR REDUCED TO) ALT. 14½°		
					Blue	Green	None
Feb. 5.....	18h07m	33°–38°	−32°.0	1.9	34.4	34.9	35.4
Feb. 6.....	18 10	27–30	−21.1	1.5	31.2	31.4	30.5
Feb. 6.....	19 14	38	−20.6	1.5	24.6	25.7	26.0
Feb. 11.....	21 39	12–18	+37.4	2.4	25.7	25.1	24.1
Oct. 30.....	18 00	12–25	− 9.1	1.2	25.1	24.2	23.0
Oct. 31.....	18 33	11–26	+ 3.4	1.1	21.5	20.8	20.0
Nov. 1.....	19 07	12–20	+16.1	1.4	30.7	29.5	27.1

DATE	OBSERVED TRANSMISSION			TRANSMISSION REDUCED TO FULL			MEAN	WEIGHT
	Blue	Green	None	Blue	Green	None		
Feb. 5.....	0.037	0.035	0.034	0.070	0.066	0.065	.....	0
Feb. 6.....	.050	.049	.052	.075	.074	.078	.....	1
Feb. 6.....	.093	.079	.077	.140	.118	.116	.....	1
Feb. 11.....	.079	.087	.099	.190	.209	.238	.....	2
Oct. 30.....	.086	.099	.114	.103	.119	.137	.....	3
Oct. 31.....	.140	.152	.170	.154	.167	.187	.....	4
Nov. 1.....	0.052	0.055	0.068	0.073	0.077	0.095	.....	2
Unweighted mean.....				0.115	0.119	0.131	.....	.....
Weighted mean.....				.128	.138	.155	.....	.....
Corona *plus* sky.....				.058	.047	.049	.....	.....
Sky.....				.....	.....	.014	.....	.....
Corona only.....				.042	.034	.035	.....	.....
Ratio, corona: moon...				0.33	0.25	0.23	0.27	.....

not possible to obtain a match with the lamp in its position. This furnishes a value of 0.004 candle-power as an upper limit for it. Assuming that its actual value were half this, the sky-background about the moon would furnish less than 2 per cent of the total illumination. It has therefore been neglected. The mean ratio between corona and full moon is then deduced to be 0.27.

In order to check the transmission of the lamp-filter, on October 31 and November 1 the moon was compared with naked lamp as well as with lamp *plus* filter. Table III gives the results of fifteen comparisons of lamp 245 with the moon, with and without lamp-filter, made through the green ocular filter; eleven comparisons through the blue ocular filter; and eleven without ocular filter. Each recorded value for the transmission of the wedge depends on the mean of three settings of the wedge—so that 222 settings are represented. Two very definite systematic effects appear.

TABLE III

PERCENTAGE TRANSMISSION OF LAMP-FILTER FROM MEASURES OF FULL MOONLIGHT

DATE, 1925	OCULAR FILTER			SKY
	None	Blue	Green	
Oct. 31	0.19	0.35	0.31	Transparency good
Nov. 1	.24	.46	.40	Rather damp and foggy
Nov. 28	.23	.42	.33	Very thick, hazy
Computed	.19	.29	.23	.....
Adopted	0.19	0.32	0.26	.....
Maximum luminosity	λ 5600	λ 5200	λ 5400	.....

1. On both dates the ratio of the recorded transmission without lamp-filter to that with it changes with the ocular filters used. On October 31 the ratio without ocular filter corresponds very closely to the value obtained from a comparison of the areas under the computed curves, mentioned above; with the blue and green filters the ratio becomes greater, as was suggested by the comparison of areas given above.

2. The effect recorded for October 31 was repeated on November 1 with this notable modification—that the ratio for each filter and none was increased by about 23 per cent, i.e., the combination of lamp and filter was apparently letting through more light. The explanation is doubtful; possibly it is due to the varying amount of water-vapor in the air. Apparently, the moon measured on November 1 was a blue moon, relatively speaking, compared to the yellow moon measured the previous night.

Atmospheric conditions a month later prevented any very precise tests. On November 28 two sets of measures were made and the ratios obtained (given in Table III) lie between the two previous determinations. This would seem to preclude any change in the lamp-filter itself and throw the explanation upon selective atmospheric absorption. Mr. Parkhurst's note regarding conditions at the eclipse is as follows: "The sky was somewhat overcast with thin clouds till 8:42 when a clear area from the west reached the sun. There was very little wind, and after the clouds disappeared from the eastern sky the transparency was at least average for a winter morning." The decision as to which transmission should be used is arbitrary, and the adopted values in Table III are means of the computed values and those of October 31, when it may be supposed that conditions were most like those at the eclipse.

CANDLE-POWER OF THE CORONA AND FULL MOON

The steps taken in deducing the candle-power of the corona are shown in Table IV. The candle-power of lamp 245, placed at a distance of 1.05 m from the microscope objective, is multiplied by the transmission of the blue lamp-filter to give the effective candle-power of lamp *plus* filter in column 5. The light from the lamp is still further diminished by the photographic wedge. The table shows the values of the transmission of the wedge when the illumination from the lamp is made to match that from corona and sky, and from sky only, whence corona only. The effective candle-power in column 5 is multiplied by these values of the transmission and further by 1.11 (to reduce the lamp from 1.05 to 1.00 m) to give for the candle-power of the corona in meter-candles a mean value of 0.04. The three determinations are not in very good agreement, but it is to be seen that the mean is close to the value obtained through the green ocular filter, which was noted by Mr. Parkhurst as giving the best match with the coronal light. "The color-match of lamp-light shining through filter 8+11 was evidently better through the green ocular filter than with other combinations, which indicated that lamp plus filter 8+11 needed a little more green to make it match the color of the light of the corona."

Table V shows the reduction of the measures of the moon, the

average of observations on two nights without the lamp-filter being shown separately from observations on five nights with the lamp-filter. As before, the quantities of columns 2 and 7 have been multiplied by the transparency of the wedge and by 1.11 to give in columns 5, 6, and 9 the candle-power in meter-candles. The mean value for the full moon comes out to be 0.16 meter-candles. All the

TABLE IV

CANDLE-POWER OF CORONA

OCULAR FILTER	MAXIMUM TRANSMISSION	C.P. OF LAMP 245 AT 1.05 M.	TRANSMISSION OF LAMP-FILTER	EFFECTIVE C.P. OF LAMP+FILTER	TRANSMISSION OF WEDGE			C.P. OF CORONA IN METER-CANDLES
					Corona+Sky	Sky	Corona Only	
Blue.....	λ 4950	4.0	0.32	1.28	0.058	.....	0.042	0.06
Green.....	5300	4.0	.26	1.04	.047	.....	.034	.04
None.....	.....	4.0	0.19	0.76	0.049	0.014	0.035	0.03
Mean....	.....	.....	.....	.....	.....	.....	.....	0.04

TABLE V

CANDLE-POWER OF FULL MOON

OCULAR FILTER	C.P. OF LAMPS 245, 241	WITHOUT LAMP-FILTER				WITH LAMP-FILTER		
		Transmission Reduced to Full		C.P. of Moon		Effective C.P. Lamp+Filter	Transmission Reduced to Full	C.P. of Moon
		Oct. 31	Nov. 1	Oct. 31	Nov. 1			
Blue.....	4.0	.....	0.032	.....	0.14	1.28	0.128	0.18
Green.....	4.0	0.050	.034	.022	.16	1.04	.138	.16
None.....	4.0	.....	0.020	.....	0.09	0.76	0.155	0.13
Mean.....	.....	.....	.....	.....	0.15	.....	.....	0.16

data of Tables IV and V refer to an altitude of $14\frac{1}{2}°$, the altitude of the eclipsed sun at Ithaca. It is to be noted that the use of different transmission factors for the lamp-filter, varying with the ocular filter, tends to bring into agreement the observations of the moon made with the lamp *plus* filter. It has the opposite effect on the measures of the corona.

It hardly seems profitable to compare these results with those of other observers who have used receiving surfaces of different color-

sensibility from that of the eye, and standards of different color. For example, Kunz and Stebbins state[1] that in 1918 Parkhurst's lamp burning at 5.4 volts gave 10.4 candles measured with their photo-electric cell K 113, compared with 4.6 candles by the visual tests of the Bureau of Standards. The observers with the cell use as standards lamps calibrated by comparison with a Hefner amyl-acetate candle. "The blue-sensitive photo-electric cell naturally gives a higher value than the eye does when a white light [filament of the electric lamp] is expressed in terms of a yellow one [amyl-acetate flame of Hefner candle]."

At the eclipse of January 24, 1925, the observers with the cell obtained a value of 0.29 candle-meters for the corona.[2] If the energy-curve of a Hefner lamp (their standard) at $T = 1875°$ be plotted and its luminosity be determined (1) to the eye, by multiplying by the visibility at corresponding wave-lengths, and (2) to the cell, by multiplying by the sensitivity of the cell,[3] it is found from the areas of the curves that the luminosity to the eye is nearly eleven times that to the cell. This would be expected since the radiation of the lamp is slight in the region to which the cell is sensitive.

YERKES OBSERVATORY
July 1926

[1] *Astrophysical Journal*, **49**, 142, 1919.

[2] *Ibid.*, **62**, 127, 1925. [3] *Ibid.*, **49**, 141, 1919.

PROVISIONAL ELEMENTS AND DIMENSIONS OF S ANTLIAE CONSIDERED AS AN ECLIPSING BINARY[1]

By ALFRED H. JOY

ABSTRACT

Spectrographic observations.—The spectrum is similar to that of W Ursae Majoris in that it shows wide double lines, but the type for both components is estimated to be A8. Luizet's double period, 0.64833872 day, fits the observations. *Nineteen spectrograms* (Table I), obtained with a single prism, serve to determine the *elements* of the orbit: $e=0.0$ (assumed); $\gamma=-5.0$ km/sec.; $K_1=81$ km/sec.; $K_2=148$ km/sec.

Photometric orbit.—The Harvard photometric observations have been used to determine a light-curve and an orbit, the star being considered as an eclipsing variable. The results indicate that the *components* are *very close* together and greatly *elongated*. The *eclipse* is *partial*. $a_0=0.36$; $k=0.77$; $i=62^\circ\ 10'$. Judged from their spectra, the light of the brighter star is twice that of the fainter.

Absolute dimensions.—The spectrographic and photometric observations are combined to give the dimensions of the stars and the system: radius of relative orbit = 2,300,000 km; semi-major axis of large star = 1,160,000 km; semi-major axis of small star = 896,000 km; distance of surfaces = 251,000 km; $m_1=0.75\ \odot$; $m_2=0.42\odot$:, $\rho_1=0.31\ \odot$; $\rho_2=0.38\ \odot$.

The light-changes of the southern variable, S Antliae ($9^h\ 29^m.7$, $-28^\circ\ 11'$, 1900), were first detected by H. M. Paul[2] at Washington in 1888. Its period was then the shortest known. The early observers, Sawyer, Yendell, and Chandler, placed the variable in the Algol class on account of the sharp minimum and flat maximum; but, in 1896, E. C. Pickering[3] made a series of observations with the meridian photometer and concluded that the star was not an eclipsing variable, because the minimum occupied such a large portion of the period and because the light-change at maximum was continuous. O. C. Wendell[4] observed portions of four minima in 1898 with the polarizing photometer, finding odd and even minima of nearly equal depth. Luizet,[5] in 1904, compared his observations with earlier measures and gave corrected elements of such accuracy as to hold very closely up to the time of the present observations. Since

[1] *Contributions from the Mount Wilson Observatory*, No. 322.

[2] *Astronomical Journal*, **9**, 180, 1890.

[3] *Astronomische Nachrichten*, **142**, 12, 1896.

[4] *Annals of the Harvard College Observatory*, **69**, 44, 1909.

[5] *Astronomische Nachrichten*, **165**, 291, 1904.

the light-curve does not differ widely from that which would be given by a single rotating ellipsoid, Shapley[1] included the star in his list of such objects. Plummer[2] has noted certain irregularities in the light-curve which led him to associate it with the short-period cluster-type of variables.

TABLE I

SPECTROGRAPHIC OBSERVATIONS

	Plate	Date	G.M.T.	Phase	Velocity		O−C		Wt.	
					Prim.	Sec.	Prim.	Sec.	Prim.	Sec.
					km/sec.	km/sec.	km/sec.	km/sec.		
γ	6397.....	1917 Nov. 27	$0^h\ 47^m$	0.3279	+19	.....	+21	.....	1.0	.....
	6435.....	Dec. 4	0 52	.1996	−67	+137	+14	+ 4	0.5	1.0
	6505.....	9	22 36	.1717	−80	+149	+ 1	+ 1	1.0	0.5
	6727.....	1918 Mar. 2	19 12	.1411	−87	+149	− 3	+ 9	0.5	0.5
	6810.....	30	17 20	.1848	−82	+122	+ 2	−17	0.5	0.5
	7798.....	1919 Jan. 18	21 25	.0091	−26	.....	−14	.....	1.0	.....
	7970.....	Mar. 17	18 12	.1729	−84	+146	+ 2	+ 4	1.0	1.0
	8023.....	Apr. 10	15 35	.0761	−68	+ 55	− 9	−39	1.0	1.0
	8024.....	10	16 35	.1171	−76	+135	+ 2	− 7	1.0	1.0
	8037.....	11	16 14	.4542	+55	−137	−17	+ 9	1.0	0.5
C	798.....	1920 Nov. 29	1 10	.0581	−56	+ 69	− 6	− 4	1.0	1.0
C	939.....	1921 Mar. 16	17 37	.0776	−51	+ 91	+ 9	− 5	1.0	1.0
γ	10082.....	Apr. 16	15 50	.5731	+54	−146	+ 5	−42	1.0	0.5
	10084.....	16	17 05	.6252	+14	.....	+ 3	.....	1.0	.....
	10089.....	17	15 21	.2564	−77	+ 57	−23	−27	0.5	0.5
	10092.....	17	17 07	.3300	− 4	.....	− 3	.....	1.0	.....
	10109.....	21	15 40	.3795	+35	−102	− 2	−21	1.0	0.5
	10123.....	25	16 39	.5304	+83	−172	+15	−33	0.5	0.5
C	1012.....	May 13	16 02	0.3512	+22	.....	+ 6	.....	0.5	.....

SPECTROGRAPHIC OBSERVATIONS

The Harvard estimate of the spectral type is Fo. The first photographs of the spectrum obtained at this observatory were taken for the purpose of determining the absolute magnitude and parallax. It was immediately seen[3] that the spectrum is very different from that of Cepheid or cluster-type variables, the lines being wide and hazy, because of a large rotational effect like that found in W Ursae Majoris. In some cases the lines appeared to be double. On account of the character of the spectrum, the plates are extremely difficult to

[1] *Astronomische Nachrichten*, **194**, 353, 1913.

[2] *Monthly Notices of the Royal Astronomical Society*, **73**, 659, 1913.

[3] Adams and Joy, *Publications of the Astronomical Society of the Pacific*, **31**, 41, 1919.

measure and the results are accordingly uncertain, especially in the case of the secondary spectrum. As more observations were obtained, it became evident that the period of light-variation could be used to plot the velocity changes only if the double period of sixteen

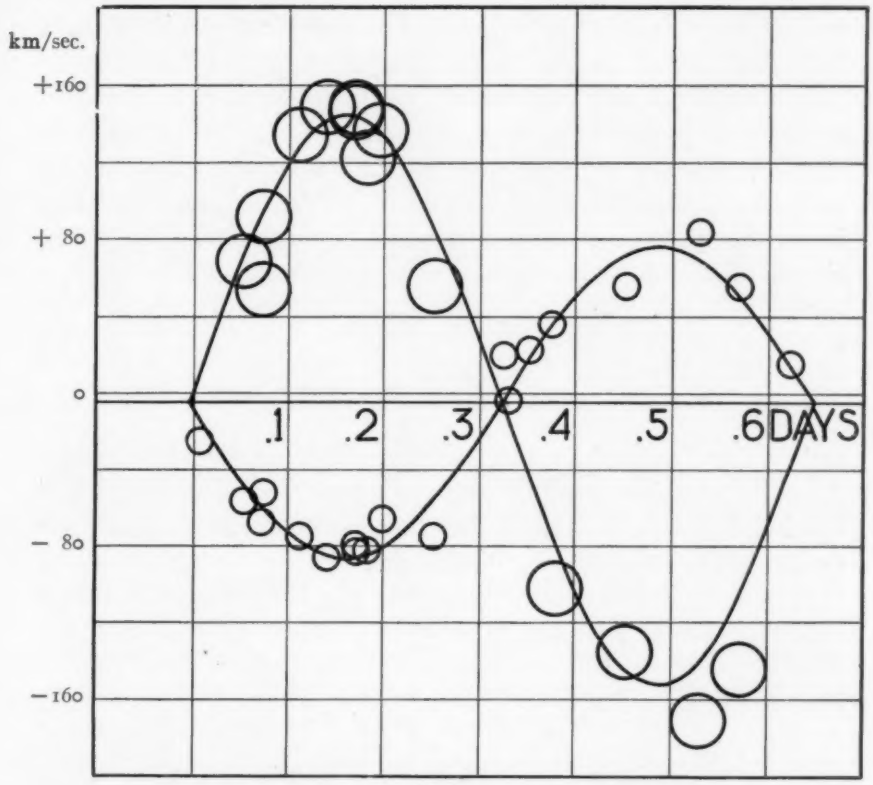

FIG. 1.—Velocity-curves of the components of S Antliae

hours were adopted. The predicted maximum of light occurs at the time of maximum separation of the two components of the spectrum, and minimum of light when the spectrum is single. It is therefore concluded that the star must be an eclipsing binary having ellipsoidal components of nearly the same surface brightness which partially eclipse each other. The spectral type is estimated as A8 for each star, but there is much uncertainty in the case of the fainter spectrum. On many of the plates, the weaker lines of both compo-

nents are lacking, and the stronger lines very poorly defined. The lines of the secondary are always measured with difficulty. The low altitude of the star caused some of the spectrograms to be weak in the violet region.

Nineteen plates were obtained as given in Table I. All were measured at least once by the writer, and the weight for most of them is increased by the measures of Mr. Adams and Miss Burwell.

Since neither the photometric observations nor the velocity-curve show any indication of eccentricity, the orbit is assumed to be circular. Separate solutions were made to determine the correction to the remaining elements of the primary and secondary. The velocity of the system, γ, was not included in the secondary solution, since it was considered to be more accurately defined by the solution for the primary. When the period is doubled, the photometric elements of Luizet,

$$\text{Min.} = \text{J.D. } 2410741.5248 + 0.64833872 \text{ day (G.M.T.)}$$

satisfy the observations very exactly. Since more than eighteen thousand complete revolutions have taken place since the initial epoch, it is evident that the period cannot have changed by as much as one-tenth of a second in thirty years.

The corrected elements of the spectrographic orbit as determined by the observations are:

$e = 0.0$ (assumed)	$a_1 \sin i = 722{,}000$ km
$\gamma = -5.0 \pm 1.8$ km/sec.	$a_2 \sin i = 1{,}320{,}000$ km
$K_1 = 81 \pm 2.5$ km/sec.	$m_1 \sin^3 i = 0.52$
$K_2 = 148 \pm 11.6$ km/sec.	$m_2 \sin^3 i = 0.29$

The residuals in the seventh and eighth columns of Table I are computed from these elements.

PHOTOMETRIC ORBIT

The outcome of the spectroscopic observations makes it worth while to re-examine the available photometric data, with a view to the determination of other facts concerning this well-known variable. It is of especial interest to see whether it is possible to account for

the observed light-changes by assuming that the two bodies are ellipsoidal stars partially eclipsing each other.

The observations with the meridian photometer by Pickering[1] in 1896 and those of Wendell[2] in 1898 with the sliding-prism polarizing photometer have been used, the latter being adjusted to the meridian observations by applying a correction of +0.16 mag. The measures were grouped according to time in twenty-three normal places as given in Table II. The phases were determined from Luizet's elements.

TABLE II

HARVARD PHOTOMETRIC OBSERVATIONS

Mean Mag.	Mean Phase	No.	Mean Mag.	Mean Phase	No.	Mean Mag.	Mean Phase	No.
6.84.....	0.006	6	6.45.....	0.227	12	6.38.....	0.435	4
6.75.....	.016	7	6.53.....	.251	7	6.46.....	.460	18
6.67.....	.028	7	6.61.....	.272	7	6.38.....	.502	17
6.56.....	.051	9	6.76.....	.318	4	6.41.....	.545	3
6.52.....	.065	5	6.79.....	.325	5	6.55.....	.576	19
6.38.....	.098	6	6.71.....	.349	17	6.67.....	.610	15
6.31.....	.146	7	6.65.....	.371	23	6.79.....	0.636	16
6.39.....	0.204	28	6.53.....	0.398	8			

The observations show large errors, probably because of the southern declination of the star. Too much confidence should not be placed upon the arbitrary light-curve, which has been drawn as shown in Figure 2. It is evident, however, that the minima are not exactly equal in depth, and that after allowing for a considerable ellipticity, there remains a small percentage loss of light which may be caused by eclipse.

Using Russell's[3] method and notation, we find by plotting $\cos^2\theta$ against $1-L^2$, the magnitudes being reduced to intensities, that $z=0.340$. The rectified curve then shows that the loss of light because of eclipse is 0.145 at primary and 0.120 at secondary minimum. The loss because of the ellipticity of the stars is 0.188.

By setting different values for a_0 and k in the equation

$$a_0 = 1-\lambda_1+\frac{1-\lambda_2}{k^2},$$

[1] *Harvard Annals*, **46**, 124, 1903.

[2] *Ibid.*, **69**, 44, 1909.

[3] *Astrophysical Journal*, **35**, 315; **36**, 54, 1912.

it is seen that the orbit would be largely indeterminate were it not for the assistance of the spectroscopic data at this point. The spectrograms indicate that one star is brighter than the other in the ratio of approximately 2:1. After calculating the ratio of surface brightnesses by comparing the minima and the total light of the two stars, the ratio of the radii, k, is found to be 0.775. Had the ratio 3:2 been used instead of 2:1, the resulting dimensions of the stars would have been changed by less than 10 per cent. A light-curve was computed with $k=0.775$ and $a_0=0.36$ which fits the rectified light-curve at minimum within the uncertainties of the observations.

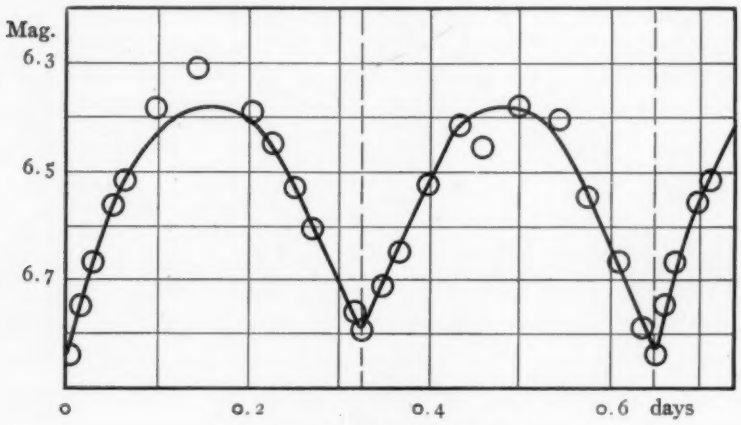

FIG. 2.—Light-curve of S Antliae

If we take 0.09 day before minimum as the beginning of eclipse, the corresponding value of the longitude, θ', may be computed, and the inclination, $i=62^\circ\ 10'$, may be found from the equations

$$a_1^2(1-z)[1+kp(k, a_0)]^2=\cos^2 i$$

$$a_1^2(1-z\cos^2\theta')\,(1+k)^2=\cos^2 i\cos^2\theta'+\sin^2\theta'.$$

The dimensions of the stars in terms of the radius of the relative orbit are:

Semi-major axis of larger star	a_1	0.502
Semi-minor axis of larger star	b_1	.377
Semi-major axis of smaller star	a_2	.389
Semi-minor axis of smaller star	b_2	0.292

The value of the inclination of the orbit having been determined from the photometric observations, it is possible to give absolute values for the dimensions of the system by combining the photometric and spectroscopic elements. We thus find:

Period	P	0.64833872 day
Orbital eccentricity	e	0.00 (assumed)
Light of bright star	L_1	0.67
Ratio of surface brightness	J_b/J_f	1.2
Spectral type, both stars		A8
Ratio of radii of stars	k	0.775
Percentage of eclipse	a_0	0.36
Duration of eclipse		0.180 day
Magnitude at maximum		6.39
Magnitude at primary minimum		6.83
Magnitude at secondary minimum		6.79
Inclination of orbit	i	62° 10′
Radius of relative orbit	a_1+a_2	2,300,000 km
Radius of primary orbit	a_1	817,000
Radius of secondary orbit	a_2	1,490,000
Semi-major axis, large star		1,160,000
Semi-minor axis, large star		870,000
Semi-major axis, small star		896,000
Semi-minor axis, small star		674,000
Distance of surfaces		251,000
Mass, primary large star	m_1	0.75 ⊙
Mass, secondary small star	m_2	0.42
Density, large star	ρ_1	0.31
Density, small star	ρ_2	0.38
Absolute magnitude, bright star	M	2.9
Parallax		0″.017

The difference in velocity at the two limbs of the larger star due to rotation is 225 km/sec., which easily accounts for the character of the spectral lines. For determining the absolute magnitude the brighter star was assumed to have a surface brightness 1.1 mag. brighter than that of the sun. No darkened solution was attempted on account of the inaccuracy of the light-curve, but it seems probable from inspection that the observations would have been somewhat better represented by the assumption of darkening at the limb.

It therefore appears that the variable S Antliae should be classed among the eclipsing binaries. The light-changes can be accounted for by ellipticity of the stars and by the partial eclipse of the larger, brighter, and more massive star at primary minimum. The star will repay further accurate photometric observation, for the present results must be affected by a considerable degree of uncertainty.

Of those variable stars which have been suggested as single rotating ellipsoids, not one has been found to meet the necessary spectrographic requirements.

MOUNT WILSON OBSERVATORY
August 1926

GENERAL CHARACTERISTICS OF ELECTRICALLY EXPLODED WIRES[1]

By J. A. ANDERSON and SINCLAIR SMITH

ABSTRACT

A general discussion of the condenser circuit shows that *efficiency in producing high temperatures* with the method of electrically exploded wires requires primarily *high voltage;* secondarily, *large capacity* and *low inductance.* The best value for the resistance of the wire is $\sqrt{L/C}$, and the resistance of the rest of the circuit should be negligible.

Several methods of studying the explosions are outlined: (1) From *direct photographs* the temperature of the vapor may be measured when its pressure is equal to that of the surrounding atmosphere. (2) A convenient form of *rotating-mirror camera* is described, which is well adapted for studying sparks or explosions in circuits whose frequency is not much greater than 10^6 cycles. (3) *Rotating-mirror spectrograph.* (4) *Velocity-of-sound method.* The sound pulse produced by the explosion is reflected back and caused to pass through the hot metallic vapor. Its path is photographed with the rotating-mirror camera. From this the *velocity of sound in the vapor* can be determined at various instants of time after the beginning of the explosion. A simple calculation then gives the *true temperature of the vapor* at these instants. The method does not apply to the early stages when the temperature exceeds 10,000° on account of the opacity of the vapor. (5) *Optical focal-plane shutter.* In the mechanical focal-plane shutter the image is stationary while the shutter moves. This is reversed in the present apparatus. The *image moves at high speed* produced by reflection from one face of a rotating mirror. After passing the opening in the shutter it is *reflected from a second face of the mirror* which exactly stops the motion, allowing the photograph to be made. Exposures of about 10^{-6} second are easily obtained. A motion-picture camera taking several such exposures in quick succession is suggested. Photographs made with this apparatus showing various phases of explosions are reproduced. (6) *Magneto-optic shutter.* A cell containing water is placed between crossed nicols. A small coil of wire connected in series with the wire to be exploded is wound around the cell. The coil is so designed that with the maximum current a rotation of the plane of polarization of about 20° is produced. With a suitable resistance in the circuit it follows that the shutter is open only near the maximum of the first half-cycle. Photographs of an early stage of the explosions are reproduced and discussed briefly. (7) *Parallel spark-gap.* A spark-gap parallel to the wire to be exploded is so adjusted that the current is shunted into it immediately after the wire is vaporized. This is possible for all metals tried except tungsten. A photograph of the wire then shows practically nothing but the very beginning of the explosion.

The appearance of explosions at the very beginning indicates that *the particles evaporating from electrically heated wires at high temperatures are charged.*

Six years ago one of us published an account of the spectra of electrically exploded wires[2] in which was included a description of some of the phenomena of an explosion. Since then methods and apparatus have been devised which greatly facilitate the study of such transient phenomena, and these, together with some of the conclusions we have reached, form the subject of the present paper.

[1] *Contributions from the Mount Wilson Observatory,* No. 323.

[2] Anderson, *Mt. Wilson Contr.,* No. 178; *Astrophysical Journal,* **51,** 37, 1920.

The chief aim of the investigation is to produce very high temperatures. The method is that used first by Singer and later by Nipher, namely, to pass the current from a large condenser through a fine wire. Since by this means currents having an instantaneous value of several thousand amperes are readily obtained, it follows that a small wire will be heated and turned into vapor very suddenly. The word "explosion" was used by Nipher to describe the phenomenon, and we have followed him in this, although we do not agree with the reasoning which appears to have led him to choose this term.

In order to specify more or less precisely the conditions which favor the development of high temperatures it will be desirable to recall the well-known formulae which have been developed for condenser circuits. Such a circuit is defined by four constants, namely, the capacity (C) of the condenser, the inductance (L), the resistance (R) of the circuit, and the voltage (V) of the charged condenser. The current (i) is then given by

$$i=\frac{Ve^{-\frac{RT}{2L}}}{L\sqrt{\frac{1}{LC}-\frac{R^2}{4L^2}}}\sin t\sqrt{\frac{1}{LC}-\frac{R^2}{4L^2}}, \tag{1}$$

provided R is less than $2\sqrt{L/C}$, and by

$$i=\frac{Ve^{-\frac{RT}{2L}}}{L\sqrt{\frac{R^2}{4L^2}-\frac{1}{LC}}}\sinh t\sqrt{\frac{R^2}{4L^2}-\frac{1}{LC}} \tag{2}$$

in the general case.

It will be convenient to regard the resistance R as made up of two parts, the resistance of the wire (r) and that of the rest of the circuit (R_0). Heat energy is developed in the wire at a rate given by i^2r, and in the rest of the circuit at the rate i^2R_0. Consequently, it is necessary that r be large as compared to R_0, if the greater part of the energy is to appear in the wire. Practically, this means that R_0 must be made very small, for it will be shown later that the total resistance $r+R_0$ may not be large. The current i which appears in the expression for the rate of energy input is of first importance, because

it enters with the exponent 2. The product i^2r must be made as large as possible. From equation (1) it follows that i^2R will be a maximum when $R=\sqrt{L/C}$ nearly, and since r will not differ very materially from R, this is very nearly the best value for the resistance of the wire.

There remains now to find what the relative values of the other constants C, L, and V should be. Inserting in (1) the value of R just found, we find that the maximum value of i^2 is

$$\tfrac{1}{3}V^2\frac{C}{L}e^{-\frac{C}{L}t}.$$

Hence, i^2 varies as V^2C/L, from which it follows that a large value of V is of first importance; that C should be large also, and L as small as possible.

Four condensers have been used in this work, and the constants of their circuits are given in Table I.

TABLE I

Condenser No.	Capacity Microfarads	Inductance Millihenrys	Voltage Kilovolts	i Max. Amperes	Frequency	Energy Joules
1	0.4	0.0033	18–20	7,000	140,000	80
2	1.0	.0034	18–20	10,800	87,000	200
3	0.6	.0011	55–60	45,000	200,000	1080
4	2.0	0.0036	35–40	30,000	60,000	1600

Condensers 1 and 2 were built of sheets of window glass coated with tinfoil. Condenser 3 is of special plate glass, 11 mm thick. The electrodes are sheets of wire gauze imbedded in the center of each plate. These plates were made to order by the Mississippi Wire Glass Company, of New York, to whom, and especially to the superintendent of their factory, Mr. H. L. Carspecken, we are deeply grateful. Condenser 4 is made of window glass, but is coated with thin sheet copper, allowing the leads to be soldered on, thus insuring good electric contact throughout. It is made in eight units, each having a capacity of 1.0 microfarad. These units may be connected in various ways giving a number of different capacities and voltages. The arrangement for which constants are given in Table I is four pairs in series-parallel.

All of the condensers have been used in air, that is, not immersed in oil or any other special insulator, for the reason that in this kind of work glass plates occasionally fail, and if the condenser were immersed in oil, its repair would in general be a rather tedious matter, requiring much unpleasant work and a considerable loss of time.

METHODS OF STUDY

1. *Direct photographs.*—Photographs[1] taken with a stop small enough to avoid over-exposure show the explosion to consist of two distinct parts: an inner very bright cylinder, usually from 2 to 3 cm in diameter and a little longer than the wire, and a much fainter flame, very irregular, both in shape and brightness, surrounding this cylinder. In the first paper, these parts were supposed to correspond to the limiting volume of vapor during the first and second half-oscillations of the current in the condenser circuit, but later methods of observation have shown that the flame develops chiefly after the current has ceased to flow. During the main explosion the vapor, which at first occupies a volume not much larger than the wire, expands with diminishing speed until, after two or three oscillations of the circuit, its volume becomes constant, or nearly so. It is this constant volume which is outlined by the bright inner cylinder shown by the direct photographs. In cooling, the vapor combines with the oxygen of the surrounding air, and this reaction produces the flame seen around the bright cylinder. Since the flame is caused by oxidation, it is in reality not a part of the explosion proper. A few wires have been exploded in atmospheres of hydrogen and of carbon dioxide; in these cases the bright cylinder appeared without the surrounding flame.

The fact that the bright cylinder soon attains a constant size is easy to explain and leads to a simple method of estimating the temperature. When first formed the metallic vapor must have a high pressure. As a result, it expands rapidly and the pressure falls. Equilibrium obtains only when the pressure becomes equal to that of the surrounding air, and observations described below show that this state is reached after a very few oscillations of the circuit, in something like 1/25,000 sec.

[1] *Mt. Wilson Contr.*, No. 178; *Astrophysical Journal*, 51, 40, Plate VII*d*, *e*, 1920.

The volume occupied by the metallic vapor at atmospheric pressure may be determined from a direct photograph made to a known scale. The mass of the vapor is known, for it is equal to the mass of the wire used in the explosion. From the gas equation we then have

$$T=\frac{mvp}{MR}\,, \tag{3}$$

where T is the absolute temperature, m the molecular weight, v the volume, p the pressure, M the mass, and R the gas constant. There are two unknown quantities T and m, and hence another equation is required. The equation first given by Saha, viz.,

$$\log_{10}\frac{x^2}{1-x^2}P=-\frac{5036\,I}{T}+2.5\log_{10}T-6.49\,, \tag{4}$$

will do since it involves only I, the ionization potential, and x, the percentage ionization. The ionization potential is known for most metallic elements, and x is just what is required to compute the molecular weight of the vapor. At high temperatures metallic vapors are monatomic, and, consequently, if A is the atomic weight, the mean molecular weight m is given by

$$m=\frac{A}{1+x}\,. \tag{5}$$

With $p=1$, and I equal to the ionization potential of the metal studied, a curve is drawn giving x as a function of T on the basis of equation (4). A value of T is found from equation (3) by inserting the observed value of v, and taking $m=A$. In general, this value of T will be much too high, but from the curve the corresponding value of x is read off, which, inserted in m, gives a first approximation to the molecular weight. A new value of T is then found from (3), which gives a second value of x, and hence by (5) a second approximation to m, and so on, until the correct value is found. The process converges quite rapidly, but in case the first value of x is 0.5 or larger, the process can be much shortened by arbitrarily using one-half of this value in computing the first approximation to m.

The value of T found by this process probably represents the average temperature of the vapor when the pressure has reached that

of the surrounding atmosphere. This will be considerably lower than the highest temperature attained. There is every reason for believing that the maximum temperature is reached near the middle of the first half-oscillation of the circuit, because at this time the current has its greatest value, and the radiating surface of the mass of vapor is very much smaller than at later stages. Further, the photographs discussed in the following section show that the brightness is greatest during the first half-cycle. Still, for comparing explosions of different substances, or of the same substance produced under different conditions, this method of determining T should prove of value.

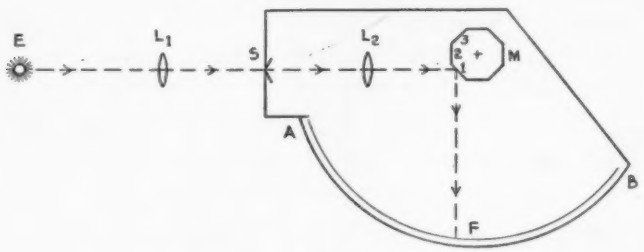

FIG. 1

2. *Rotating-mirror camera.*—The essential features of this apparatus may be seen in Figure 1. E is the source (spark, explosion, etc.) to be studied. The lens L_1 forms an image of E on the slit S, which is perpendicular to the plane of the paper. L_2 forms an image of S on the photographic film F after reflection from one of the faces of the mirror M. When M is rotated, this image moves along the film from A to B. The arc AB is one-fourth of a circle, and, as the mirror has eight faces, it follows that when the slit image reflected from face 1 is just leaving the film at B, the image reflected from face 2 is just entering the film at A. Consequently, if the phenomenon at E does not last longer than the time required for the slit image to move from A to B, it must necessarily be recorded on the film, and by varying the speed of rotation of the mirror this condition can always be satisfied.

The distance from M to F is 25 cm. Hence, if M makes 150 revolutions per second, the linear speed of the slit image along F is $25\times 2\pi\times 300=47{,}250$ cm per second, which is sufficient for a study

PLATE X

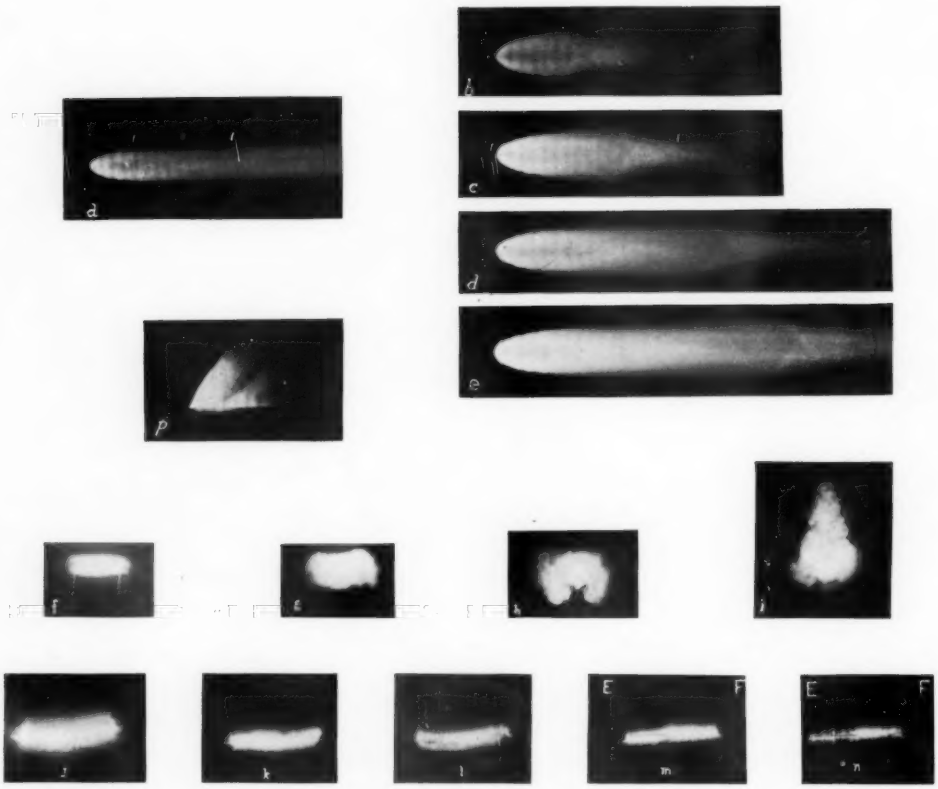

PHOTOGRAPHS OF IRON WIRE EXPLOSIONS

Rotating-mirror camera: *a*, open air explosion, end on; *p*, confined explosion, end on; *b*, *c*, *d*, *e*, photographs showing passage of sound pulses through iron vapor.

Direct photographs of explosions: *f*, *g*, *h*, *i*, with optical focal-plane shutter; *j*, *k*, *l*, *m*, *n*, magneto-optic shutter.

of sparks in circuits whose frequency does not exceed one million cycles.

A photograph of the explosion of an iron wire taken with this camera is reproduced in Plate X*a*. The frequency of the circuit was eighty-seven thousand cycles, so that the time interval between the bright bands which are faintly visible near the left end of the picture was 5.7×10^{-6} sec. The slit was 1/50 mm in width, and its image moved from left to right. The beginning of the explosion is therefore at the left.

3. *Rotating-mirror spectrograph.*—The apparatus has been described by one of us.[1] The work done with the instrument shows that throughout at least the first half-cycle the spectrum of the explosion is continuous, and, consequently, that the vapor radiates essentially like a black body. Beginning with the second cycle, the continuous spectrum weakens rapidly and is replaced by a spectrum of bright lines similar to that of an arc.

4. *Velocity-of-sound method.*—This simple application of the rotating-mirror camera furnishes valuable information about the temperature, especially during the later stages when the vapor no longer radiates as a black body, and when, in consequence, it is impossible to make temperature determinations by radiation methods.

The explosion *E* (Fig. 1) is projected on the slit *S* end-on. A sound pulse is made to traverse the explosion in a direction parallel to that of the slit, that is, at right angles to the plane of the paper. If the sound pulse is a compression, the temperature within it will be somewhat higher than outside, and since it travels parallel to the slit, its trace on the photographic film will be a bright line inclined at some angle to the direction of travel of the slit image. The sound pulse utilized is that produced in the air by the rapid initial expansion of the explosion vapor. Two concave cylindrical mirrors are placed one on each side of the wire to reflect the sound pulse back to the explosion. In Figure 1, one of these mirrors would be directly above the plane of the paper at *E*, the other directly below. If their distances from the wire are exactly equal, the two reflected pulses will arrive simultaneously, and the two traces on the photo-

[1] Sinclair Smith, *Mt. Wilson Contr.*, No. 285; *Astrophysical Journal*, **61**, 186, 1925.

graphic film will cross at the center of the slit image. Several photographs of this sort are reproduced in Plate X*b*, *c*, *d*, *e*.

The velocity of sound (V) in the vapor is readily determined by measuring the angle (θ) between the two traces, the ratio (M) of the size of an object at E to its image on the film F, and the linear speed (V_0) of the slit image on F. In the diagram (Fig. 2), let AB and CD be the two traces on the photograph. The sound wave travels the distance $M \times AP$ while the slit image moves from P to O. Hence $M \times AP = Vt$; $PO = V_0 t$; therefore

$$\left.\begin{aligned} &\frac{AP}{PO} = \tan\frac{\theta}{2} = \frac{V}{MV_0}\,; \\ \text{or} \qquad &V = MV_0 \tan\frac{\theta}{2}\,. \end{aligned}\right\} \tag{6}$$

The velocity of sound in a gas is given by

$$V = \sqrt{\frac{\gamma RT}{m}}\,, \tag{7}$$

where γ is the ratio of the specific heats, and may be taken as 1.66 for all monatomic gases such as the metallic vapors at high temperatures. R is the gas constant 8.316×10^7, T is the absolute temperature, and m the molecular weight. Hence, when V has been determined by observation, equation (7) gives the ratio T/m, and consequently T, since m may be found by the method discussed in connection with equations (4) and (5). This value of T is the actual average temperature of the vapor at the moment when it is traversed by the sound pulse. By changing the distance between the wire and the cylindrical mirrors, the time interval between the beginning of the explosion and the moment at which the temperature is determined may be varied through a considerable range. It has been found that very good traces are obtained when the mirrors are from 3 to 7 cm from the wire. Since the radius of the cylinder of vapor is of the order of 1.5 cm, this gives from 3 to 11 cm for the length of path traveled by the sound pulse in air before it enters the hot vapor. The corresponding times measured from the beginning of the explosion are about 1/11,000 to 1/3000 sec. Fair traces are recorded when the

mirrors are placed 2.5 cm from the wire, giving a path of 2 cm and an interval of about 1/17,000 sec. With the mirrors at 2 cm the traces are poorly defined and very difficult to measure. Probably this indicates that at such an early stage (less than 1/30,000 sec. from the beginning of the explosion) the vapor is not very transparent. Figure 3 will make this clear.

Let E represent the vapor cylinder of the explosion, R one of the reflectors, and ABC the sound wave passing through E in the direction given by the arrows. The projecting lens and slit are at L and S. The surface ABC is at a slightly higher temperature than the surrounding vapors of E, and, if

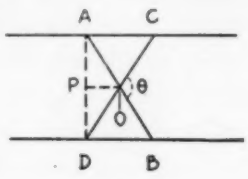

FIG. 2

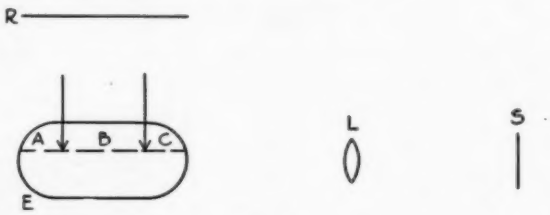

FIG. 3

these are fairly transparent, light from all points of ABC will reach the slit S. If, however, the body of E is only partially transparent, the lens L will receive light from only a short distance within the vapor. Now in the neighborhood of C the temperature is not uniform, and, consequently, the sound pulse will travel with a lower velocity near the boundary than inside. The result will be a poorly defined image of the sound pulse, just as is observed when the mirrors are placed less than 2.5 cm from the wire.

Table II gives the results of one series of measures made on explosions of iron wires.

5. *Optical focal-plane shutter.*[1]—The rotating-mirror camera records only what happens in some one plane passed through the

[1] The absence of literature references does not mean that we regard any of the devices described in this paper as new. The principles are all well known, and they have been frequently applied in the construction of apparatus by research workers everywhere.

source E, and it is often desirable to know just what the source as a whole looks like at any instant. It is certain that great changes take place in the explosion in 10^{-5} sec., and, at the beginning, in even much shorter time. Consequently, a camera is required which will take a picture of the source in something like 10^{-6} sec. Still better would be a motion-picture camera taking pictures with this exposure at the rate of say 500,000 per second. While neither of these requirements has been satisfied, a first step has been taken with the optical focal-plane shutter, and with the magneto-optic shutter described in the next section.

The optical focal-plane shutter, which is an adaptation of the rotating-mirror camera, is shown diagrammatically in Figure 4. A lens forms a small image of the source in the widely opened slit at

TABLE II

Distance from Wire to Mirrors in Centimeters	Inclination of Trace $=\theta/2$	Percentage Ion. x	Temp. (Ion. Pot. Assumed = 7 V.)
3	66°0	40	8800° K
4	62.8	20	7650
5	61.7	14	7260
6	60.4	9	6880
7	59.35	6	6410

I. The lens L_2 focuses this image after reflection from face 1 of the mirror M at some point on the circular arc FF ordinarily occupied by the photographic film. As M rotates, this image travels along FF. At m is placed a small plane mirror which reflects the light to face 2 of the rotating mirror. The length of m in the direction perpendicular to the plane of the paper is equal to the length of M in the same direction, while in the direction of travel of the image it is usually diaphragmed down to 1 mm or less as may be desired. The light, after reflection from M_2, passes through the lens L_3, which brings it to a focus on a photographic plate at P. Since the angular speed of M_2 is just one-half the angular speed of the light beam from m, it follows that the image at P is stationary. When M is rotating, the appearance on a ground-glass at P when the image of m sweeps by is precisely the same as that seen on the ground-glass of a camera fitted with a focal-plane shutter when the slot passes by. Hence, the name

"optical focal-plane shutter" is suggested for this device. It has, of course, all the faults of the ordinary shutter of this type. If, for example, the image I is wide compared to the width of m, and is changing very rapidly in position or shape, there is a certain amount of distortion of the picture produced at P. As far as speed is concerned, however, this device is much superior to the mechanical shutter. The linear speed of the latter does not often exceed 10 m per second, while in the present camera we have used 500 m per second regularly, and this can easily be increased.

In photographing the explosions, the image I, formed by a good lens, was about one-fifth of the natural size. Hence, the diameter of

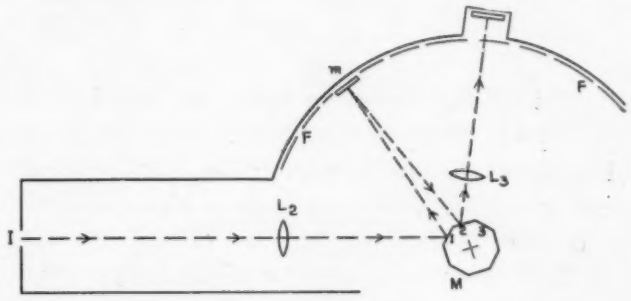

FIG. 4

the bright cylinder at I measured about 5 mm. The image at m was of the same size as at I, while at P it was reduced in the ratio 7:5. The actual exposure time is that required for any point of the image to move across m; and, as this was 1 mm in width, it follows that a given point on the plate was illuminated for 1/500,000 sec. This always resulted in over-exposure for the bright cylinder, but was about right for the flame. The time required for the whole image to be impressed on the plate P is, of course, the time required for the image to move across m, and thus depends on the size of this image. In our case this time was about 1/100,000 sec.

Unfortunately, there is no way of synchronizing the explosion and the rotation of the mirror. Consequently, the beginning of the explosion may fall at any point along the arc FF, while only that stage is recorded which happens to fall on the small mirror m. Many photographs must therefore be taken in order to show all stages in

the development of the phenomenon. In Plate X*f*, *g*, *h*, *i*, are reproduced four photographs out of a series of seventy-five taken with this camera; *f* shows the explosion in a very early stage when the cylinder of vapor is expanding very rapidly. In Plate X*g* it has reached its normal size, corresponding approximately to atmospheric pressure; *h* is somewhat later, while *i* shows the flame produced by the oxidation of the iron vapor.

If, in Figure 4, a second mirror like *m* were placed quite near to *m*, but so adjusted as to reflect the light to face 3 instead of to face 2,

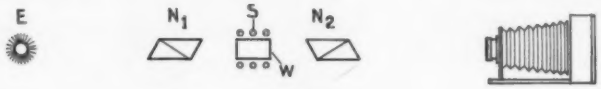

FIG. 5

and if the light so reflected were received by a second lens and plate like L_3 and P, properly placed, we should have an arrangement which would always take two photographs in quick succession. Indeed, the time interval separating them would be equal to the time required for the mirror M to turn through one-half the angle subtended by the two mirrors *m* as seen from M, and this could be made very short indeed. In general, it will be clear that if the mirror M has n faces, one could employ $(n/4)^2$ mirrors like *m*, and hence obtain $(n/4)^2$ photographs at perfectly arbitrary time intervals. With $n = 16$, this would give a series of sixteen pictures showing sixteen successive stages of the explosion.

6. *Magneto-optic shutter.*—This device utilizes the magnetic rotation of the plane of polarization by a liquid such as water. A water-cell W (Fig. 5) is placed between crossed nicols N_1 and N_2 directly in front of the camera C, suitable diaphragms being placed so that no light can enter the camera except that which has passed through the water cell. A few turns of wire, S, connected directly in the discharge circuit, are wound about W. The number of turns is so chosen that the plane of polarization for the average wave-length of photographic light is rotated some 10°–20° when the current has its first maximum value, and sufficient resistance is inserted in the circuit to make sure that the current in the second half-cycle will not "open" the shutter appreciably. Consequently, the photograph shows the explosion as

it appears during the middle of the first half-cycle. One might therefore conclude that the method has no flexibility but must always show only one phase of the explosion. This is not the case, for, by varying the current and, simultaneously, the number of turns in the coil *S*, the shutter-opening can be maintained sensibly constant while the phase of the explosion may be varied through a considerable range. For example, let the current be chosen so that the vaporization of the wire is completed just before the maximum value is reached; then if enough turns of wire have been placed around the water-cell to open the shutter the required amount, a photograph will be obtained showing a very early phase of the explosion. On the other hand, if the maximum possible current is used with say only one turn of wire in *S*, the vaporization of the wire will have been completed long before the shutter opens, and hence a relatively late phase will be recorded.

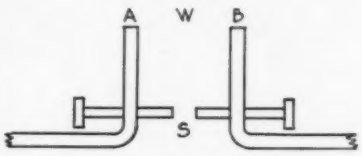

FIG. 6

Five photographs selected from a large number taken with this shutter are reproduced in Plate X *j*, *k*, *l*, *m*, *n*. These were made with condenser 3 operated at a frequency of approximately one hundred thousand cycles. The coil *S* had ten turns of wire, and was not changed during the experiments. Some variation was produced by changing the current: the voltage of the condenser was varied from 40 to about 18 kv. In Plate X, *j*, *k*, and *l* show explosions of nickel wires with voltages of 40, 30, and 22 kv, respectively. In Plate X, *m* and *n* were taken with thin aluminum ribbons so placed that approximately half of the ribbon presented the flat face to the camera, the other half the edge. These are marked *f* and *e*. The peculiarities exhibited by these photographs will be considered in the discussion.

7. *Parallel spark-gap.*—This method enables us to photograph a very early stage of the explosion of all metals tried except tungsten. As seen in Figure 6, a spark-gap *S* is connected in parallel with the wire *W* and as close to the latter as possible. At the beginning of the discharge the current flows only through the conducting path *AWB*,

and it continues to do so until the voltage drop across AB becomes greater than the potential difference required to break down the gap S, after which it flows through S. If S is made very short, this will in general happen before the wire is vaporized; but by a proper adjustment of the spark-gap one can always insure that the wire is completely vaporized before the change of path takes place. A photograph of AB shows in this case the early stage, plus the flame resulting from oxidation, if the experiment is performed in air. The flame can be largely suppressed, however, by the expedient of taking the picture with a heavily silvered quartz lens. This transmits only the 3150 A region of the spectrum, in which the flame is rather weak. Plate XI*s*, *t*, shows two photographs made with this arrangement.

By projecting both the wire and the spark-gap simultaneously on the slit of the rotating-mirror camera, a photograph is obtained which shows clearly that the current jumps suddenly from the wire to the gap and stays there during the remainder of the discharge. Such a photograph, taken when W was an aluminum wire and the spark-gap had a length of 12 mm, is reproduced in Plate XI*o*. When a tungsten wire is used, the current does not pass wholly to the spark-gap, but divides, part going each way.

This method is interesting and very easy to apply. It has the disadvantage that it always shows the same very early phase of the explosion. Just why it works with most metals and cannot be made to work with tungsten is a problem which thus far has not been entirely solved.

8. *Miscellaneous studies.*—If the wire is placed in a slot 3 or 4 mm wide, 2 cm deep, and a little longer than the wire itself, the explosion differs very materially from one taken in the open air. Plate X*p* shows a photograph of such an explosion made with the rotating-mirror camera (cf. this with the open-air explosion shown in Plate X*a*). The luminosity of the vapor lasts only through the first three or three and one-half cycles, and the flame, as well as the long tail following the oscillations in the open-air exposition, is completely suppressed. The rotating-mirror spectrograph shows[1] that the spectrum remains continuous during the whole time. This will be called the

[1] *Mt. Wilson Contr.*, No. 285; *Astrophysical Journal*, **61**, 191–193, and Plate VIII*c*, 1925.

PLATE XI

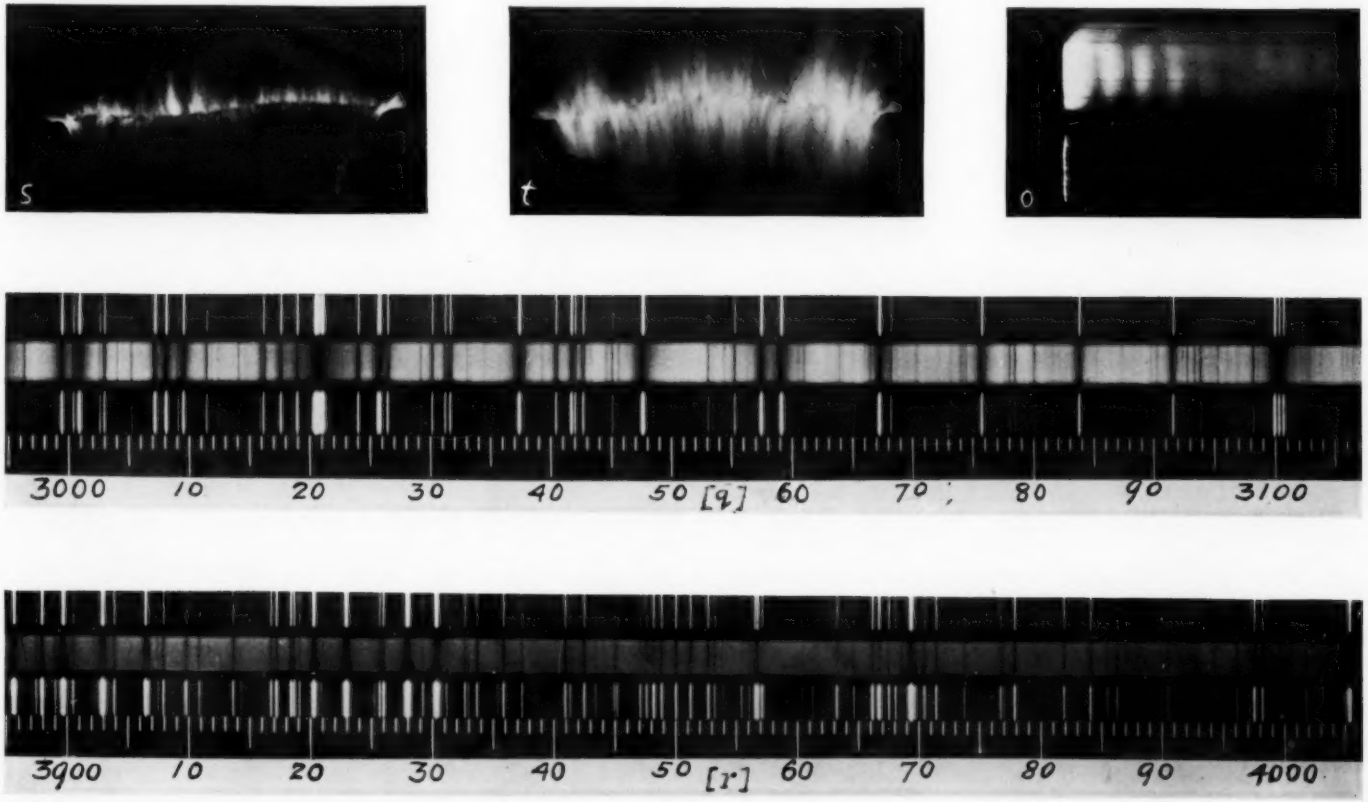

PHOTOGRAPHS OF WIRE EXPLOSIONS

o, Rotating-mirror camera, with parallel spark-gap, spark-gap above; *s*, *t*, direct photographs through silvered quartz lens, with parallel spark-gap; *q*, *r*, sections of iron spectrum, confined explosion in middle, iron-arc comparison outside.

"confined explosion" to distinguish it from the ordinary or "open-air" explosion. It has been used in most of the spectroscopic studies because all the arc lines and many spark lines appear in absorption. The spectrum of iron was photographed in the first and second orders of a 15-ft. concave grating, and a map extending from 2600 to 6600 A has been prepared from these plates. Plate XI*q*, *r*, shows two sections of this map, which give a good idea of the richness of the spectrum and the character of the lines.

Energy curves of the confined explosion of iron have been determined by employing a vacuum thermocouple mounted so that it could be moved along the focal curve of a small quartz spectrograph. Ample deflections were obtained throughout the range 0.2–3μ. Such a curve is not easy to interpret, since the radiation is integrated over the whole duration of the explosion, and in this time the temperature varies enormously. When reduced to a normal spectrum, so that the ordinates are proportional to E_λ, the maximum ordinate was found near 2650 A, with a second maximum of very nearly the same value at 2100 A. Throughout the ultra-violet region, low values of E_λ were always found roughly to correspond to the larger groups of strong iron absorption lines.

Spectrograms of open-air explosions, which have been obtained for most of the metals, are difficult to interpret, because they are composite pictures of a number of different phenomena. During the first cycle the spectrum is mainly continuous with absorption lines. Beginning with the second cycle, the continuous spectrum decreases rapidly in intensity, and bright lines make their appearance, the spark lines showing first. Very soon the whole arc spectrum appears in emission, the low-temperature lines being strongly reversed. The flame which follows probably affects the integrated spectrum very little, owing to its inferior intensity. The spectrogram consequently shows a strong continuous background with the low-temperature arc lines appearing as rather narrow absorption lines; the spark lines and some high-temperature arc lines show bright, while lines of intermediate temperature classes may be practically absent. The appearance varies in different parts of the spectrum. In the ultra-violet, where reversals are relatively easy to obtain, many spark and most of the arc lines appear dark. In the visible portion most spark lines

are bright and only the low-temperature arc lines appear in absorption. Near the red end of the spectrum dark lines are not frequently observed.

It is useless to attempt to draw conclusions from the study of an integrated spectrum such as this. Consider for a moment the photographs shown in Plate X*b*, *c*, *d*, *e*. It will be observed that the passage of the sound wave through the vapor very soon quenches the luminosity of that stage which follows the oscillations and which has been referred to above as the "tail." Now this stage emits bright lines (the arc spectrum) with little or no continuous spectrum. Hence, by arranging two reflectors near the explosion, one can gradually remove from the integrated spectrum all the bright-line emission by merely moving the reflectors closer to the wire, without changing in any way the discharge conditions in the circuit. In fact, all stages between the open-air and the confined explosion can be produced in this way.

A somewhat more interesting series of changes can be produced by introducing self-induction into the circuit when studying open-air explosions. With a fair amount of inductance the continuous spectrum is suppressed entirely, and the spectrum approximates very closely a normal arc spectrum. Reducing the amount of inductance causes the spectrum to change gradually into that of the open-air explosion. In this case, the circuit conditions are changed. The current intensity, and hence the temperature, increases as the inductance is decreased.

Since the confined explosion has a continuous spectrum, it follows that the vapor should be opaque to radiation, unless the spectrum is due to minute solid or liquid particles, as is the case in the flame of a candle. It does not seem likely that the light of the confined explosion can come from solid or liquid particles, for its maximum brightness is equal to that of a black body at a temperature of about 20,000° C. The temperature of the supposed particles would have to be at least this high, and this is obviously impossible. The following experiment was tried, however, to test the point in question. An iron wire was used for the explosion. Close to the wire, but between it and the slit of the spectrograph, was placed a spark-gap with zinc terminals. This gap was connected in series with the

wire so that the spark would be exactly simultaneous with the explosion. In a second experiment the arrangement was similar, except that the spark-gap was placed behind the explosion, so that the light from the spark passed through the iron vapor of the explosion on its way to the spectrograph. The exposures were made just sufficient to show the continuous spectrum of the explosion clearly. In the first experiment the bright zinc spark lines were very prominent on the weak continuous spectrum, while in the second no trace of any bright lines could be seen. It was estimated that if 5 per cent of the light from the spark had been transmitted, the strongest zinc lines should have been visible on the spectrogram. It follows that the layer of iron vapor 5 cm in thickness transmitted less than 5 per cent of the light. This gives an absorption coefficient per centimeter of at least 0.6, or a mass absorption coefficient of about 2000, if we take the average density of the iron vapor as 3×10^{-4}. At 20,000° C. this corresponds to a pressure of about 10 atmospheres. The average density is certainly no higher than this, for the zinc lines reach their greatest brightness in the second, third, and fourth half-cycles, and it is only during the first half-cycle that the pressure can exceed 10 atmospheres.

DISCUSSION

The following is a general description of what probably takes place during an explosion:

1. The wire is heated, melted, and vaporized while the current through it increases from zero to a few thousand amperes. This part of the process may be followed quite easily by numerical calculation, for all the constants are fairly well known. Such a computation for condenser 2, with an iron wire weighing 1 mg, is plotted as a time-temperature curve in Figure 7. It shows that the wire was completely vaporized 6.4×10^{-7} sec. after the beginning of the discharge. The current at this instant was 3,900 amp. Vaporization began at 4.5×10^{-7} sec., when the current was 2,800 amp. The maximum possible diameter[1] of the cylinder of vapor at 6.4×10^{-7} sec. may be found by assuming that the vapor moved outward during the vapor-

[1] It is here assumed that the evaporated particles are neutral atoms or molecules leaving the surface with the average velocity of molecular motion due to temperature. It appears from the photographs discussed in section 4 that in reality the phenome-

ization with the molecular velocity of iron at 2690° C., the boiling-point of iron. This diameter comes out 0.3 mm, and hence the pressure of the vapor would be high—in round numbers, 500 atmospheres. Beyond this point calculation fails, for the conductivity of iron vapor is not known.

2. Shortly after the wire has been completely vaporized the resistance is probably high, especially for metals which vaporize below 3000° C. This is indicated by the fact that the method of the

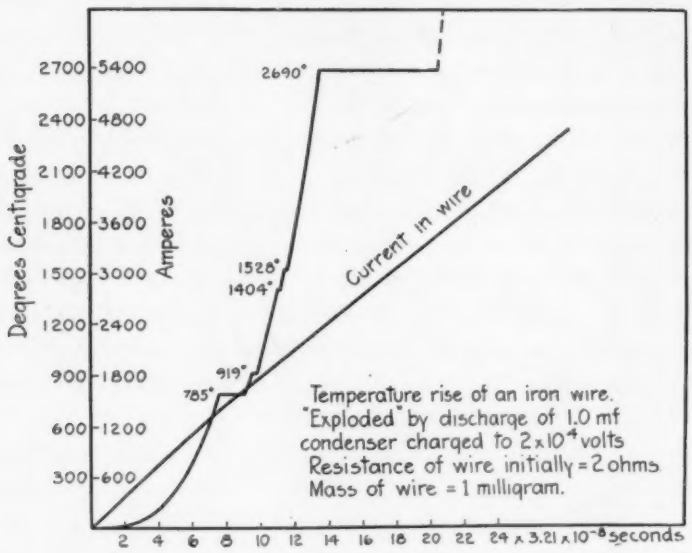

FIG. 7

parallel spark-gap works for just these metals. Tungsten, for which that method fails, is probably not completely vaporized until the temperature is well above 5000° C., and at such a high temperature it is probable that the ionization is appreciable, and, hence, that the conductivity is sufficient for the current to flow in spite of the parallel spark-gap.

For most metals, then, the voltage rises sharply immediately

---

non is not so simple as this. The particles forming the "jets" shown on the photographs escape from the wire with velocities up to 2 km per second. Consequently, the cylinder has at first no such regular boundary as assumed in the test, and the pressure is undoubtedly lower than the computed value.

after vaporization is complete. This means a very rapid rise in temperature, since the current is large, and, until the ionization becomes appreciable, the resistance is high. Ionization becomes important when the temperature reaches 10,000° C. From this point on, the resistance diminishes rapidly on account of increasing ionization due to both rising temperature and falling pressure caused by the rapid expansion.

The maximum temperature will be reached when the energy lost by radiation from the surface of the vapor is just equal to the input i^2r. Unfortunately, the resistance r is unknown. It is quite certain, however, that a temperature of at least 20,000° C. is reached toward the end of the first quarter-cycle. The radiating area of the vapor may be measured from photographs taken with the rotating-mirror camera, the current is known, and consequently a value of the apparent resistance at this stage can be calculated. The result is in the neighborhood of 0.2 ohm. This includes, of course, the effect of the potential drop at the cold electrodes, which may be appreciable.

3. After the first quarter-cycle, the phenomena may be readily followed with the aid of the rotating-mirror camera. The temperature oscillates, but its trend is steadily downward. The pressure decreases and becomes sensibly equal to that of the surrounding air at the end of the second cycle. (A frequency of 10^5 cycles is assumed.)

4. The photographs reproduced in Plate X*j*, *k*, *l*, *m*, *n*, showing the earliest stages of explosions, are somewhat surprising, and suggest that the vaporization of the wire is not such a simple process as was assumed above. Instead of small smooth cylinders, these photographs show a complicated structure consisting chiefly of streamers issuing from the wire.

Two interpretations of the appearance suggest themselves at once: (*a*) that we have to do with a brush discharge from the wire to the air around it; (*b*) that the vapor escapes from the wire in the form of jets irregularly distributed over its surface. Photographs reproduced in Plate X*m* and *n* show quite clearly that we are not dealing with a brush discharge, for the apparent jets all originate on the flat surface of the ribbons, the edge being quite free from any appearance of a discharge. If it were a brush discharge, practically all

the brushes would spring from the edge, and few, if any, from the flat sides. Hence we must conclude that these are real jets of vapor issuing from the wire. A study of all the photographs taken with the magneto-optic shutter shows that the jets appear first at the places where the magnetic field produced by the current in the wire is weakest, for example, on the flat face of a ribbon, or around the outside angle of a wire bent sharply, etc. The intensity of the magnetic field at the surface of a wire when vaporization begins is generally from 10^5 to 10^6 gausses. It is easy to see that a charged particle would have some difficulty in escaping from the wire against such a field, but it could have no effect on a neutral atom. These photographs therefore indicate that the particles evaporating from an electrically heated wire at high temperatures are charged when they leave the wire.

MOUNT WILSON OBSERVATORY
September 1926

A METHOD FOR CHECKING MEASUREMENTS OF SPECTRAL LINES

By C. RUNGE

ABSTRACT

The *method* is an extension of the way in which *equidistant ordinates* are treated by the calculus of differences. In order to detect an irregularity among equidistant ordinates it is the custom to form the first and second differences. The smooth run of the second differences then guarantees a smooth run of the ordinates, while an irregularity in the ordinates causes a relatively large irregularity in the second differences.

With ordinates that are not equidistant, the method must be modified. The differences must be divided by the differences of the corresponding abscissae, and the quotients must be associated with the mean of the abscissae. The same operation is then repeated with these values. With certain corrections of the abscissae the second set is then plotted and serves the same purpose as the second differences in the calculus of differences. Reversing operations, the method can also be used for interpolation.

Let x_ν, y_ν $(\nu = 1, 2, \ldots . n)$ denote the co-ordinates of a number of consecutive points of a curve. Let x_ν, for instance, designate the measurements along a spectroscopic plate and y_ν the wave-lengths of the corresponding lines, and let us assume that the curve can with sufficient accuracy be represented by an equation of the form

$$y = a + b(x - x_0) + c(x - x_0)^2 + d(x - x_0)^3 , \qquad (1)$$

x_0 designating an intermediate abscissa. We now divide the differences $y_{\nu+1} - y_\nu$ by $x_{\nu+1} - x_\nu$ and associate the quotient with the mean of x_ν and $x_{\nu+1}$. Let us write

$$\bar{y}_\nu = \frac{y_{\nu+1} - y_\nu}{x_{\nu+1} - x_\nu} , \quad \bar{x}_\nu = \frac{x_{\nu+1} + x_\nu}{2} .$$

From equation (1) it follows that

$$\bar{y}_\nu = b + 2c(\bar{x}_\nu - x_0) + 3d(\bar{x}_\nu - x_0)^2 + \frac{d}{4}(x_{\nu+1} - x_\nu)^2 , \qquad (2)$$

or

$$\bar{y}_\nu = \left(\frac{dy}{dx}\right)_\nu + \frac{d}{4}(x_{\nu+1} - x_\nu)^2 , \qquad (2a)$$

$\left(\frac{dy}{dx}\right)_\nu$ designating the value of $\frac{dy}{dx}$ for $x = \bar{x}_\nu$. From this equation it

is evident that for an irregular distribution of the abscissae the points $\bar{x}_\nu$, $\bar{y}_\nu$ must deviate irregularly from a parabola.

Let us now repeat the same operation and write

$$\bar{\bar{y}}_\nu = \frac{\bar{y}_{\nu+1} - \bar{y}_\nu}{\bar{x}_{\nu+1} - \bar{x}_\nu}, \quad \bar{\bar{x}}_\nu = \frac{\bar{x}_{\nu+1} + \bar{x}_\nu}{2}.$$

Then we obtain from equation (2)

$$\bar{\bar{y}}_\nu = 2c + 6d(\bar{\bar{x}}_\nu - x_0) + \frac{d}{2}\Delta^2 x_\nu, \tag{3}$$

$\Delta^2 x_\nu$ being written for $(x_{\nu+2} - x_{\nu+1}) - (x_{\nu+1} - x_\nu)$, or

$$\bar{\bar{y}}_\nu = 2c + 6d\left(\bar{\bar{x}}_\nu + \frac{\Delta^2 x_\nu}{12} - x_0\right). \tag{3a}$$

That is to say, the points

$$\text{Abscissa} = \bar{\bar{x}}_\nu + \frac{\Delta^2 x_\nu}{12}; \quad \text{Ordinate} = \bar{\bar{y}}_\nu$$

must lie in a straight line. Deviations from a straight line indicate inaccuracies in the points x_ν, y_ν.

Equation (3a) may also be written

$$\bar{\bar{y}}_\nu = \left(\frac{d^2 y}{dx^2}\right)_\nu,$$

the differential coefficient being calculated for $x = \bar{\bar{x}}_\nu + \frac{\Delta^2 x_\nu}{12}$.

Assuming that in equation (1) the term $d(x - x_0)^3$ is small in comparison to $c(x - x_0)^2$, $d(x - x_0)$ will be small in comparison with c. Therefore, in equation (3a), $\bar{\bar{y}}_\nu$ will not differ much from $2c$ relatively, so that we can plot $\bar{\bar{y}}_\nu$ in a large scale to a moderate scale of $\bar{\bar{x}}_\nu + \frac{\Delta^2 x_\nu}{12}$ and thus detect even small errors of $\bar{\bar{y}}_\nu$.

As an example I will consider measurements made by St. John and Miss Ware on a plate taken with a plane grating mounted in the Littrow fashion and given explicitly in their admirable paper, "Ter-

tiary Standards with the Plane Grating," *Astrophysical Journal*, **36**, 23, 1912.

They compare the "International Secondary Standards" with "Kayser's Adjusted Values" and find that the latter are less accurate. Their data are contained in Table I.

TABLE I

ν	$x_{\nu+1}-x_\nu$	Int. Standards	Kayser's Values
1	45.7586	6191.568	6191.568
2	40.2802	6230.734	6230.734
3	62.0582	6265.145	6265.145
4	20.3567	6318.028	6318.031
5	68.6640	6335.341	6335.339
6	44.0138	6393.612	6393.612
7	76.0395	6430.859	6430.848
8	.....	6494.993	6494.994

From these data we calculate (Table II):

TABLE II

ν	$\bar{y}_\nu$ Int. St.	$\bar{y}_\nu$ Kayser	$\bar{y}_{\nu+1}-\bar{y}_\nu$ Int. St.	$\bar{y}_{\nu+1}-\bar{y}_\nu$ Kayser	$\bar{x}_{\nu+1}-\bar{x}_\nu$
1	0.85593	0.85593	−0.00164	−0.00164	43.0
2	.85429	.85429	.00214	.00209	51.2
3	.85215	.85220	.00167	.00196	41.2
4	.85048	.85024	.00184	.00157	44.5
5	.84864	.84867	.00238	.00266	56.3
6	.84626	.84601	−0.00283	−0.00242	60.0
7	0.84343	0.84359	.....	.....	.....

The values of $\bar{\bar{y}}_\nu$ may now be calculated with the slide-rule (Table III):

TABLE III

$\bar{\bar{y}}_\nu$ Int. St.	$\bar{\bar{y}}_\nu$ Kayser	$\bar{\bar{x}}_\nu+\frac{\Delta^2 x_\nu}{12}$
$-3.82\ 10^{-6}$	$-3.82\ 10^{-6}$	43.9
$4.18\ 10$	$4.08\ 10$	93.3
$4.05\ 10$	$4.75\ 10$	134.2
$4.14\ 10$	$3.53\ 10$	184.6
$4.23\ 10$	$4.73\ 10$	228.9
$-4.72\ 10^{-6}$	$-4.03\ 10^{-6}$	291.8

Figure 1 shows at a glance that the international standards correspond more closely to the measurements than Kayser's values.[1]

By drawing an approximate straight line as in Figure 1, we obtain an approximation for $2c+6d(x-x_0)$ and thus for c and d and for

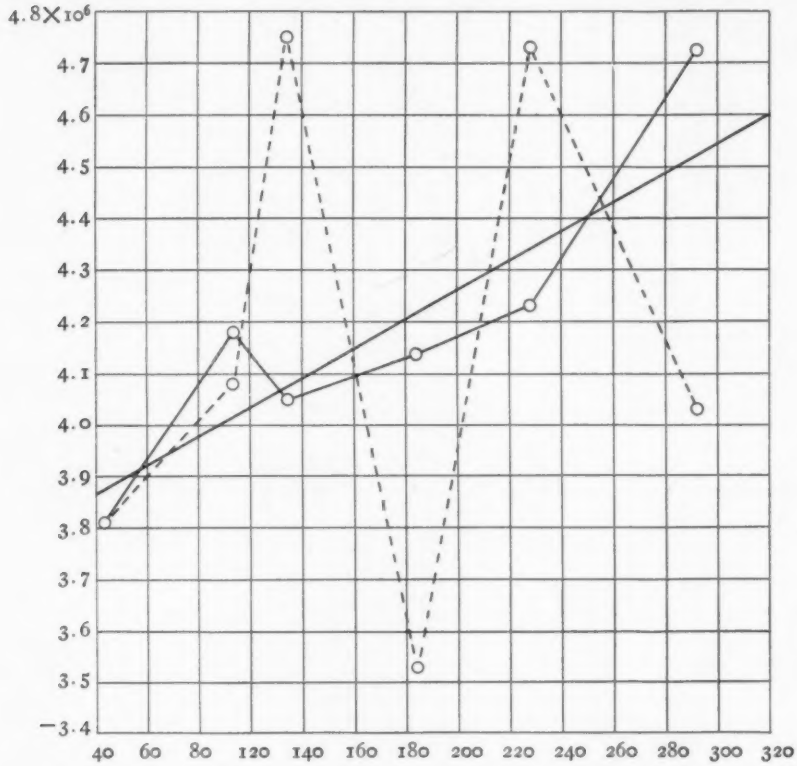

FIG. 1.—Broken line represents International Standards; dotted line, Kayser's values.

the third and fourth term of equation (1). In this way we can determine the values

$$y_\nu-[c(x_\nu-x_0)^2+d(x_\nu-x_0)]^3 ,$$

which now have to be approximated by a linear function

$$a+b(x_\nu-x_0) .$$

[1] St. John and Ware plot $\bar{y}_\nu$ as ordinates to the abscissae $\frac{y_{\nu+1}+y_\nu}{2}$ and draw a smooth curve through the points. This is not legitimate generally, although in their case the error is negligible.

A convenient way to proceed is this. We read the values of $\bar{\bar{y}}_\nu$ along the approximate straight line in Figure 1. Multiplying by $(\bar{x}_{\nu+1}-\bar{x}_\nu)$ we find $(\bar{y}_{\nu+1}-\bar{y}_\nu)$, and assuming a convenient value for $\bar{y}_1$, we calculate $\bar{y}_\nu$. Again multiplying by $(x_{\nu+1}-x_\nu)$, we obtain $(y_{\nu+1}-y_\nu)$, and assuming a convenient value for y_1, we get approximate values for y_ν. The differences between these approximate values and the observed values y_ν have finally to be corrected by a linear function

$$\alpha+\beta(x-x_0)$$

to suit the observed values as closely as possible.

We may at the same time and by the same procedure interpolate values of y for any intermediate values of x. Let us, for instance, calculate y for a value of x in the middle of the fifth interval $x_6-x_5=68.6640$, so that there are two intervals,

$$x_6-x_5=34.3320\ ; \qquad x_7-x_6=34.3320\ ,$$

to be introduced into the table instead of the interval 68.6640. We then have (Table IV):

TABLE IV

ν	$x_{\nu+1}-x_\nu$	$\Delta^2 x_\nu$	$\bar{x}_{\nu+1}-\bar{x}_\nu$	$\bar{\bar{x}}_\nu+\frac{\Delta^2 x_\nu}{12}$	$\bar{\bar{y}}_\nu 10^6$	$(\bar{y}_{\nu+1}-\bar{y}_\nu)10^6$	$\bar{y}_\nu$
1.....	45.7586	− 5.4	43.0	43.9	−3.82	−164	0.85593
2.....	40.2802	+21.8	51.2	93.3	4.04	207	.85429
3.....	62.0582	−41.7	41.2	134.2	4.14	170	.85222
4.....	20.3567	+14.0	27.3	173.2	4.24	116	.85052
5.....	34.3320	0.0	34.3	202.8	4.31	148	.84936
6.....	34.3320	+ 9.7	39.2	240.3	4.41	173	.84788
7.....	44.0138	+32.0	60.0	291.8	−4.53	−272	.84615
8.....	76.0395	.....	.....	.....	.....	.....	0.84343

So far the multiplications can be done with the slide-rule. The last step is done with the calculating machine, which gives at once x_ν and y_ν (Table V). For y_1 we have assumed the observed value and for $\bar{y}_1$ the value deduced from the first two observed values. The differences, international standards *minus* y_ν, may now be plotted to the abscissae x_ν, and a straight line approximating these

points (Fig. 2) furnishes corrections to be applied to the calculated values y_p.

TABLE V

p	x_p	y_p	Int. St.	Int. St. $-y_p$
1.....	0.0000	6191.5680	.568	.0000
2.....	45.7586	6230.7342	.734	−.0002
3.....	86.0388	6265.1451	.145	.0001
4.....	148.0970	6318.0324	.028	.0044
5.....	168.4537	6335.3462	.341	.0052
6.....	202.7857	6364.5064	.....	.....
7.....	237.1177	6393.6158	.612	−.0038
8.....	281.1315	6430.8581	.859	+.0009
9.....	357.1710	6494.9921	.993	+.0009

The final residues will not be larger than 0.003, but they cannot all be reduced to a much smaller amount, unless we should make use of a formula with more than four arbitrary constants.

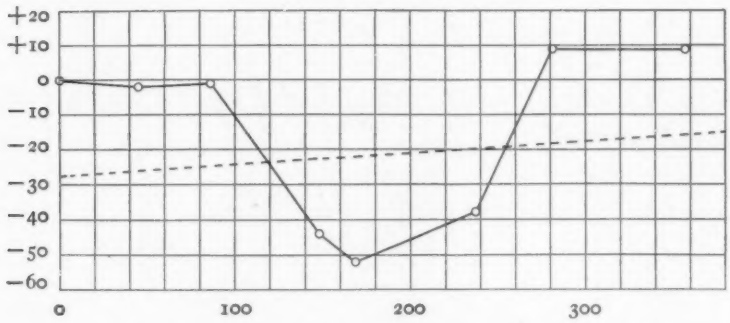

FIG. 2.—Corrections to be applied to the computed values of y_p

But when the number of constants approaches the number of observations, the conception of a smooth approximation becomes futile. In other words, it remains doubtful whether the deviations from the straight line in Figure 2 are accidental or systematic.

GÖTTINGEN
June 15, 1926

EXTRA-GALACTIC NEBULAE[1]

By EDWIN HUBBLE

ABSTRACT

This contribution gives the results of a statistical investigation of 400 extra-galactic nebulae for which Holetschek has determined total visual magnitudes. The list is complete for the brighter nebulae in the northern sky and is representative to 12.5 mag. or fainter.

The classification employed is based on the forms of the photographic images. About 3 per cent are irregular, but the remaining nebulae fall into a sequence of type forms characterized by rotational symmetry about dominating nuclei. The sequence is composed of two sections, the elliptical nebulae and the spirals, which merge into each other.

Luminosity relations.—The distribution of magnitudes appears to be uniform throughout the sequence. For each type or stage in the sequence, the total magnitudes are related to the logarithms of the maximum diameters by the formula,

$$m_T = C - 5 \log d ,$$

where C varies progressively from type to type, indicating a variation in diameter for a given magnitude or vice versa. By applying corrections to C, the nebulae can be reduced to a standard type and then a single formula expresses the relation for all nebulae from the Magellanic Clouds to the faintest that can be classified. When the minor diameter is used, the value of C is approximately constant throughout the entire sequence. The coefficient of $\log d$ corresponds with the inverse-square law, which suggests that the nebulae are all of the same order of absolute luminosity and that apparent magnitudes are measures of distance. This hypothesis is supported by similar results for the nuclear magnitudes and the magnitudes of the brightest stars involved, and by the small range in luminosities among nebulae whose distances are already known.

Distances and absolute dimensions.—The mean absolute visual magnitude, as derived from the nebulae whose distances are known, is -15.2. The statistical expression for the distance in parsecs is then

$$\log D = 4.04 + 0.2\, m_T ,$$

where m_T is the total apparent magnitude. This leads to mean values for absolute dimensions at various stages in the sequence of types. Masses appear to be of the order of 2.6×10^8 $\odot$.

Distribution and density of space.—To apparent magnitude about 16.7, corresponding to an exposure of one hour on fast plates with the 60-inch reflector, the numbers of nebulae to various limits of total magnitude vary directly with the volumes of space represented by the limits. This indicates an approximately uniform density of space, of the order of one nebula per 10^{17} cubic parsecs or 1.5×10^{-31} in C.G.S. units. The corresponding radius of curvature of the finite universe of general relativity is of the order of 2.7×10^{10} parsecs, or about 600 times the distance at which normal nebulae can be detected with the 100-inch reflector.

Recent studies have emphasized the fundamental nature of the division between galactic and extra-galactic nebulae. The relationship is not generic; it is rather that of the part to the whole. Galactic

[1] *Contributions from the Mount Wilson Observatory*, No. 324.

nebulae are clouds of dust and gas mingled with the stars of a particular stellar system; extra-galactic nebulae, at least the most conspicuous of them, are now recognized as systems complete in themselves, and often incorporate clouds of galactic nebulosity as component parts of their organization. Definite evidence as to distances and dimensions is restricted to six systems, including the Magellanic Clouds. The similar nature of the countless fainter nebulae has been inferred from the general principle of the uniformity of nature.

The extra-galactic nebulae form a homogeneous group in which numbers increase rapidly with diminishing apparent size and luminosity. Four are visible to the naked eye;[1] 41 are found on the Harvard "Sky Map";[2] 700 are on the Franklin-Adams plates;[3] 300,000 are estimated to be within the limits of an hour's exposure with the 60-inch reflector.[4] These data indicate a wide range in distance or in absolute dimensions. The present paper, to which is prefaced a general classification of nebulae, discusses such observational material as we now possess in an attempt to determine the relative importance of these two factors, distance and absolute dimensions, in their bearing on the appearance of extra-galactic nebulae.

The classification of these nebulae is based on structure, the individual members of a class differing only in apparent size and luminosity. It is found that for the nebulae in each class these characteristics are related in a manner which closely approximates the operation of the inverse-square law on comparable objects. The presumption is that dispersion in absolute dimensions is relatively unimportant, and hence that in a statistical sense the apparent dimensions represent relative distances. The relative distances can be reduced to absolute values with the aid of the nebulae whose distances are already known.

PART I. CLASSIFICATION OF NEBULAE

GENERAL CLASSIFICATION

The classification used in the present investigation is essentially the detailed formulation of a preliminary classification published in

[1] These are the two Magellanic Clouds, M 31, and M 33.

[2] Bailey, *Harvard Annals*, 60, 1908.

[3] Hardcastle, *Monthly Notices*, 74, 699, 1914.

[4] This estimate by Seares is based on a revision of Fath's counts of nebulae in Selected Areas (*Mt. Wilson Contr.*, No. 297; *Astrophysical Journal*, 62, 168, 1925).

a previous paper.[1] It was developed in 1923, from a study of photographs of several thousand nebulae, including practically all the brighter objects and a thoroughly representative collection of the fainter ones.[2] It is based primarily on the structural forms of photographic images, although the forms divide themselves naturally into two groups: those found in or near the Milky Way and those in moderate or high galactic latitudes. In so far as possible, the system is independent of the orientation of the objects in space. With minor changes in the original notation, the complete classification is as follows, although only the extra-galactic division is here discussed in detail:

CLASSIFICATION OF NEBULAE

	Symbol	Example
I. Galactic nebulae:		
A. Planetaries	P	N.G.C. 7662
B. Diffuse	D	.....
1. Predominantly luminous	DL	N.G.C. 6618
2. Predominantly obscure	DO	Barnard 92
3. Conspicuously mixed	DLO	N.G.C. 7023
II. Extra-galactic nebulae:		
A. Regular:		
1. Elliptical	E*n*	N.G.C. 3379 E0 221 E2 4621 E5 2117 E7
(n=1, 2, ... , 7 indicates the ellipticity of the image without the decimal point)		

[1] "A General Study of Diffuse Galactic Nebulae," *Mt. Wilson Contr.*, No. 241; *Astrophysical Journal*, **56**, 162, 1922.

[2] The classification was presented in the form of a memorandum to the Commission on Nebulae of the International Astronomical Union in 1923. Copies of the memorandum were distributed by the chairman to all members of the Commission. The classification was discussed at the Cambridge meeting in 1925, and has been published in an account of the meeting by Mrs. Roberts in *L'Astronomie*, **40**, 169, 1926. Further consideration of the matter was left to a subcommittee, with a resolution that the adopted system should be as purely descriptive as possible, and free from any terms suggesting order of physical development (*Transactions of the I.A.U.*, **2**, 1925). Mrs. Roberts' report also indicates the preference of the Commission for the term "extra-galactic" in place of the original, and then necessarily non-committal, "non-galactic."

Meanwhile K. Lundmark, who was present at the Cambridge meeting and has since been appointed a member of the Commission, has recently published (*Arkiv för Matematik, Astronomi och Fysik, Band 19B*, No. 8, 1926) a classification, which, except for nomenclature, is practically identical with that submitted by me. Dr. Lundmark makes no acknowledgments or references to the discussions of the Commission other than those for the use of the term "galactic."

CLASSIFICATION OF NEBULAE—*Continued*

	Symbol	Example
2. Spirals:		
a) Normal spirals	S	.....
(1) Early	Sa	N.G.C. 4594
(2) Intermediate	Sb	2841
(3) Late	Sc	5457
b) Barred spirals	SB	.....
(1) Early	SBa	N.G.C. 2859
(2) Intermediate	SBb	3351
(3) Late	SBc	7479
B. Irregular	Irr	N.G.C. 4449

Extra-galactic nebulae too faint to be classified are designated by the symbol "Q."

REGULAR NEBULAE

The characteristic feature of extra-galactic nebulae is rotational symmetry about dominating non-stellar nuclei. About 97 per cent of these nebulae are regular in the sense that they show this feature conspicuously. The regular nebulae fall into a progressive sequence ranging from globular masses of unresolved nebulosity to widely open spirals whose arms are swarming with stars. The sequence comprises two sections, elliptical nebulae and spirals, which merge into each other.

Although deliberate effort was made to find a descriptive classification which should be entirely independent of theoretical considerations, the results are almost identical with the path of development derived by Jeans[1] from purely theoretical investigations. The agreement is very suggestive in view of the wide field covered by the data, and Jeans's theory might have been used both to interpret the observations and to guide research. It should be borne in mind, however, that the basis of the classification is descriptive and entirely independent of any theory.

Elliptical nebulae.—These give images ranging from circular through flattening ellipses to a limiting lenticular figure in which the ratio of the axes is about 1 to 3 or 4. They show no evidence of resolution,[2] and the only claim to structure is that the luminosity

[1] *Problems of Cosmogony and Stellar Dynamics*, 1919.

[2] N.G.C. 4486 (M 87) may be an exception. On the best photographs made with the 100-inch reflector, numerous exceedingly faint images, apparently of stars, are found around the periphery. It was among these that Belanowsky's nova of 1919 appeared. The observations are described in *Publications of the Astronomical Society of the Pacific*, **35**, 261, 1923.

PLATE XII

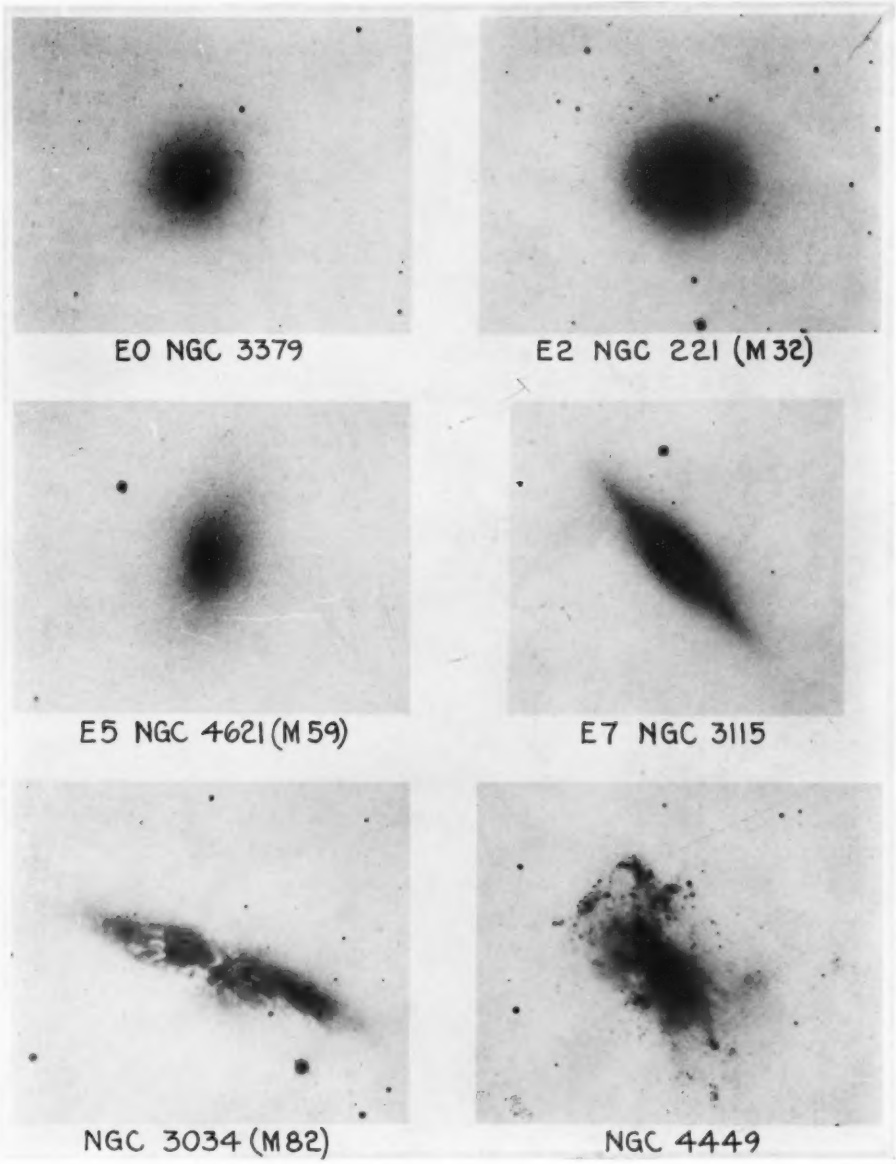

ELLIPTICAL AND IRREGULAR NEBULAE

fades smoothly from bright nuclei to indefinite edges. Diameters are functions of the nuclear brightness and the exposure times.

The only criterion available for further classification appears to be the degree of elongation. Elliptical nebulae have accordingly been designated by the symbol "E," followed by a single figure, numerically equal to the ellipticity $(a-b)/a$ with the decimal point omitted. The complete series is E0, E1, ... , E7, the last representing a definite limiting figure which marks the junction with the spirals.

The frequency distribution of ellipticities shows more round or nearly round images than can be accounted for by the random orientation of disk-shaped objects alone. It is presumed, therefore, that the images represent nebulae ranging from globular to lenticular, oriented at random. No simple method has yet been established for differentiating the actual from the projected figure of an individual object, although refined investigation furnishes a criterion in the relation between nuclear brightness and maximum diameters. For the present, however, it must be realized that any list of nebulae having a given apparent ellipticity will include a number of tilted objects having greater actual ellipticities. The statistical average will be too low, except for E7, and the error will increase with decreasing ellipticity.

Normal spirals.—All regular nebulae with ellipticities greater than about E7 are spirals, and no spirals are known with ellipticities less than this limit. At this point in the sequence, however, ellipticity becomes insensitive as a criterion and is replaced by conspicuous structural features which now become available for classification. Of these, practically speaking, there are three which fix the position of an object in the sequence of forms: (1) relative size of the unresolved nuclear region; (2) extent to which the arms are unwound; (3) degree of resolution in the arms. The form most nearly related to the elliptical nebulae has a large nuclear region similar to E7, around which are closely coiled arms of unresolved nebulosity. Then follow objects in which the arms appear to build up at the expense of the nuclear regions and unwind as they grow; in the end, the arms are wide open and the nuclei inconspicuous. Early in the series the arms begin to break up into condensations, the resolution

commencing in the outer regions and working inward until in the final stages it reaches the nucleus itself. In the larger spirals where critical observations are possible, these condensations are found to be actual stars and groups of stars.

The structural transition is so smooth and continuous that the selection of division points for further classification is rather arbitrary. The ends of the series are unmistakable, however, and, in a general way, it is possible to differentiate a middle group. These three groups are designated by the non-committal letters "a," "b," and "c" attached to the spiral symbols "S," and, with reference to their position in the sequence, are called "early," "intermediate," and "late" types.[1] A more precise subdivision, on a decimal scale for example, is not justified in the present state of our knowledge.

In the early types, the group Sa, most of the nebulosity is in the nuclear region and the arms are closely coiled and unresolved. N.G.C. 3368 and 4274 are among the latest of this group.

The intermediate group, Sb, includes objects having relatively large nuclear regions and thin rather open arms, as in M 81, or a smaller nuclear region with closely coiled arms, as in M 94. These two nebulae represent the lateral extension of the sequence in the intermediate section. The extension along the sequence is approximately represented by N.G.C. 4826, among the earliest of the Sb, and N.G.C. 3556 and 7331, which are among the latest. The resolution in the arms is seldom conspicuous, although in M 31, a typical Sb, it is very pronounced in the outer portions.

[1] "Early" and "late," in spite of their temporal connotations, appear to be the most convenient adjectives available for describing relative positions in the sequence. This sequence of structural forms is an observed phenomenon. As will be shown later in the discussion, it exhibits a smooth progression in nuclear luminosity, surface brightness, degree of flattening, major diameters, resolution, and complexity. An antithetical pair of adjectives denoting relative positions in the sequence is desirable for many reasons, but none of the progressive characteristics are well adapted for the purpose. Terms which apply to series in general are available, however, and of these "early" and "late" are the most suitable. They can be assumed to express a progression from simple to complex forms.

An accepted precedent for this usage is found in the series of stellar spectral types. There also the progression is assumed to be from the simple to the complex, and in view of the great convenience of the terms "early" and "late," the temporal connotations, after a full consideration of their possible consequences, have been deliberately disregarded.

PLATE XIII

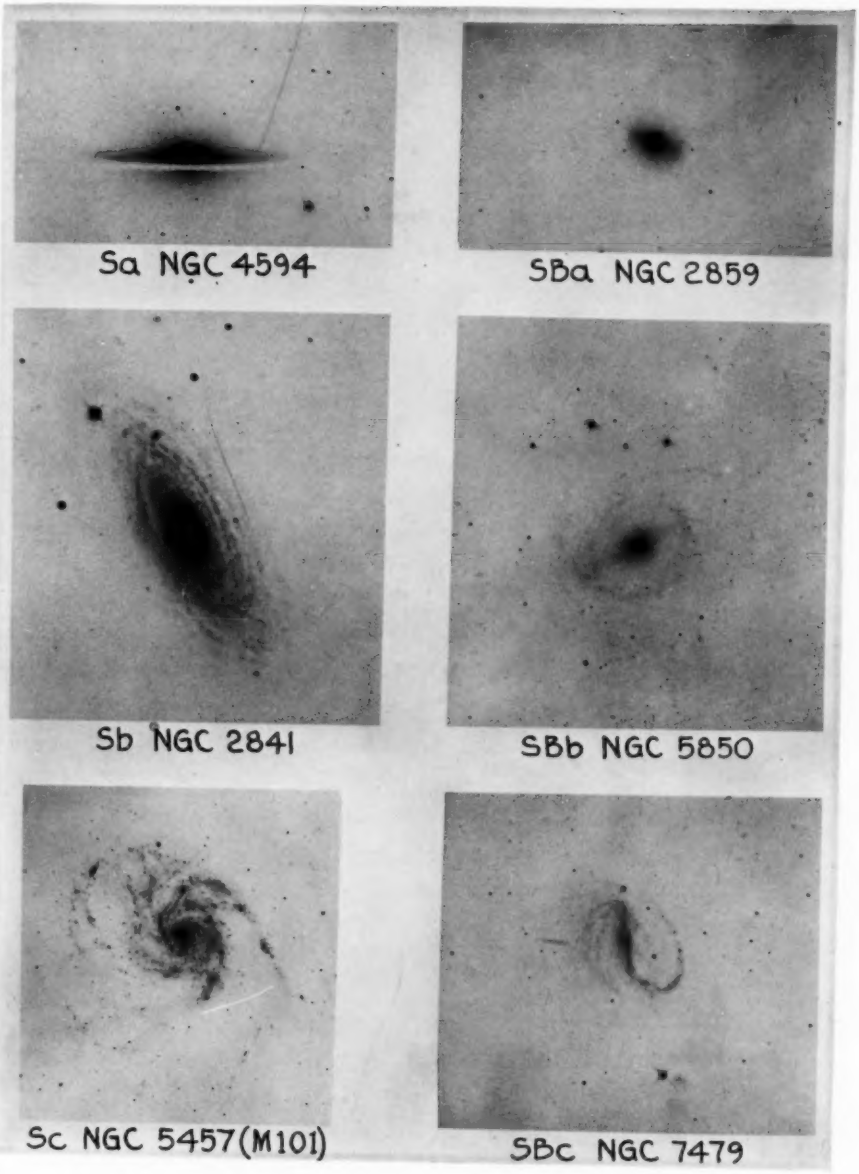

NORMAL AND BARRED SPIRALS

The characteristics of the late types, the group Sc, are more definite—an inconspicuous nucleus and highly resolved arms. Individual stars cannot be seen in the smaller nebulae of this group, but knots are conspicuous, which, in larger objects, are known to be groups and clusters of stars. The extent to which the arms are opened varies from M 33 to M 101, both typical Sc nebulae.

Barred spirals.—In the normal spiral the arms emerge from two opposite points on the periphery of the nuclear region. There is, however, a smaller group, containing about 20 per cent of all spirals, in which a bar of nebulosity extends diametrically across the nucleus. In these spirals, the arms spring abruptly from the ends of this bar. These nebulae also form a sequence, which parallels that of the normal spirals, the arms apparently unwind, the nuclei dwindle, the condensations form and work inward.

H. D. Curtis[1] first called attention to these nebulae when he described several in the intermediate stages of the series and called them ϕ-type spirals. The bar, however, never extends beyond the inner spiral arms, and the structure, especially in the early portion of the sequence, is more accurately represented by the Greek letter θ. From a dynamical point of view, the distinction has considerable significance. Since Greek letters are inconvenient for cataloguing purposes, the English term, "barred spiral," is proposed, which can be contracted to the symbol "SB."

The SB series, like that of the normal spirals, is divided into three roughly equal sections, distinguished by the appended letters "a," "b," and "c." The criteria on which the division is based are similar in general to those used in the classification of the normal spirals. In the earliest forms, SBa, the arms are not differentiated, and the pattern is that of a circle crossed by a bar, or, as has been mentioned, that of the Greek letter θ. When the bar is oriented nearly in the line of sight, it appears foreshortened as a bright and definite minor axis of the elongated nebular image. Such curious forms as the images of N.G.C. 1023 and 3384 are explained in this manner. The latest group, SBc, is represented by the S-shaped spirals such as N.G.C. 7479.

[1] *Publications of the Lick Observatory*, 13, 12, 1918.

IRREGULAR NEBULAE

About 3 per cent of the extra-galactic nebulae lack both dominating nuclei and rotational symmetry. These form a distinct class which can be termed "irregular." The Magellanic Clouds are the most conspicuous examples, and, indeed, are the nearest of all the extra-galactic nebulae. N.G.C. 6822, a curiously faithful miniature of the Clouds, serves to bridge the gap between them and the smaller objects, such as N.G.C. 4214 and 4449. In these latter, a few individual stars emerge from an unresolved background, and occasional isolated spots give the emission spectrum characteristic of diffuse nebulosity in the galactic system, in the Clouds, and in N.G.C. 6822.[1] These features are found in other irregular nebulae as well, notably in N.G.C. 1156 and 4656, and are just those to be expected in systems similar to the Clouds but situated at increasingly greater distances.

The system outlined above is primarily for the formal classification of photographic images obtained with large reflectors and portrait lenses. For each instrument, however, there is a limiting size and luminosity below which it is impossible to classify with any confidence. Except in rare instances, these small nebulae are extra-galactic, and their numbers, brightness, dimensions, and distribution are amenable to statistical investigation. For cataloguing purposes, they require a designating symbol, and the letter "Q" is suggested as convenient and not too widely used with other significations.

PART II. STATISTICAL STUDY OF EXTRA-GALACTIC NEBULAE

THE DATA

The most homogeneous list of nebulae for statistical study is that compiled by Hardcastle[2] containing all nebulae found on the Franklin-Adams charts. These are uniform exposures of two hours on fast plates made with a Cooke astrographic lens of 10-inch aperture and 45-inch focal length. The scale is 1 mm = 3′. The entire sky is cov-

[1] $H\beta$ is brighter than N_2. Patches with similar spectra are often found in the arms of late-type spirals—N.G.C. 253, M 33, M 101. The typical planetary spectrum, where $H\beta$ is fainter than N_2, is found in the rare cases of apparently stellar nuclei of spirals; for instance, in N.G.C. 1068, 4051, and 4151. Here also the emission spectra are localized and do not extend over the nebulae.

[2] *Monthly Notices*, **74**, 699, 1914.

PLATE XIV

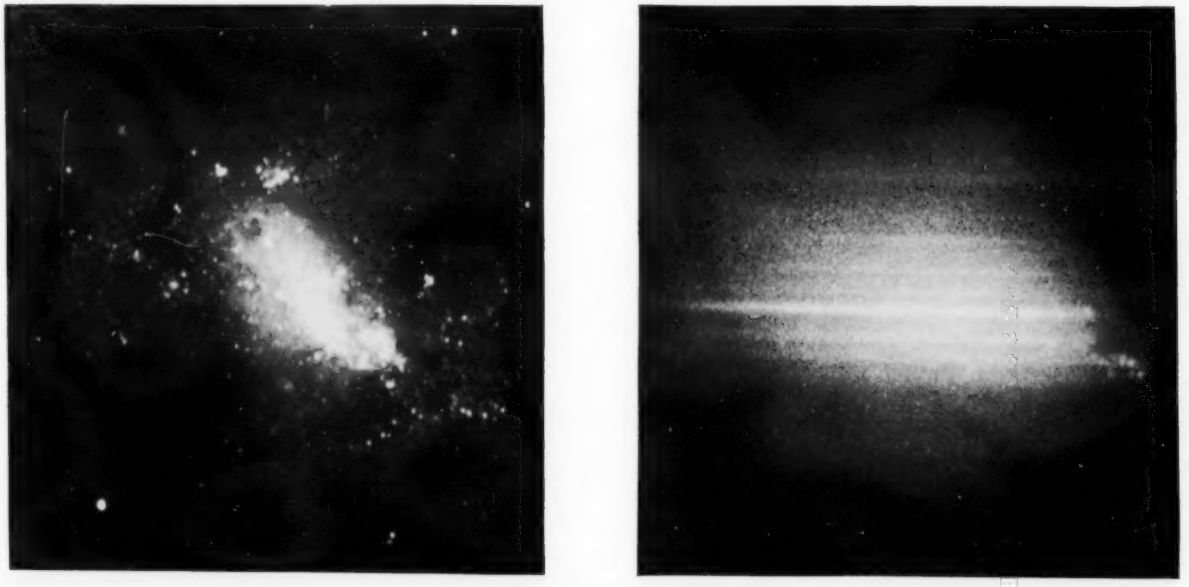

IRREGULAR NEBULA N.G.C. 4214

Direct photograph with 100-inch reflector March 18, 1925. Scale 1 mm=3″.3
Slitless spectrogram at primary focus of 100-inch reflector, March 19, 1925

ered, but since the plates are centered about 15° apart and the definition decreases very appreciably with distance from the optical axis, the material is not strictly homogeneous. Moreover, the published list suffers from the usual errors attendant on routine cataloguing; for instance, four conspicuous Messier nebulae, M 60, M 87, M 94, and M 101, are missing. In general, however, the list is thoroughly representative down to about the thirteenth photographic magnitude and very few conspicuous objects are overlooked. It plays the rôle of a standard with which other catalogues of the brighter nebulae may be compared for completeness, and numbers in limited areas may be extended to the entire sky.

When known galactic nebulae, clusters, and the objects in the Magellanic Clouds are weeded out, the remaining 700 nebulae may be treated as extra-galactic. Very few can be classified from the Franklin-Adams plates; for this purpose photographs on a much larger scale are required. Until further data on the individual objects are available, Hardcastle's list can be used only for the study of distribution over the sky. This shows the well-known features—the greater density in the northern galactic hemisphere, the concentration in Virgo, and the restriction of the very large nebulae to the southern galactic hemisphere.

Fortunately, numerical data do exist in the form of total visual magnitudes for many of the nebulae in the northern sky. These determinations were made by Holetschek,[1] who attempted to observe all nebulae within reach of his 6-inch refractor. He later restricted his program; but the final list is reasonably complete for the more conspicuous nebulae north of declination −10°, and is representative down to visual magnitude about 12.5. Out of 417 extra-galactic nebulae in Holetschek's list, 408 are north of −10°, as compared with 400 in Hardcastle's. The two lists agree very well for the brighter objects, but diverge more and more with decreasing luminosity. At the twelfth magnitude about half of Holetschek's nebulae are included by Hardcastle. Since the two lists compare favorably in completeness over so large a region of the sky, Holetschek's may be chosen as the basis for a statistical study and advantage taken of the valuable numerical data on total luminosities.

[1] *Annalen der Wiener Sternwarte*, **20**, 1907.

Hopmann[1] has revised the scale of magnitudes by photometric measures of the comparison stars used by Holetschek. New magnitudes were thus obtained for 85 individual nebulae and from these were derived mean correction tables applicable to the entire list. The revised magnitudes are used throughout the following discussion. Hopmann's corrections extend to about 12.0 mag., and have been extrapolated on the assumption that they are constant for the fainter magnitudes. The errors involved are unimportant in view of selective effects which must be present among the observed objects near the limit of visibility.

The nebulae were classified and their diameters measured from photographs of about 300 of them taken with the 60-inch and 100-inch reflectors at Mount Wilson. Most of the others are included in the great collection of nebular photographs at Mount Hamilton, which have been described by Curtis;[2] and, through the courtesy of the Director of the Lick Observatory, it has been possible to confirm the classification inferred from the published description by actual inspection of the original negatives.

Types, diameters, and total visual magnitudes are thus available for some 400 of the nebulae in Holetschek's list. The few unclassified objects are all fainter than 12.5 mag. The data are listed in Tables I–IV, in which the N.G.C. numbers, the total magnitudes, and the logarithms of the maximum diameters in minutes of arc are given for each type separately. A summary is given in Table V, in which the relative frequencies and the mean magnitudes of the various types will be found.

RELATIVE LUMINOSITIES OF THE VARIOUS TYPES

The frequency distribution of magnitudes for all types together and for the elliptical nebulae and the spirals separately is shown in Table VI and Figure 1. With the exception of the two outstanding spirals, M 31 and M 33, the apparent luminosities are about uniformly distributed among the different types. The relative numbers of the elliptical nebulae as compared with the spirals decrease somewhat with decreasing luminosity, but this is very probably an effect

[1] *Astronomische Nachrichten*, 214, 425, 1921.

[2] *Publications of the Lick Observatory*, 13, 1918.

TABLE I

Elliptical Nebulae

N.G.C.	m_T	log d
E0 (17)		
404	11.1	+0.11
474	12.6	− .40
1407	10.9	.15
3348	11.8	− .15
3379*	9.4	+ .30
4283	12.2	− .52
4486*	9.7	+ .30
4494*	10.1	− .15
4552*	9.9	+ .23
4589	11.4	− .30
4648	12.3	.52
5044	11.8	.30
5216	13.3	.70
5273	12.1	.52
5557	12.3	.40
5812	12.0	− .40
5846	10.9	0.0
Mean	11.40	−0.204
E1 (13)		
467	13.0	−0.70
596	11.8	.22
1400	11.1	.22
2880	12.0	.52
3226	12.0	.10
3962	11.8	− .30
4278*	10.8	.0
4374*	9.9	+ .08
4472	8.8	+ .30
4478	11.5	− .10
4636	10.9	+ .08
5813	12.6	− .30
7626	12.3	−0.30
Mean	11.43	−0.177
E2 (14)		
221*	8.8	+0.42
1453	11.9	− .10
2672	12.8	− .40
3193	12.1	0.0
3599	12.0	−0.30
3608	11.6	.22
3640	11.1	− .05
4261	11.1	+ .20
4291	12.3	− .52
4377	11.9	− .05
4406*	10.0	+ .30
4476	12.8	− .30
4649*	9.5	+ .30
5127	13.3	−0.52
Mean	11.52	−0.088
E3 (10)		
1052	11.8	−0.15
1600	12.7	+ .17
3222	13.3	− .15
4319	12.8	− .52
4365	11.4	+ .04
4386	12.3	− .52
5322*	9.6	+ .15
5982	11.4	.0
7562	12.8	− .22
7619	11.8	−0.15
Mean	11.99	−0.133
E4 (13)		
584	10.9	+0.30
1700	12.5	− .10
2974	11.8	.15
3605	12.5	− .52
3610	11.8	+ .15
3894	12.8	− .05
4125*	10.3	+ .30
4378	12.1	− .15
4382*	10.0	+ .48
4551	12.8	+ .04
4742	12.3	.0
5576	12.3	− .15
7454	13.3	0.0
Mean	11.95	−0.011

E2 —*Continued*

TABLE I—*Continued*

N.G.C.	m_T	log d
E5 (6)		
720	10.9	+0.11
2693	12.3	− .15
3377	10.9	+ .17
4473	10.3	.11
4621*	10.0	+ .30
4660	11.4	0.0
Mean	10.97	+0.090
E6 (7)		
821	11.8	0.0
2768	10.7	+ .18
3613	11.8	.25
4179	11.8	.34
4435*	10.5	.11
4546*	10.3	.18
4697*	9.6	+0.48
Mean	10.93	+0.220
E7 (5)		
3115*	9.5	+0.60
4111	10.1	.54
4270	12.1	.0
4570	11.1	.38
5308	12.3	+0.28
Mean	11.02	+0.360
Peculiar (8)		
185	12.3	+0.48
205*	9.3	.90
524†	11.9	.41
3607†	9.9	.11
3998†	12.1	+ .23
4459‡	11.3	− .22
5485‡	12.3	.05
5739	13.3	−0.40

of selection. The elliptical nebulae are more compact than the spirals and become more stellar with decreasing luminosity. For this reason some of the fainter nebulae are missed when small-scale instruments are used, although the same luminosity spread over a larger area would still be easily detected. The effect is very pronounced on photographic plates. It accounts also for the slightly brighter mean magnitude of the elliptical nebulae as compared with the spirals in Table V.

The various types are homogeneously distributed over the sky, their spectra are similar, and the radial velocities are of the same general order. These facts, together with the equality of the mean magnitudes and the uniform frequency distribution of magnitudes, are consistent with the hypothesis that the distances and absolute luminosities as well are of the same order for the different types. This is an assumption of considerable importance, but unfortunately it cannot yet be subjected to positive and definite tests. None of the individual similarities necessarily implies the adopted interpretation, but the totality of them, together with the intimate series relations

among the types, which will be discussed later, suggests it as the most reasonable working hypothesis, at least until inconsistencies should appear.

TABLE II

BARRED SPIRALS

N.G.C.	m_T	log d
SBa (26)		
936	11.1	+0.48
1023*	10.2	.78
2732	12.3	.11
2781	12.3	.11
2787	11.4	.36
2859	11.1	.28
2950	11.6	.15
3384*	10.7	.48
3412*	11.2	+ .40
3418	13.1	.0
3458	12.8	− .22
3945	11.5	+ .20
4026	11.1	.48
4203	11.1	.36
4346	12.0	.20
4371	12.0	.18
4421	12.8	.17
4442	10.9	.50
4477	10.9	.40
4596	12.0	.25
4643	11.1	.26
4754	10.9	.48
5473	12.0	+ .08
5574	13.0	− .05
5689	12.0	+ .30
5701	12.3	+0.17
Mean	11.66	+0.267
SBb (16)		
1022	11.8	+0.04
2650	12.8	.0
3351*	11.4	+ .48
3400	12.5	− .10
3414	11.5	+ .26
3504	11.4	.30
3718	11.8	+0.48
4102	12.0	+0.36
4245	11.1	.15
4394	11.5	.60
4548	11.1	.60
4699*	10.0	.57
4725*	9.2	.70
5218	12.8	.25
5566	11.1	.20
7723	11.8	+0.18
Mean	11.48	+0.317
SBc (15)		
613	10.6	+0.60
779	12.1	.48
3206	13.3	.45
3344	11.4	.60
3346	12.3	.40
3625	13.3	.0
3686	12.0	.30
3769	12.8	.43
3953	11.1	.74
3992	11.5	.85
4303*	10.6	.78
4579*	9.7	.45
5383	12.6	.40
5921	12.8	.70
7479	12.1	+0.48
Mean	11.87	+0.509
Peculiar (2)		
2782	12.3	+0.26
4314	11.1	+0.34

RELATION BETWEEN LUMINOSITIES AND DIAMETERS

Among the nebulae of each separate type are found linear correlations between total magnitudes and logarithms of diameters. These

TABLE III

NORMAL SPIRALS

N.G.C.	m_T	log d	N.G.C.	m_T	log d
		Sa (49)			
488	11.8	+0.48	4281	11.5	+0.18
676	13.3	.30	4429	11.5	.48
1332	10.9	.43	4452	12.6	.15
2655	11.1	.60	4526	11.1	.70
2681	10.7	.48	4550	12.1	.43
2775	10.9	.32	4570	11.1	.38
2811	12.3	.28	4594	9.1	.85
2855	12.8	.11	4665	11.8	+ .08
3169§	12.3	.60	4684	12.2	− .22
3245	11.8	.30	4698	11.9	+ .43
3301	12.4	.15	4710	11.8	.54
3368*	10.0	.85	4762	11.5	.57
3516	12.1	.20	4866	12.0	.50
3619	12.3	.0	4958	11.4	.60
3626*	11.3	.28	5377	11.8	.48
3665	12.0	.0	5389	12.5	.25
3682	12.1	.08	5422	12.1	+ .40
3898	12.0	.43	5631	12.0	− .05
3941	10.3	.30	5866*	11.7	+ .48
4036	10.9	.60	7013	12.8	.08
4138	12.1	.20	7457	12.8	.30
4143	11.3	.11	7727	11.3	.43
4150	12.0	.11	7814*	11.4	+0.48
4251	10.4	.26			
4268	12.8	.0	Mean	11.69	+0.333
4274	11.1	+0.54			
		Sb (70)			
224	5.0	+2.25	3556	11.1	+0.90
672	12.8	0.54	3593	11.9	.60
772	11.1	.70	3623*	9.9	.90
949	13.3	.0	3627*	9.1	0.90
955	12.9	.40	3628§	11.4	+1.08
1068	9.1	.40	3632	13.3	−0.10
1309	12.0	.15	3675	11.4	+ .48
2639	12.2	.0	3681	13.0	.0
2715	12.5	.40	3684	13.0	+ .08
2748	12.0	.32	3895	13.3	− .05
2841*	9.4	.78	3900	12.1	+ .25
2985	11.4	0.48	3938	12.1	.65
3031*	8.3	+1.20	4020	12.3	.17
3182	12.9	−0.22	4030	11.1	.30
3190	11.9	+ .48	4051*	11.9	.60
3227	12.0	.48	4085	12.5	.36
3277	12.6	.0	4151	12.0	.40
3310	10.4	+ .18	4192	10.9	.90
3380	12.1	− .05	4216*	10.8	0.85
3489*	11.2	+0.40	4244§	12.3	+1.11

TABLE III—*Continued*

N.G.C.	m_T	log d	N.G.C.	m_T	log d
		Sb—*Continued*			
4258*.....	8.7	+1.30	5394.....	13.3	+0.17
4273.....	11.8	0.20	5633.....	13.0	− .10
4438*.....	10.3	.54	5713.....	12.3	+ .32
4448.....	11.8	.48	5740.....	12.3	.48
4450.....	10.6	+ .57	5746.....	10.4	.87
4451.....	12.8	− .15	5750.....	12.8	.15
4500.....	12.8	+0.17	5772.....	12.0	.25
4565*§.....	11.0	1.17	5806.....	12.3	.30
4736*.....	8.4	0.70	5985.....	12.0	.60
4750.....	11.8	.26	6207.....	11.8	.30
4800.....	11.8	.04	6643.....	11.9	.48
4814.....	12.7	.56	7331*.....	10.4	.95
4826.....	9.0	.90	7541.....	12.7	.41
5055*.....	9.6	.90	7606.....	12.0	+0.78
5376.....	12.8	+ .17			
5379.....	12.9	−0.05	Mean.....	11.55	+0.471
		Sc (115)			
157.....	11.4	+0.40	3395.....	12.6	+0.11
253.....	9.3	1.34	3396.....	13.3	− .10
278.....	12.0	0.08	3430.....	12.6	+ .49
470.....	13.1	0.20	3432.....	12.0	.79
598.....	7.0	1.78	3437.....	12.4	.28
615.....	12.3	0.43	3445.....	13.1	.08
628*.....	10.6	.90	3448.....	12.3	.26
908.....	11.9	.60	3486.....	11.8	.58
1084.....	11.4	.34	3488.....	12.8	.25
1087.....	12.1	.36	3512.....	12.3	.0
1637.....	12.6	.48	3521*.....	10.1	.65
2339.....	13.1	0.28	3549.....	13.3	.43
2403*.....	8.7	1.20	3596.....	13.3	.60
2532.....	13.3	0.17	3631.....	11.8	.66
2683.....	9.9	1.00	3642.....	12.0	.73
2712.....	12.3	0.20	3655.....	11.9	.04
2742.....	11.8	.40	3666.....	11.8	.54
2776.....	12.3	0.34	3672.....	13.0	.54
2903*.....	9.1	1.04	3683.....	12.0	.15
2964.....	11.6	0.40	3780.....	13.0	.40
2976.....	12.0	.50	3810.....	11.3	.62
3003§.....	13.3	.78	3813.....	12.3	.32
3021.....	12.3	.11	3877.....	11.8	.64
3079§.....	12.0	.90	3887.....	12.3	.40
3147.....	11.4	.30	3893.....	11.8	.61
3166.....	12.0	.0	3949.....	11.8	.34
3184.....	12.7	.78	3982.....	12.1	.36
3198.....	13.0	.95	4013.....	13.3	.60
3254.....	12.8	.60	4041.....	11.4	.30
3294.....	12.0	.48	4062.....	12.6	.48
3389.....	13.1	+0.30	4088.....	11.5	+0.72

TABLE III—*Continued*

N.G.C.	m_T	log d	N.G.C.	m_T	log d
		Sc—*Continued*			
4096	12.3	+0.78	4995	11.8	+0.36
4100	12.3	.60	5005*	11.1	.70
4145	12.3	.70	5012	11.9	.43
4157§	12.3	.77	5033*	11.8	0.78
4212	12.3	.30	5194*	7.4	1.08
4220	12.1	0.40	5204	12.8	0.59
4236	12.8	1.04	5236	10.4	1.00
4254	10.4	0.65	5247	13.3	0.70
4321*	10.5	.70	5248	11.5	.50
4414	10.1	.48	5290	12.5	.48
4419	11.8	.36	5297	12.6	.60
4460	12.1	.20	5364	13.3	.60
4490*	10.2	.60	5395	12.8	0.30
4501*	10.5	.70	5457	9.9	1.34
4504	12.1	0.48	5474	12.0	0.60
4517§	12.5	1.00	5585	12.3	.60
4536§	12.3	0.85	5676	11.8	.48
4559	10.7	.90	5678	11.8	.41
4569*	10.9	.65	5832	13.1	0.56
4580	12.3	.15	5907§	11.9	1.04
4605	9.9	0.48	6181	12.5	0.30
4631*	9.5	1.08	6217	12.1	.25
4632	13.1	0.50	6503	9.9	.70
4666	12.0	.60	7448	11.8	+ .30
4713	12.3	.38	7671	13.3	−0.15
4781	11.8	.48			
4793	12.4	.20	Mean	11.75	+0.537
4808	12.6	+0.34			
		Peculiar Spirals (Unclassified)			
972	13.3	+0.17			
2537	13.3	.0			
4900	11.8	+0.23			

are shown in Figures 2–5 for the beginning, middle, and end of the sequence of types and also for the irregular nebulae. In Figures 2 and 3 adjacent types have been grouped in order to increase the material, and in Figure 5 the Magellanic Clouds have been added to increase the range.

The correlations can be expressed in the form

$$m_T = C - K \log d \,, \qquad (1)$$

where K is constant from type to type, but C varies progressively throughout the sequence. The value of K cannot be accurately de-

termined from the scattered data for any particular type, but, within the limits of uncertainty, it approximates the round number 5.0, the value which is represented by the lines in Figures 2–5.

When K is known, the value of C can be computed from the mean magnitude and the logarithm of the diameter for each type. This amounts to reading from the curves the magnitudes corresponding to a diameter of one minute of arc, but avoids the uncertainty of establishing the curves where the data are limited.

TABLE IV

IRREGULAR NEBULAE

N.G.C.	m_T	log d	N.G.C.	m_T	log d
2968.....	12.6	+0.08	4656§.....	11.5	+1.30
3034*.....	9.0	.85	4753.....	11.4	+0.43
3077.....	11.4	.48	5144.....	12.8	− .30
3729.....	11.8	.17	5363.....	11.1	+0.20
4214*.....	11.3	.90			
4449*.....	9.5	.65	Mean.....	11.34	+0.469
4618.....	12.3	+0.40			

NOTES TO TABLES I–IV

* Magnitude from Hopmann.

† N.G.C. 524 and 3998 are late elliptical nebulae in which the equatorial planes are perpendicular to the line of sight. They might be included with the E6 or E7 nebulae.

§ Absorption very conspicuous.

‡ N.G.C. 3607, 4459, and 5485 appear to be elliptical nebulae with narrow bands of absorption between the nuclei and the peripheries.

The progressive change in the value of C throughout the sequence may be expressed as a variation either in the magnitude for a given diameter or in the diameter for a given magnitude. Both effects are listed in Table VII and are illustrated in Figure 6, in which magnitudes and diameters thus found are plotted against types. With the exception of the later elliptical nebulae, for which the data are wholly inadequate for reliable determinations, the points fall on smooth curves. In the region of the earlier elliptical nebulae, the curves should be somewhat steeper in order to allow for objects of great ellipticities which are probably included.

REDUCTION OF NEBULAE TO A STANDARD TYPE

The slope, K, in the formula relating magnitudes with diameters, appears to be closely similar for the various types, but accurate de-

terminations are restricted by the limited and scattered nature of the data for each type separately. With a knowledge of the parameter C, however, it is possible to reduce all the material to a standard

TABLE V

FREQUENCY DISTRIBUTION OF TYPES

Type	Number	Percentage	Mean Mag.
Elliptical Nebulae			
E0	17	18	11.40
1	13	14	11.43
2	14	15	11.52
3	10	11	11.99
4	13	14	11.95
5	6	6	10.97
6	7	8	10.93
7	5	5	11.02
Pec	8	9	11.55
Total	93	23*	11.53
Normal Spirals			
Sa	49	21	11.69
b	70	29	11.55
c	115	49	11.75
Pec	3	1	12.80
Total	237	59*	11.68
Barred Spirals			
SBa	26	44	11.66
b	16	27	11.48
c	15	26	11.87
Pec	2	3	11.70
Total	59	15*	11.66
Irregular Nebulae			
	11	3*	11.34
Totals			
All types	400	100	11.63

* Percentages of 400, the total number of nebulae investigated. The percentages of the subtypes refer to the number of nebulae in the particular type.

type and hence to determine the value of K from the totality of the data. The mean of E7, SBa, and Sa was chosen for the purpose, as representing a hypothetical transition-point between the elliptical nebulae and the spirals, and was designated by the symbol "So." The corresponding value of C, in round numbers, is 13.0. Corrections

TABLE VI

FREQUENCY DISTRIBUTION OF MAGNITUDES

MAGNITUDE INTERVAL	NUMBERS OF NEBULAE		
	E	S	All
8.1– 8.5	0	2	2
8.6– 9.0	2	4	7
9.1– 9.5	4	6	11
9.6–10.0	7	7	19
10.1–10.5	7	13	20
10.6–11.0	8	14	32
11.1–11.5	9	24	49
11.6–12.0	21	57	88
12.1–12.5	20	52	86
12.6–13.0	10	33	51

were applied to the logarithms of the diameters of the nebulae of each observed class, amounting to

$$\Delta \log d = 0.2\,(13.0 - C)$$

where C is the observed value for a particular class.[1] When the values of C are read from the smooth curve in Figure 6, these corrections are as shown in Table VIII.

The corrected values of $\log d$ were then plotted against the observed magnitudes. This amounts to shifting the approximately parallel correlation curves for the separate types along the axis of $\log d$ until they coincide. Since the mean magnitudes of the various types are nearly constant, the relative shifts will very nearly equal the differences in the mean observed $\log d$, and hence the effect of errors in the first approximation to the values of K will be negligible.

The plot is shown in Figure 7, in which the two Magellanic

[1] Since C is constant for all nebulae in a given class, the linear relation between $\Delta \log d$ and C for the different classes is something more than a mere geometrical relation arising from the observed equality of the mean m_T in the various classes.

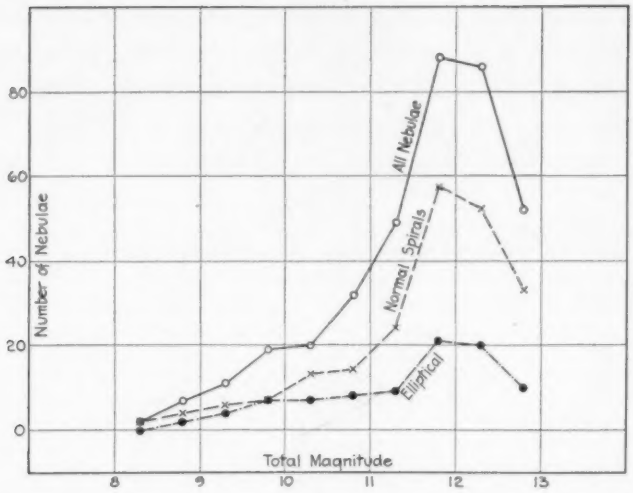

FIG. 1.—Frequency distribution of apparent magnitudes among nebulae in Holetschek's list.

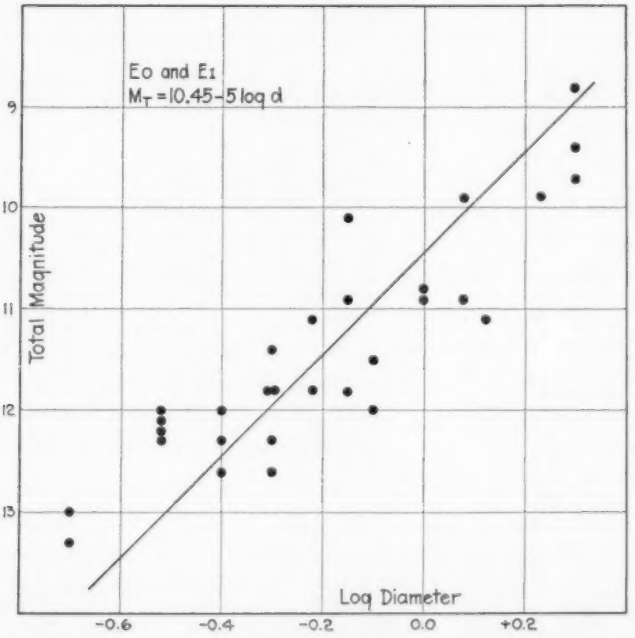

FIG. 2.—Relation between luminosity and diameter among nebulae at the beginning of the sequence of types—Eo and E1 nebulae.

Clouds have been included in order to strengthen the bright end of the curve which would otherwise be unduly influenced by the single

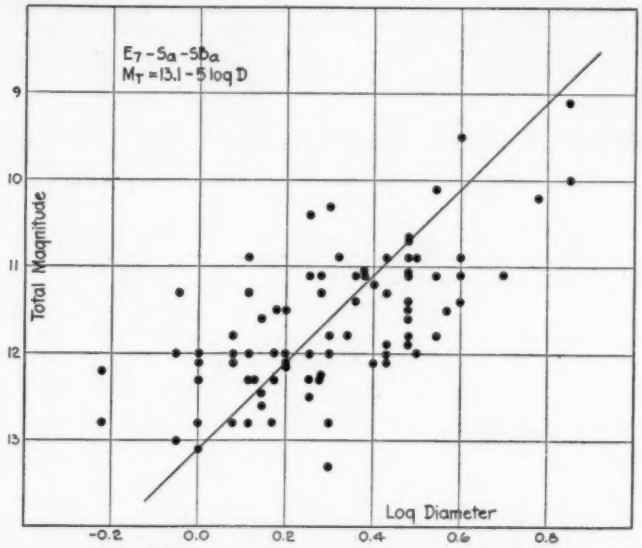

FIG. 3.—Relation between luminosity and diameter among nebulae at the middle of the sequence of types—E7, Sa, and SBa nebulae.

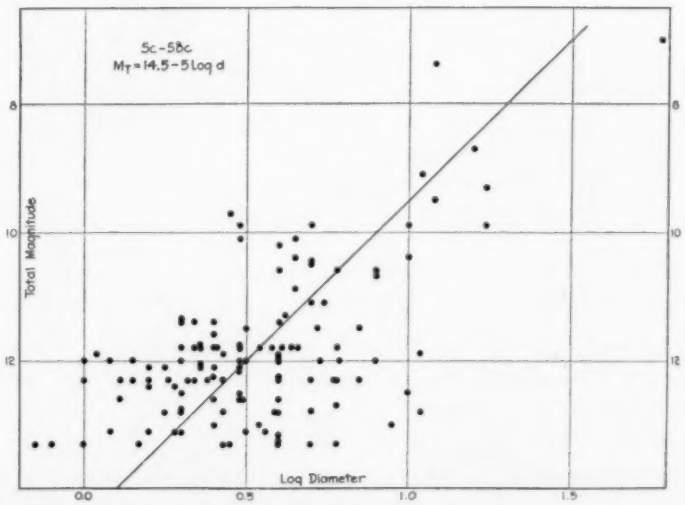

FIG. 4.—Relation between luminosity and diameter among nebulae at the end of the sequence of types—Sc and SBc nebulae.

object, M 31. The magnitudes +0.5 and +1.5, which were assigned to the Clouds, are estimates based upon published descriptions.

The correlation of the data is very closely represented by the formula

$$m_T = 13.0 - 5 \log d \,. \qquad (2)$$

This falls between the two regression curves derived from least-square solutions and could be obtained exactly by assigning appro-

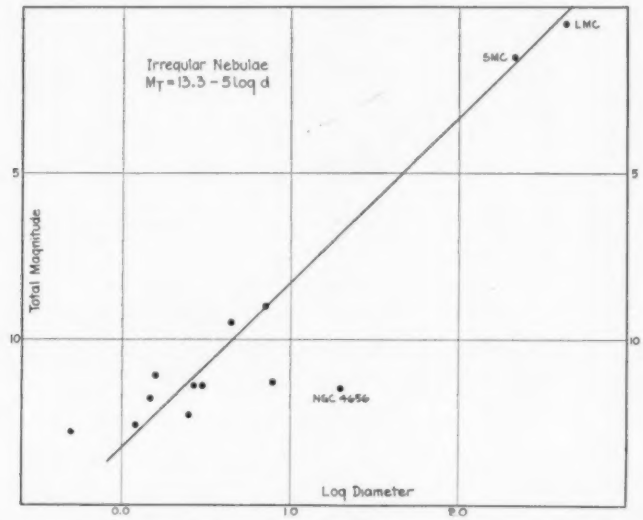

FIG. 5.—Relation between luminosity and diameter among the irregular nebulae. The Magellanic Clouds are included. N.G.C. 4656 is an exceptional case in that it shows a narrow, greatly elongated image in which absorption effects are very conspicuous; hence the maximum diameter is exceptionally large for its apparent luminosity.

priate weights to the two methods of grouping. The nature of the data is such that a closer agreement can scarcely be expected. No correction to the assumed value of the slope appears to be required. The material extends over a range of 12 mag., and the few cases which have been investigated indicate that the correlation can be extended another 3 mag., to the limit at which nebulae can be classified with certainty on photographs made with the 100-inch reflector. The relation may therefore be considered to hold throughout the entire range of observations.

The residuals without regard to sign average 0.87 mag., and there appears to be no systematic effect due either to type or luminosity. The scatter, however, is much greater for the spirals, especially in the later types, than for the elliptical nebulae. The limiting cases are explained by peculiar structural features. The nebulae which fall well above the line usually have bright stellar nuclei, and those which fall lowest are spirals seen edge-on in which belts of absorption are conspicuous.

TABLE VII

Type	$\overline{m_T}$	$\overline{\log d}$	C^*	$d\dagger$
Eo	11.40	−0.204	10.38	1.2
1	11.43	.177	10.54	1.3
2	11.52	.088	11.08	1.6
3	11.99	.133	11.33	1.8
4	11.95	− .011	11.90	2.4
5	10.97	+ .090	11.42	1.9
6	10.93	.220	12.03	2.5
7	11.02	.360	12.82	3.7
Sa	11.69	.333	13.35	4.7
b	11.55	.471	13.90	6.0
c	11.74	.540	14.44	7.7
SBa	11.66	.267	13.00	4.0
b	11.48	.317	13.16	4.3
c	11.87	.509	14.41	7.6
Irr	11.34	+0.469	13.68	5.4

* $C=\overline{m_T}+5\,\overline{\log d}$.
† $\log d=0.2\,(C-m_T)$; $m_T=10.0$.

EFFECTS OF ORIENTATION

The effect of the orientation is appreciable among the spirals in general. In order to illustrate this feature, they have been divided into three groups consisting of those whose images are round or nearly round, elliptical, and edge-on, or nearly so. The mean values of $m_T+5\log d$ were then computed and compared with the theoretical value, 13.0. The residuals are negative when the nebulae are too bright for their diameters and positive when they are too faint. The results are given in Table IX, where mean residuals are followed by the numbers of nebulae, in parentheses, which are represented by the means.

The numbers of the barred spirals are too limited to inspire confidence in the results, but among the normal spirals there is conclusive evidence that the highly tilted and edge-on nebulae are fainter for a given diameter than those seen in the round. A study of the individual images indicates that the effect is due very largely to dark

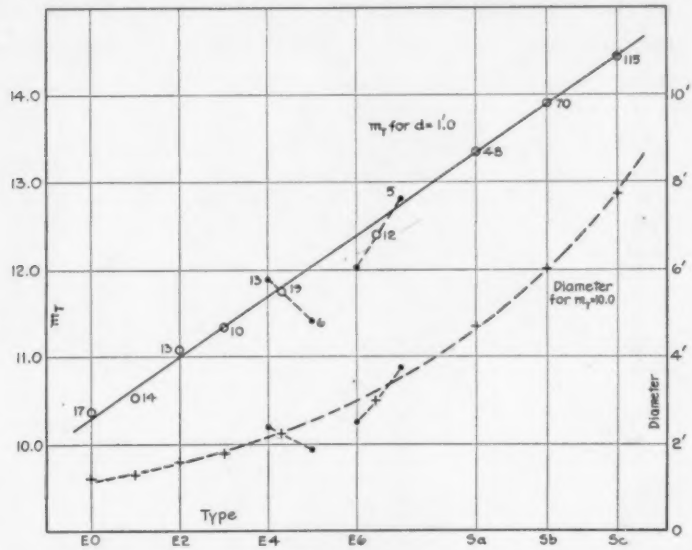

FIG. 6.—Progressive characteristics in the sequence of types. The upper curve represents the progression in total magnitude with type for nebulae having maximum diameters of one minute of arc. The elliptical nebulae and the normal spirals are included as representing the normal sequence, but the barred spirals and the irregular nebulae are omitted. The figures give the number of objects observed in each type. Among the later elliptical nebulae the numbers are so small that means of adjacent types have been plotted. The lower curve represents the progression in diameter along the normal sequence for nebulae of the tenth magnitude.

absorption clouds, which become more conspicuous when the nebulae are highly tilted. These clouds are generally, but not universally, peripheral features. An extensive investigation will be necessary before any residual effect due to absorption by luminous nebulosity can be established with certainty. Even should such exist, it clearly cannot be excessive.

SIGNIFICANCE OF THE LUMINOSITY RELATION

The correlations thus far derived are between total luminosities and maximum diameters. In the most general sense, therefore, they

express laws of mean surface brightness. The value, $K = 5.0$, in formula (1) indicates that the surface brightness is constant for each separate type. The variations in C indicate a progressive diminution

TABLE VIII

Type	C	$\Delta \log d$	Type	C	$\Delta \log d$
Eo	10.30	+0.54	Sa	13.31	−0.06
1	10.65	.47	Sb	13.90	.18
2	11.00	.40	Sc	14.45	.29
3	11.35	.33	SBa	13.00	.00
4	11.70	.26	SBb	13.16	.03
5	12.05	.19	SBc	14.41	.28
6	12.40	.12	Irr	13.68	−0.14
7	12.75	+0.05			

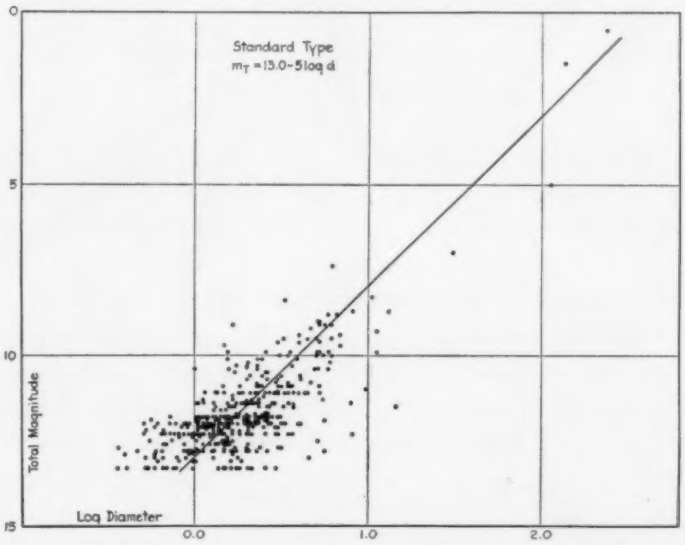

FIG. 7.—Relation between luminosity and diameter among extra-galactic nebulae. The nebulae have been reduced to a standard type, So, which, being the mean of E7, Sa, and SBa, represents a hypothetical transition point between elliptical nebulae and spirals. The Magellanic Clouds have been included in order to strengthen the brighter end of the plot.

in the surface brightness from class to class throughout the entire sequence. The consistency of the results amply justifies the sequence as a basis of classification, since a progression in physical dimensions

is indicated, which accompanies the progression in structural form. Although the correlations do not necessarily establish any generic relation among the observed classes, they support in a very evident manner the hypothesis that the various stages in the sequence represent different phases of a single fundamental type of astronomical body. Moreover, the quantitative variation in C is consistent with this interpretation, as is apparent from the following considerations.

Among the elliptical nebulae it is observed that the nuclei are sharp and distinct and that the color distribution is uniform over

TABLE IX

RESIDUALS IN m_T+5 LOG d AS A FUNCTION OF ORIENTATION

Type	Round	Elliptical	Edge-On
Sa	−0.02 (13)	−0.27 (13)	+0.57 (23)
Sb	.77 (24)	.0 (35)	1.71 (11)
Sc	−0.08 (35)	−0.13 (57)	+0.66 (22)
All S	−0.26 (72)	−0.11 (105)	+0.83 (56)
SBa	0.0 (10)	−0.30 (7)	+0.31 (8)
SBb	− .16 (10)	+ .07 (6)	.....
SBc	+0.19 (9)	−0.50 (4)	+0.32 (2)
All SB	+0.01 (29)	−0.21 (17)	+0.31 (10)
All spirals	−0.22 (101)	−0.13 (122)	+0.73 (66)

the images. This indicates that there is no appreciable absorption, either general or selective, and hence that the luminosity of the projected image represents the total luminosity of the nebula, regardless of the orientation. If the observed classes were pure, that is, if the apparent ellipticities were the actual ellipticities, formula (1) could be written

$$C_e = m_T + 5 \log b - 5 \log (1-e) , \qquad (3)$$

where b is the minor diameter in minutes of arc and e is the ellipticity. The term $m + 5 \log b$ is observed to be constant for a given type. If it were constant for all elliptical nebulae, then the term $C_e + 5 \log (1-e)$ would be constant also. On this assumption,

$$C_e + 5 \log (1-e) = C_0 ,$$

where C_0 is the value of C for the pure class Eo. Hence

$$C_e - C_0 = -5 \log (1-e) , \qquad (4)$$

a relation which can be tested by the observations. An analysis of the material indicates that this is actually the case, and hence that among the elliptical nebulae in general, the minor diameter determines the total luminosity, at least to a first approximation.[1]

The observed values of C vary with the class, as is seen in Table VII and Figure 6, but, excepting that for E7, they are too large because of the mixture of later types of nebulae among those of a given observed class. It is possible, however, to calculate the values of $C_e - C_0$ for the pure classes and then to make approximate corrections for the observed mixtures on the assumption that the nebulae of any given actual ellipticity are oriented at random. In this manner, mean theoretical values can be compared with the observed values. The comparisons are shown in Table XII in the form $C_7 - C_e$, because E7 is the only observed class that can be considered as pure. The significance of the table will be discussed later.

The following method has been used to determine the relative frequencies with which nebulae of a given actual ellipticity, oriented at random, will be observed as having various apparent ellipticities.

In Figure 8, let the co-ordinate axes OX and OY coincide with the major and minor axes, a and b, of a meridian section of an ellipsoid of revolution. Let OO' be the line of sight to the observer, making an angle i with OX, and let OR be perpendicular to OO'. Let PP' be a

[1] This is apparent even among the observed classes. Referring to formula (3), $m_T + 5 \log b$ will be constant in so far as $C_e + 5 \log (1-e)$ is constant. The following table indicates that the latter term is approximately constant throughout the sequence of elliptical nebulae. The values of C_e were read from the smooth curve in Fig. 6.

e	C_e	$5 \log (1-e)$	C_0	Res.
0	10.30	0.0	10.30	−0.14
1	10.65	− .23	10.42	− .02
2	11.00	.48	10.52	+ .10
3	11.35	0.78	10.57	+ .13
4	11.70	1.11	10.59	+ .15
5	12.05	1.50	10.55	+ .11
6	12.40	1.99	10.41	− .03
7	12.75	−2.62	10.13	−0.31
Mean	.....	.....	10.44	0.12

tangent to the ellipse, parallel to and at a distance b_1 from OO'. Let x_0 and y_0 be the intercepts of the tangent on the X- and Y-axis, respectively. The apparent ellipticity is determined by b_1, which, for various values of the angle i, ranges from b to a. The problem is to determine the relative areas on the surface of a sphere whose center is O, within which the radius OY must pass in order that the values of b_1, and hence of the apparent ellipticity, e_1, may fall within certain designated limits. This requires that the angle i be expressed in terms of b_1.

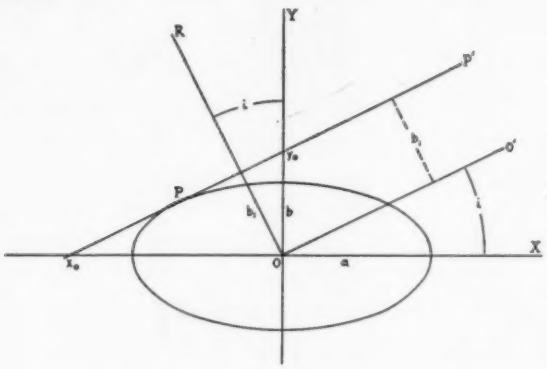

FIG. 8

From the equation of the tangent, PP',

$$y=-x\tan i+\sqrt{a^2\tan^2 i+b^2}$$

$$y_0=\sqrt{a^2\tan^2 i+b^2}\,.$$

Since

$$b_1=y_0\cos i$$

$$b_1^2=a^2\sin^2 i+b^2\cos^2 i\,.$$

Let $a=1$, then

$$\cos^2 i=\frac{1-b_1^2}{1-b^2}\,,$$

where

$$b_1=1-e_1\,,\qquad b=1-e\,.$$

From these equations, the values of i can be determined for all possible values of e_1. The limits for the observed classes Eo to E7 were chosen midway between the consecutive tenths, Eo ranging

from $e=0$ to $e=0.05$; E1, from $e=0.05$ to $e=0.15$; E7, from $e=0.65$ to $e=0.75$. The relative frequencies of the various observed classes are then proportional to the differences in sin i corresponding to the two limiting values of e_1. These frequencies must be calculated separately for nebulae of different actual ellipticities.

The results are given in Table X, where the actual ellipticities, listed in the first column, are followed across the table by the percentages which, on the assumption of random orientation, will be observed as having the various apparent ellipticities. The bottom row will be seen to show the percentages of apparent ellipticities

TABLE X

Actual	Apparent								
	E0	E1	E2	E3	E4	E5	E6	E7	Total
E7	0.055	0.111	0.114	0.116	0.121	0.132	0.164	0.187	1.000
6	.059	.123	.126	.133	.148	.187	0.224	.....	.....
5	.067	.140	.148	.166	.216	0.263	.....	.....	.....
4	.079	.169	.190	.250	0.312	.....	.....	.....	.....
3	.100	.225	.299	0.376	.....	.....	.....	.....	.....
2	.145	.378	0.477	.....	.....	.....	.....	.....	.....
1	0.300	0.700	.....	.....	.....	.....	.....	.....	.....
0	1.000	.....	.....	.....	.....	.....	.....	.....	.....
Total	1.805	1.846	1.354	1.041	0.797	0.582	0.388	0.187	8.000
	0.226	0.231	0.169	0.130	0.100	0.073	0.049	0.023	1.000

observed in an assembly of nebulae in which the numbers for each actual ellipticity are equal and all are oriented at random.

From this table and the actual numbers in the observed classes as read from a smoothed curve, the numbers of each actual ellipticity mingled in the observed classes can be determined. For instance, the four nebulae observed as E7 represent 0.187 of the total number of actual E7. The others are distributed among the observed classes Eo to E6 according to the percentages listed in Table X. Six nebulae are observed as E6, but 3.6 of these are actually E7. The remaining 2.4 actual E6 nebulae represent 0.224 of the total number of that actual ellipticity, the others, as before, being scattered among the observed classes Eo to E5. Table XI gives the complete analysis and is similar to Table X except that the percentages in the latter are replaced by the actual numbers indicated by the observations.

Finally, the mean values of $C_7 - C_e$ are calculated from the numbers of nebulae in the various columns of Table XI together with the values of $C_7 - C_e$ for the pure classes as derived from formula (4). The results are listed in the fourth column of Table XII following those for the pure and the observed classes. In determining the observed values, N.G.C. 524 and 3998 are included as E0 and E1, although in Table I they are listed as peculiar, because they are obviously much flattened nebulae whose minor axes are close to the line of sight.

The observed values in general fall between those for the pure classes and those corresponding to random orientation. They are of

TABLE XI

Actual	Apparent								
	E0	E1	E2	E3	E4	E5	E6	E7	Total
E7	1.2	2.4	2.5	2.5	2.6	2.9	3.6	4.0	21.7
6	0.6	1.3	1.4	1.5	1.6	2.0	2.4	.....	10.8
5	.8	1.7	1.8	2.0	2.7	3.1	.....	.....	12.1
4	.8	1.7	1.9	2.5	3.1	.....	.....	.....	10.0
3	0.9	2.1	2.8	3.5	.....	.....	.....	.....	9.3
2	1.1	2.9	3.6	.....	.....	.....	.....	.....	7.6
1	1.7	3.9	.....	.....	.....	.....	.....	.....	5.6
0	9.9	.....	.....	.....	.....	.....	.....	.....	9.9
Total*	17.0	16.0	14.0	12.0	10.0	8.0	6.0	4.0	87.0

* The totals represent the numbers in the observed classes as read from a smooth curve.

the same order as the latter, and the discrepancies are perhaps not unaccountably large in view of the nature and the limited extent of the material. There is a systematic difference, however, averaging about 0.2 mag., in the sense that the observed values are too large, and increasing with decreasing ellipticity. One explanation is that the observed classes are purer than is expected on the assumption of random orientation. This view is supported by the relatively small dispersion in C, as may be seen in Table I and Figure 2, among the nebulae of a given class, but it is difficult to account for any such selective effect in the observations. The discrepancies may be largely eliminated by an arbitrary adjustment of the numbers of nebulae with various degrees of actual ellipticity; for instance, the values in

the last column of Table XII, calculated on the assumption of equal numbers, agree very well with the observed values, although the resulting numbers having the various apparent ellipticities differ slightly from those observed. The observed values, however, can again be accounted for by the inclusion of some flatter nebulae among the classes E6 and E7. Very early Sa or SBa nebulae might easily be mistaken for E nebulae when oriented edge-on, although they would be readily recognized when even slightly tilted. If the numerical results fully represented actual statistical laws, the explanation would

TABLE XII

DIFFERENTIAL VALUES OF *C*

CLASS	PURE CLASSES	OBSERVED	RANDOM ORIENTATION	
			No. as Observed	Equal No.
C7–C7.....	0.00	0.00	0.00	0.00
C6.....	0.63	0.35*	0.25	0.35
C5.....	1.10	0.70*	0.58	0.70
C4.....	1.51	0.85	0.87	1.01
C3.....	1.84	1.42	1.11	1.28
C2.....	2.13	1.67	1.33	1.55
C1.....	2.39	2.01†	1.54	1.83
Co.....	2.62	2.17†	2.15	2.25

* Read from smooth curve in Fig. 6. The small numbers of observed E5 and E6 nebulae justify this procedure. The other values are the means actually observed.

† N.G.C. 524 and 3998 are included as Eo and E1, respectively.

be sought in the physical nature of the nebulae. The change from ellipsoidal to lenticular figures, noticeable in the later-type nebulae, would affect the results in the proper direction, as would also a progressive shortening of the polar axis. The discrepancies, however, are second-order effects, and since they may be due to accidental variations from random orientation, a further discussion must await the accumulation of more data.

Meanwhile, it is evident that, to a first approximation at least, the polar diameters alone determine the total luminosities of all elliptical nebulae, and the entire series can be represented by the various configurations of an originally globular mass expanding equatorially. A single formula represents the relation, in which the value of *C* is that corresponding to the pure type Eo. From Table

XII, this is found to be 2.62 mag. less than the value of C_7. The latter is observed to be 12.75, hence

$$m_T + 5 \log b = 10.13 . \qquad (5)$$

If this relation held for the spirals as well, the polar diameters could be calculated from the measured magnitudes. Unfortunately, it has not been possible to measure accurately the polar diameters directly, and hence to test the question, but they have been computed for the mean magnitudes of the Sa, Sb, and Sc nebulae as given in Table III, and the ratios of the axes have been derived by a comparison of these hypothetical values with the means of the measured maximum diameters. The results, 1 to 4.4, 1 to 5.7, and 1 to 7.3, respectively, although of the right order, appear to be somewhat too high. An examination of the photographs indicates values of the order of 1 to 5.5, 1 to 8, and 1 to 10, but the material is meager and may not be representative. The comparison emphasizes, however, the homogeneity and the progressive nature of the entire sequence of nebulae and lends some additional color to the assumption that it represents various aspects of the same fundamental type of system.

From the dynamical point of view, the empirical results are consistent with the general order of events in Jeans's theory. Thus interpreted, the series is one of expansion, and the scale of types becomes the time scale in the evolutionary history of nebulae. In two respects this scale is not entirely arbitrary. Among the elliptical nebulae the successive types differ by equal increments in the ellipticity or the degree of flattening, and among the spirals the intermediate stage is midway between the two end-stages in the structural features as well as in the luminosity relations.

One other feature of the curves may be discussed from the point of view of Jeans's theory before returning to the strictly empirical attitude. The close agreement of the diameters for the stages E7 and Sa suggests that the transition from the lenticular nebula to the normal spiral form is not cataclysmic. If the transition were gradual, however, we should expect to observe occasional objects in the very process, but among the thousand or so nebulae whose images have been inspected, not one clear case of a transition form has been detected. The observations jump suddenly from lenticular nebulae

with no trace of structure to spirals in which the arms are fully developed.

If the numerical data could be fully trusted, the SBa forms would fill the gap. Among these nebulae, the transition from the lenticular to the spiral with arms is gradual and complete. It is tempting to suppose that the barred spirals do not form an independent series parallel with that of the normal spirals, but that all or most spirals begin life with the bar, although only a few maintain it conspicuously throughout their history. This would also account for the fact that the relative numbers of the SBa nebulae are intermediate to those of the lenticular and of the Sa. The normal spirals become more numerous as the sequence progresses, while the numbers of barred spirals, on the contrary, actually decrease with advancing type.

RELATION BETWEEN NUCLEAR LUMINOSITIES AND DIAMETERS

Visual magnitudes have been determined by Hopmann for the nuclei of 37 of the nebulae included in the present discussion. These data, together with types and diameters of the nebulae, are listed in Table XIII. When the magnitudes are plotted directly against the logarithms of the diameters, they show little or no correlation. When, however, the nebulae are reduced to the standard type (by applying corrections for differences in diameter along the sequence), a decided correlation is found whose coefficient is 0.76. This is shown in Figure 9. The simple mean of the two regression curves is

$$m_n = 14.45 - 4.94 \log d\,, \qquad (6)$$

where the slope differs by about 1 per cent from that in formula (2). The list contains 16 elliptical nebulae, 15 normal, and 6 barred spirals. The nebulae are fairly representative, except that few late-type spirals are included. This is an effect of selection due to the fact that nuclei become less and less conspicuous as the sequence progresses.

The same result can be derived from a study of the differences, $m_n - m_T$, for the individual nebulae. The mean value is 1.55 ± 0.08, and the average residual is 0.60 mag. Means for the separate types are to be found in Table XIV.

The low value for Sa–SBa is due to N.G.C. 5866, for which the

magnitude difference of 0.06 is certainly in error, and the high value for Sc and SBc, to M 51, for which the difference of 3.98 mag. is not representative. The latter is accounted for in part by the fact that

TABLE XIII

DIAMETERS AND NUCLEAR MAGNITUDES

N.G.C.	Type	log d	m_n Hopmann	m_n Reduced
221	E2	+0.42	9.84	11.85
1023	SBa	.78	11.86	11.86
2841	Sb	0.78	12.08	11.19
3031	Sb	1.20	10.94	10.05
3115	E7	0.60	10.83	11.09
3351	SBb	.48	12.31	12.15
3368	Sa	.85	11.68	11.43
3379	E0	.30	11.55	14.27
3412	SBa	.40	11.59	11.59
3489	Sb	.40	11.54	10.65
3626	Sa	.28	12.37	12.12
3627	Sb	.90	12.03	11.14
4125	E4	.30	11.74	13.04
4216	Sb	.85	11.65	10.76
4278	E1	.0	12.02	14.38
4374	E1	.08	11.43	13.79
4382	E4	.48	11.77	13.07
4435	E6	.11	11.65	12.26
4438	Sb	.54	11.83	10.94
4486	E0	.30	11.23	13.95
4546	E6	.18	11.75	12.36
4552	E0	.23	11.59	14.31
4569	Sc	.65	12.05	10.57
4579	SBc	.45	11.48	10.07
4621	E5	.30	11.60	12.56
4636	E1	.08	11.97	14.33
4649	E2	.30	11.57	13.58
4697	E6	.48	10.90	11.51
4699	SBb	.57	10.72	10.56
4725	SBb	.70	11.97	11.81
4736	Sb	.70	10.36	9.47
5005	Sc	.70	12.04	10.56
5033	Sc	0.78	12.38	10.90
5194	Sc	1.08	11.38	9.90
5322	E3	0.15	12.10	13.76
5866	Sa	.48	11.76	11.51
7331	Sb	+0.95	11.82	10.93
Means ...	.....	+0.509	11.60	11.90

the m_T refers to the combined magnitude of the main spiral and the outlying mass, N.G.C. 5195. When these two cases are discarded, the final mean becomes 1.52 ± 0.05, and the average residual, 0.52 mag., is consistent with the probable errors of the magnitude de-

terminations. The small numbers of objects within each class are insufficient for reliable conclusions concerning slight variations along the sequence. From the constancy of $m_n - m_T$, the relation expressed by formula (6) necessarily follows, the small difference in the constant being accounted for by the different methods of handling the data.

The parallelism of the two curves representing formulae (2) and (6) indicates that the regular extra-galactic nebulae, when reduced

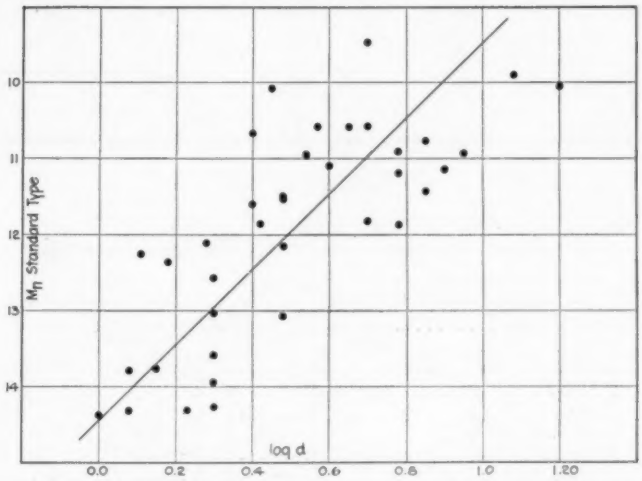

FIG. 9.—Relation between nuclear magnitudes and diameters. The nebulae have been reduced to the standard type by applying corrections to the magnitudes.

to the standard type, are similar objects. The mean surface brightness is constant, and the luminosity of the nucleus, as measured by Hopmann, is a constant fraction, about one-fourth, of the total luminosity of the nebulae. If there is a considerable range in absolute magnitude and hence in actual dimensions, the smaller nebulae must be faithful miniatures of the larger ones.

ABSOLUTE MAGNITUDES OF EXTRA-GALACTIC NEBULAE

Reliable values of distances, and hence of absolute magnitudes, are restricted to a very few of the brightest nebulae. These are derived from a study of individual stars involved in the nebulae, among which certain types have been identified whose absolute magnitudes in the galactic system are well known. The method assumes that the

stars involved in the nebulae are directly comparable with the stars in our own system, and this is supported by the consistency of the results derived from the several different types which have been identified.

TABLE XIV

Types	$m_n - m_T$	Number
Eo–E3	1.64	(9)
E4–E7	1.43	(7)
Sa–SBa	0.97	(5) 1.27 when N.G.C. 5866 is omitted
Sb–SBb	1.70	(11)
Sc–SBc	1.76	(5) 1.19 when N.G.C. 5194 is omitted
Unweighted mean	1.50	(37) 1.45 (35)
Weighted mean	1.55	(37) 1.52 (35)

TABLE XV

ABSOLUTE MAGNITUDES OF NEBULAE

System	M_T	M_S
Galaxy	.....	− 5.5
M 31	−17.1	6.5
L M C	17.0	8.0
S M C	16.0	5.5
M 33	15.1	6.5
N.G.C. 6822	13.7	5.8
M 101	13.5	− 6.3
M 32	−13.3	.....
	.....	− 6.3
	.....	− 9.0 $= M_S - M_T$
Means	−15.1	−15.3
Adopted	−15.2	

In Table XV are listed absolute magnitudes of the entire system and of the brightest stars involved, for the galaxy and the seven nebulae whose distances are known. The data for the Magellanic Clouds are taken from Shapley's investigations. The absolute magnitudes of the remaining nebulae were derived from Holetschek's apparent magnitudes and the distances as determined at Mount Wilson, where the stellar magnitudes were also determined. M 32 is generally assumed to be associated with the great spiral M 31, because the radial velocities are nearly equal and are unique in that

they are the only large negative velocities that have been found among the extra-galactic nebulae. M 101 has been added to the list on rather weak evidence. The brightest stars involved are slightly brighter than apparent magnitude 17.0, and several variables have been found with magnitudes at maxima fainter than 19.0. Sufficient observations have not yet been accumulated to determine the light-curves of the variables, but from analogy with the other nebulae they are presumed to be Cepheids. On this assumption, both the star counts and the variables lead to a distance of the order of 1.7 times the distance of M 33. The inclusion of M 101 does not change the mean magnitude of the brightest stars involved, but reduces the mean magnitude of the nebulae by 0.2.

The range in the stars involved is about 2.5 mag., and in the total luminosities of the nebulae, about 3.8 mag. This latter is consistent with the scatter in the diagram exhibiting the relation between total luminosities and diameters. The associated objects, M 31 and 32, represent the extreme limits among the known systems, and the mean of these two is very close to the mean of them all.

LUMINOSITY OF STARS INVOLVED IN NEBULAE

The number of nebulae of known distance is too small to serve as a basis for estimates of the range in absolute magnitude among nebulae in general. Further information, however, can be derived from a comparison of total apparent magnitudes with apparent magnitudes of the brightest stars involved, on the reasonable assumption, supported by such evidence as is available, that the brightest stars in isolated systems are of about the same intrinsic luminosity.

The most convenient procedure is to test the constancy of the differences in apparent magnitude between the brightest stars involved and the nebulae themselves, over as wide a range as possible in the latter quantities.

An examination of the photographs in the Mount Wilson collection has revealed no stars in the very faint objects or in the bright elliptical nebulae and early-type spirals. This was to be expected from the conclusions previously derived. Observations were therefore confined to intermediate- and late-type spirals and the irregular

nebulae to the limiting visual magnitude 10.5. The Magellanic Clouds and N.G.C. 6822 were added to the nebulae in Holetschek's

TABLE XVI

DIFFERENCE IN MAGNITUDE BETWEEN NEBULAE AND THEIR BRIGHTEST STARS

N.G.C.	m_s	m_T	$m_s - m_T$
	Sb		
224	15.5	5.0	10.5
1068	17.5	9.1	8.4
2841	>19.5	9.4	>10.1
3031	18.5	8.3	10.2
3310	>19.0	10.4	> 8.6
3623	>20.0	9.9	>10.1
3627	18.5	9.1	9.4
4438	>19.0	10.3	> 8.7
4450	19.5	10.0	9.5
4736	17.3	8.4	8.9
4826	>19.5	9.2	>10.3
5055	>19.0	9.6	> 9.4
5746	>19.5	10.4	> 9.1
7331	19.0	10.4	8.6
	SBb		
4699	>19.5	10.0	> 9.5
	Sc		
253	18.3	9.3	9.0
598	15.6	7.0	8.6
2403	17.3	8.7	8.6
2683	>20.0	9.9	>10.1
2903	19.0	9.1	9.9
4254	18.5	10.4	8.1
4321	18.8	10.5	8.3
4414	>19.5	10.1	> 9.4
4490	18.8	10.2	8.6
5194	17.3	7.4	9.9
5236	18.6	10.4	8.2
5457	17.0	9.9	7.1
	Irr.		
L M C	9.5	0.5	9.0
S M C	12.0	1.5	10.5
3034	>19.5	9.0	>10.5
4449	17.8	9.5	8.3
6822	15.8	8.5	7.3

list. Altogether, data were available for 32 objects, or about 60 per cent of the total number in the sky to the adopted limit. For this reason it is believed that the results are thoroughly representative.

The data are listed in Table XVI and are shown graphically in Figure 10. The luminosities of the brightest stars are given in photographic magnitudes. For the Magellanic Clouds, M 33, and N.G.C. 6822, these were obtained from published star counts. For M 31, 51,

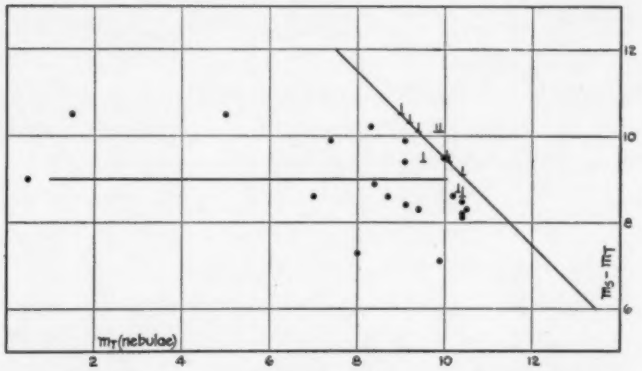

FIG. 10.—Relation between total magnitudes of extra-galactic nebulae and magnitudes of the brightest stars involved. Differences between total visual magnitudes of nebulae and the photographic magnitudes of the brightest stars are plotted against the total magnitudes. The dots represent cases in which the stars could actually be detected; the incomplete crosses represent cases in which stars could not be detected, and hence give lower limits for the magnitude differences. The diagonal line indicates the approximate limits of observation, fixed by the circumstance that, in general, stars fainter than 19.5 probably would not be detected on the nebulous background.

63, 81, 94, and N.G.C. 2403, they depend upon unpublished counts, for which the magnitudes were determined by comparisons with Selected Areas. For the remaining nebulae, the magnitudes of stars were estimated with varying degrees of precision, but are probably less than 0.5 mag. in error.

The sloping line to the right in Figure 10 represents the limits of the observations, for, from a study of the plates themselves, it appeared improbable that stars fainter than about 19.5 could be detected with certainty on a nebulous background. Points representing nebulae in which individual stars could not be found should lie in this excluded region above the line, and their scatter is presumably

comparable with that of the points actually determined below the line. When allowance is made for this inaccessible region, the data can be interpreted as showing a moderate dispersion around the mean ordinate

$$m_2 - m_T = 9.0 . \qquad (7)$$

The range in total magnitudes is sufficiently large in comparison with the dispersion to lend considerable confidence to the conclusion. The total range of four, and the average dispersion of less than 1 mag., are comparable with those in Table XV and in Figure 7, and agree with the former in indicating a constant order of absolute magnitude.

The mean absolute magnitude of the brightest stars in the nebulae listed in Table XV, combined with the mean difference between nebulae and their brightest stars, furnishes a mean absolute magnitude of -15.3 for the nebulae listed in Table XVI. This differs by only 0.2 mag. from the average of the nebulae in Table XV, and the mean of the two, -15.2, can be used as the absolute magnitude of intermediate- and late-type spirals and irregular nebulae whose apparent magnitudes are brighter than 10.5. The dispersion is small and can safely be neglected in statistical investigations.

This is as far as the positive evidence can be followed. For reasons already given, however, it is presumed that the earlier nebulae, the elliptical and the early-type spirals, are of the same order of absolute magnitude as the later. The one elliptical nebula whose distance is known, M 32, is consistent with this hypothesis.

Conclusions concerning the intrinsic luminosities of the apparently fainter nebulae are in the nature of extrapolations of the results found for the brighter objects. When the nebulae are reduced to a standard type, they are found to be constructed on a single model, with the total luminosities varying directly as the square of the diameters. The most general interpretation of this relation is that the mean surface brightness is constant, but the small range in absolute magnitudes among the brighter nebulae indicates that, among these objects at least, the relation merely expresses the operation of the inverse-square law on comparable objects distributed at different distances. The actual observed range covered by this restricted interpretation is from apparent magnitude 0.5 to 10.5. The

homogeneity of the correlation diagrams and the complete absence of evidence to the contrary justify the extrapolation of the restricted interpretation to cover the 2 or 3 mag. beyond the limits of actual observation.

These considerations lead to the hypothesis that the nebulae treated in the present discussion are all of the same order of absolute magnitude; in fact, they lend considerable color to the assumption that extra-galactic nebulae in general are of the same order of absolute magnitude and, within each class, of the same order of actual dimensions. Some support to this assumption is found in the observed absence of individual stars in the apparently fainter late-type nebulae. If the luminosity of the brightest stars involved is independent of the total luminosity of a nebula, as is certainly the case among the brighter objects, then, when no stars brighter than 19.5 are found, the nebulae must in general be brighter than absolute magnitude $m_T - 25.8$ where m_T is the total apparent magnitude. On this assumption, the faintest of the Holetschek nebulae are brighter than -12.5 and hence of the same general order as the brighter nebulae.

Once the assumption of a uniform order of luminosity is accepted as a working hypothesis, the apparent magnitudes become, for statistical purposes, a measure of the distances. For a mean absolute magnitude of -15.2, the distance in parsecs is

$$\log D = 0.2\, m_T + 4.04. \tag{8}$$

DIMENSIONS OF EXTRA-GALACTIC NEBULAE

When the distances are known, it is possible to derive actual dimensions and hence to calibrate the curve in Figure 6, which exhibits the apparent diameters as a function of type, or stage in the nebular sequence, for nebulae of a given apparent magnitude. The mean maximum diameters in parsecs corresponding to the different mean types are given in Table XVII. For the elliptical nebulae, values are given both for the statistical mean observed diameters and for the diameter as calculated for the pure types.

Spirals at the last stage in the observed sequence have diameters of the order of 3000 parsecs. Assuming 1:10 as the ratio of the two

axes, the corresponding volume is of the order of 1.4×10^9 cubic parsecs, and the mean luminosity density is of the order of 7.7 absolute magnitudes per cubic parsec as compared with 8.15 for the galactic system in the vicinity of the sun. These results agree with those of Seares who, from a study of surface brightness, concluded that the galactic system must be placed at the end of, if not actually outside, the series of known spirals when arranged according to density.[1]

TABLE XVII

Type	Diameter in Parsecs		Type	Diameter in Parsecs
	Obs.	Cal.		
E0	360	340	Sa	1450
E1	430	380	Sb	1900
E2	500	430	Sc	2500
E3	590	490	.....	.....
E4	700	570	SBa	1280
E5	810	680	SBb	1320
E6	960	850	SBc	2250
E7	1130	1130	Irr	1500

MASSES OF EXTRA-GALACTIC NEBULAE

Spectroscopic rotations are available for the spirals M 31[2] and N.G.C. 4594,[3] and from these it is possible to estimate the masses on the assumption of orbital rotation around the nucleus. The distances of the nebulae are involved, however, and this is known accurately only for M 31; for N.G.C. 4594 it must be estimated from the apparent luminosity.

Another method of estimating masses is that used by Öpik[4] in deriving his estimate of the distance of M 31. It is based on the assumption that luminous material in the spirals has about the same coefficient of emission as the material in the galactic system. Öpik computed the ratio of luminosity to mass for our own system in

[1] *Mt. Wilson Contr.*, No. 191; *Astrophysical Journal*, **52**, 162, 1920.

[2] Pease, *Mt. Wilson Comm.*, No. 51; *Proceedings of the National Academy of Sciences*, **4**, 21, 1918.

[3] Pease, *Mt. Wilson Comm.*, No. 32: *ibid.*, **2**, 517, 1916.

[4] *Astrophysical Journal*, **55**, 406, 1922.

terms of the sun as unity, using Jeans's value[1] for the relative proportion of luminous to non-luminous material. The relation is

$$\text{Mass} = 2.6\,L\,. \qquad (9)$$

The application of this method of determining orders of masses seems to be justified, at least in the case of the later-type spirals and irregular nebulae, by the many analogies with the galactic system itself. Moreover, when applied to M 31, where the distance is fairly well known, it leads to a mass of the same order as that derived from the spectrographic rotation:

MASS OF M 31

Spectrographic rotation	$3.5\times10^9\,\odot$
Öpik's method	1.6×10^9

The distance of N.G.C. 4594 is unknown, but the assumption that it is a normal nebula with an absolute magnitude of -15.2 places it at 700,000 parsecs. The orders of the mass by the two methods are then

MASS OF N.G.C. 4594

Spectrographic rotation	$2.0\times10^9\,\odot$
Öpik's method	2.6×10^8

Here again the resulting masses are of the same order. They can be made to agree as well as those for M 31 by the not unreasonable assumption that the absolute luminosity of the nebula is 2 mag. or so brighter than normal.

Öpik's method leads to values that are reasonable and fairly consistent with those obtained by the independent spectrographic method. Therefore, in the absence of other resources, its use for deriving the mass of the normal nebula appears to be permissible. The result, $2.6\times10^8\,\odot$, corresponding to an absolute magnitude of -15.2, is probably of the right order. The two test cases suggest that this value may be slightly low, but the data are not sufficient to warrant any empirical corrections.

NUMBERS OF NEBULAE TO DIFFERENT LIMITING MAGNITUDES

The numbers of nebulae to different limiting magnitudes can be used to test the constancy of the density function, or, on the hypoth-

[1] *Monthly Notices*, **82**, 133, 1922.

esis of uniform luminosities, to determine the distribution in space. The nebulae brighter than about the tenth magnitude are known individually. Those not included in Holetschek's list are: the Magellanic Clouds, the two nebulae N.G.C. 55 and 1097, between 9.0 and 9.5 mag., and the seven nebulae N.G.C. 134, 289, 1365, 1533, 1559, 1792, and 3726, all between 9.5 and 10.0 mag.

A fair estimate of the number between 10.0 and 11.0 mag. can be derived from a comparison of Holetschek's list with that of Hardcastle, an inspection of images on the Franklin-Adams charts and other photographs, and a correlation between known total magnitudes and the descriptions of size and brightness in Dreyer's catalogues. It appears that very few of these objects were missed by Holetschek in the northern sky—not more than six of Hardcastle's nebulae. For the southern sky, beyond the region observed by Holetschek, the results are very uncertain, but probable upper and lower limits were determined as 50 and 20, respectively. The brighter nebulae are known to be scarce in those regions. A mean value of 35 leads to a total 295 for the entire sky, and this is at least of the proper order.

The number of nebulae between 11.0 and 12.0 mag. can be estimated on the assumption that the two lists, Holetschek's and Hardcastle's, are about equally complete within this range. They are known to be comparable for the brighter nebulae, and, moreover, the total numbers included in the two lists for the same area of the sky, that north of declination $-10°$, are very nearly equal—400 as compared with 408. The percentages of Holetschek's nebulae included by Hardcastle were first determined as a function of magnitude. Within the half-magnitude interval 11.0 to 11.5, for instance, 60 per cent are in Hardcastle's list. If the two lists are equally complete and, taken together, are exhaustive, the total number in the interval will be 1.4 times the number of Holetschek's nebulae. The latter is found to be 50 from smoothed frequency curves of the magnitudes listed in Tables I–IV. The total number north of $-10°$ is therefore 70. This can be corrected to represent the entire sky by applying the factor 1.75, which is the ratio of the total number of Hardcastle's nebulae, 700, to the number north of $-10°$, 400. In this manner a reasonable estimate of 123 is obtained for the number of nebulae in

the entire sky between 11.0 and 11.5 mag. Similarly, between 11.5 and 12.0, where 50 per cent of Holetschek's nebulae are included in Hardcastle's list, the total number for the entire sky is found to be 236.

The greatest uncertainty in these figures arises from the assumption that the two lists together are complete to the twelfth magnitude. The figures are probably too small, but no standards are available by which they can be corrected. It is believed, however, that the errors are certainly less than 50 per cent and probably not more than 25 per cent. This will not be excessive in view of the possible deviations from uniform distribution where so limited a number of objects is considered.

Beyond 12.0 mag. the lists quickly lose their aspect of completeness and cannot be used for the present purpose. There are available, however, the counts by Fath[1] of nebulae found on plates of Selected Areas made with the 60-inch reflector at Mount Wilson. The exposures were uniformly 60 minutes on fast plates and cover the Areas in the northern sky down to and including the $-15°$ zone. The limiting photographic magnitudes for stars average about 18.5. The counts have been carefully revised by Seares[2] and are the basis for his estimate of 300,000 nebulae in the entire sky down to this limit.

Approximate limiting total magnitudes for the nebulae in two of the richest fields, S.A. 56 and 80, have been determined from extra-focal exposures with the 100-inch reflector. The results are 17.7 in each case, and this, corrected by the normal color-index of such objects, gives a limiting visual magnitude of about 16.7, which can be used for comparison with the counts of the brighter nebulae.

The various data are collected in Table XVIII, where the observed numbers of extra-galactic nebulae to different limits of visual magnitude are compared with those computed on the assumption of uniform distribution of objects having a constant absolute luminosity. The formula used for the computation is

$$\log N = 0.6\, m_T + \text{Constant}\,, \qquad (10)$$

[1] *Astronomical Journal*, **28**, 75, 1914.

[2] *Mt. Wilson Contr.*, No. 297; *Astrophysical Journal*, **62**, 168, 1925.

where the constant is the value of log N for $m_T=0$. The value -4.45 is found to fit the observational data fairly well.

The agreement between the observed and computed log N over a range of more than 8 mag. is consistent with the double assumption of uniform luminosity and uniform distribution or, more generally, indicates that the density function is independent of the distance.

The systematic decrease in the residuals O−C with decreasing luminosity is probably within the observational errors, but it may also be explained as due to a clustering of nebulae in the vicinity of

TABLE XVIII

NUMBERS OF NEBULAE TO VARIOUS LIMITS

m_T	log N*		O−C	log D†
	O	C		
8.5.....	0.85	0.65	+0.20	5.74
9.0.....	1.08	0.95	.13	5.84
9.5.....	1.45	1.25	.20	5.94
10.0.....	1.73	1.55	.18	6.04
10.5.....	1.95	1.85	.10	6.14
11.0.....	2.17	2.15	+ .02	6.24
11.5.....	2.43	2.45	− .02	6.34
12.0.....	2.70	2.75	.05	6.44
16.7.....	5.48	5.57	−0.09	7.38
(18.0).....	.....	(6.35)	.....	(7.64)

* Log $N=0.6\ m_T-4.45$.

† Log $D=0.2\ m_T+4.04$.

the galactic system. The cluster in Virgo alone accounts for an appreciable part. This is a second-order effect in the distribution, however, and will be discussed at length in a later paper.

Distances corresponding to the different limiting magnitudes, as derived from formula (8), are given in the last column of Table XVIII. The 300,000 nebulae estimated to the limits represented by an hour's exposure on fast plates with the 60-inch reflector appear to be the inhabitants of space out to a distance of the order of 2.4×10^7 parsecs. The 100-inch reflector, with long exposures under good conditions, will probably reach the total visual magnitude 18.0, and this, by a slight extrapolation, is estimated to represent a distance of the order of 4.4×10^7 parsecs or 1.4×10^8 light-years, within which it is expected that about two million nebulae should be found. This

seems to represent the present boundaries of the observable region of space.

DENSITY OF SPACE

The data are now available for deriving a value for the order of the density of space. This is accomplished by means of the formulae for the numbers of nebulae to a given limiting magnitude and for the distance in terms of the magnitude. In nebulae per cubic parsec, the density is

$$\left.\begin{aligned}\log \rho &= \log N - \log V \\ &= (0.6\, m_r - 4.45) - \log \frac{4\pi}{3} - 3(4.04 + 0.2\, m_r) \\ &= -17.19\end{aligned}\right\} \qquad (11)$$

This is a lower limit, for the absence of nebulae in the plane of the Milky Way has been ignored. The current explanation of this phenomenon in terms of obscuration by dark clouds which encircle the Milky Way is supported by the extra-galactic nature of the nebulae, their general similarity to the galactic system, and the frequency with which peripheral belts of obscuring material are encountered among the spirals. The known clouds of dark nebulosity are interior features of our system, and they do not form a continuous belt. In the regions where they are least conspicuous, however, the extra-galactic nebulae approach nearest to the plane of the Milky Way, many being found within 10°. This is consistent with the hypothesis of a peripheral belt of absorption.

The only positive objection which has been urged to this explanation has been to the effect that the nebular density is a direct function of galactic latitude. Accumulating evidence[1] has failed to confirm this view and indicates that it is largely due to the influence of the great cluster in Virgo, some 15° from the north galactic pole. There is no corresponding concentration in the neighborhood of the south pole.

[1] The latest and most reliable results bearing on the distribution of faint (hence apparently distant) nebulae are found in Seares's revision and discussion of the counts made by Fath on plates of the Selected Areas with the 60-inch reflector. When the influence of the cluster in Virgo is eliminated the density appears to be roughly uniform for all latitudes greater than about 25°.

If an outer belt of absorption is assumed, which, combined with the known inner clouds, obscures extra-galactic nebulae to a mean distance of 15° from the galactic plane, the value derived for the density of space must be increased by nearly 40 per cent. This will not change the order of the value previously determined and is within the uncertainty of the masses as derived by Öpik's method. The new value is then

$$\rho = 9 \times 10^{-28} \text{ nebulae per cubic parsec.} \qquad (12)$$

The corresponding mean distance between nebulae is of the order of 570,000 parsecs, although in several of the clusters the distances between members appear to be a tenth of this amount or less.

The density can be reduced to absolute units by substituting the value for the mean mass of a nebula, 2.6×10^8 ⊙. Then, since the mass of the sun in grams is 2×10^{33} and 1 parsec is 3.1×10^{18} cm,

$$\rho = 1.5 \times 10^{-31} \text{ grams per cubic centimeter.} \qquad (13)$$

This must be considered as a lower limit, for loose material scattered between the systems is entirely ignored. There are no means of estimating the order of the necessary correction. No positive evidence of absorption by inter-nebular material, either selective or general, has been found, nor should we expect to find it unless the amount of this material is many times that which is concentrated in the systems.

THE FINITE UNIVERSE OF GENERAL RELATIVITY

The mean density of space can be used to determine the dimensions of the finite but boundless universe of general relativity. De Sitter[1] made the calculations some years ago, but used values for the density, 10^{-26} and greater, which are of an entirely different order from that indicated by the present investigations. As a consequence, the various dimensions, both for spherical and for elliptical space, were small as compared with the range of existing instruments.

For the present purpose, the simplified equations which Einstein has derived for a spherically curved space can be used.[2] When

[1] *Monthly Notices*, **78**, 3, 1917.

[2] Haas, *Introduction to Theoretical Physics*, **2**, 373, 1925.

R, V, M, and ρ represent the radius of curvature, volume, mass, and density, and k and c are the gravitational constant and the velocity of light,

$$R=\frac{c}{\sqrt{4\pi k}}\cdot\frac{1}{\sqrt{\rho}}, \tag{14}$$

$$V=2\pi^2R^3, \tag{15}$$

$$M=\frac{\pi c^2}{2k}\cdot R. \tag{16}$$

Substituting the value found for ρ, 1.5×10^{-31}, the dimensions become

$$R=8.5\times10^{28}\text{ cm}=2.7\times10^{10}\text{ parsecs}, \tag{17}$$

$$V=1.1\times10^{88}\text{ cm}=3.5\times10^{32}\text{ cubic parsecs}, \tag{18}$$

$$M=1.8\times10^{57}\text{ grams}=9\times10^{22}\odot. \tag{19}$$

The mass corresponds to 3.5×10^{15} normal nebulae.

The distance to which the 100-inch reflector should detect the normal nebula was found to be of the order of 4.4×10^{7} parsecs, or about 1/600 the radius of curvature. Unusually bright nebulae, such as M 31, could be photographed at several times this distance, and with reasonable increases in the speed of plates and size of telescopes it may become possible to observe an appreciable fraction of the Einstein universe.

MOUNT WILSON OBSERVATORY
September 1926

INDEX TO VOLUME LXIV

SUBJECTS

INDEX TO VOLUME LXIV

AUTHORS